Norwegian University of Life Sciences
Faculty of Veterinary Medicine and Biosciences
Department of Chemistry, Biotechnology and Food Science

Master Thesis 2014
60 credits

Characterization of TFPIalpha and TFPIbeta on Apoptosis and Growth in Breast Cancer Cells

Marte Kirkevold

Acknowledgements

The work presented in this thesis was conducted at Ullevål University Hospital, department of Medical Genetics, from August 2013 to May 2014. The thesis was a part of the Master program in Biotechnology, at the Norwegian University of Life Sciences (NMBU), The Department for Chemistry, Biotechnology and Food Science (IKBM).

I would like to direct my gratitude to my supervisor Dr. Philos Nina Iversen for providing me the opportunity for this thesis and for support and guidance throughout the year. Many thanks to my co-supervisor Mari Tinholt for support, good advices and invaluable help during the writing process. A special thanks goes to Marit Sletten for teaching and helping me with the laboratory practical work, and for sharing all her knowledge. I would also like to thank my internal supervisor at NMBU, Prof. Leif Sigve Håvarstein. Thanks to my fellow master students for sharing up and downs in the lab, and my family and friends for support and encouragement.

Ås, May 2014

Marte Kirkevold

Sammendrag

En sammenheng mellom blod koagulasjon og kreft har vært kjent lenge. Tissue factor (TF), som har en hovedfunksjon i å initiere blod koagulasjon, har blitt foreslått til å være den viktigste forbindelse mellom disse to prosessene. Tissue factor pathway inhibitor (TFPI) er mest kjent for sin rolle som hemmer av TF indusert blod koagulasjon. I tillegg er TFPI blitt funnet uttrykt i ulike typer brystkreftcellelinjer og til å ha anti-tumor egenskaper i brystkreftceller. Dette indikerer at TFPI har en rolle i kreftbiologi. TFPI finnes i to isoformer, TFPIα og TFPIβ. Økt kunnskap om effektene av disse to isoformene av TFPI i kreftbiologi, og hvilke molekylære mekanismer som ligger til grunn for disse effektene, kan bidra til utvikling av nye kreftbehandlingsstrategier som involverer TFPI.

Effekten av nedregulert total TFPI (α + β) og bare TFPIβ på brystkreftutvikling har nylig blitt undersøkt, men kun TFPIα har enda ikke blitt nedregulert. For å ytterligere undersøke de separate effektene av TFPIα og TFPIβ på kreftutvikling ble transiente TFPIα og TFPIβ ned- og oppregulerings modeller laget i henholdsvis SUM102 and HCC1500 brystkreft celler. Effekten av modifisert TFPIα og TFPIβ ekspresjon på cellevekst og apoptose i brystkreftceller ble deretter analysert. I tillegg ble noen utvalgte proteiner og signaleringsveier analysert for sin potensielle rolle i TFPI mediert apoptose.

En reduksjon i antall celler og mengde total protein ble observert for SUM102 celler med TFPIα nedregulert (72t etter transfeksjon), mens ingen effekt ble observert for celler med nedregulert TFPIβ. Nedregulering av TFPIα og TFPIβ i SUM102 celler reduserte mengden kløyvet PARP og DNA fragmentering, mens oppregulering av TFPIα i HCC1500 celler reduserte mengden total PARP og total caspase-8, og en liten økning i DNA fragmentering ble vist for oppregulert TFPIβ. En økning i TNF-α nivåer ble også observert i HCC1500 celler med TFPIα oppregulert, mens ingen effekt ble observert i celler med oppregulert TFPIβ. I tillegg førte en nedregulering av TFPIα og TFPIβ i SUM102 celler til økt Akt fosforylering.

For å konkludere, nedregulering av TFPIα kan ha redusert cellevekst etter tre dager. TFPIα og TFPIβ effekter på apoptose ble ytterligere styrket siden ned- og oppregulering av TFPIα og TFPIβ kan henholdsvis ha redusert og indusert apoptose. I tillegg kan PI3-Kinase-Akt

signaleringsveien være involvert i TFPIα og TFPIβ regulert apoptose, og TFPIα kan muligens indusere apoptose gjennom TNF-α.

Abstract

A connection between blood coagulation and cancer has been known for a long time. Tissue factor (TF), which has a main function in initiating blood coagulation, has been indicated to be the main link between these two processes. Tissue factor pathway inhibitor (TFPI) is mainly known for its role in inhibiting TF induced blood coagulation. In addition, TFPI has been found expressed in many different cancer cell lines and to have anti-tumor properties in breast cancer cells, which indicate that TFPI plays a role in cancer biology. TFPI is alternatively spliced into two isoforms TFPIα and TFPIβ. Increased knowledge of the effects of the two TFPI isoforms in cancer biology, and of the molecular mechanisms that underline these effects may contribute to the development of new cancer treatment strategies involving TFPI.

The effect of downregulated total TFPI (α + β) and only TFPIβ on breast cancer development were recently investigated, however TFPIα has not yet been efficiently downregulated. In order to further investigate the separate effects of TFPIα and TFPIβ on cancer development, transient TFPIα and TFPIβ down- and upregulation models were made in the breast cancer cells SUM102 and HCC1500, respectively. Effects of the modified TFPIα and TFPIβ expression on cell growth and apoptosis were thereafter analysed. In addition were some selected proteins and signalling pathways analysed for their potential role in TFPI mediated apoptosis.

A reduction in number of cells and total protein was observed for SUM102 cells with TFPIα downregulated (72h after transfection), while no effect was observed in cells with TFPIβ downregulated. Downregulation of TFPIα and TFPIβ in SUM102 cells reduced the amount of cleaved PARP and DNA fragmentation, while upregulation of TFPIα in HCC1500 cells reduced the amount of total PARP and total caspase-8, and a slight increase in DNA fragmentation was observed for upregulated TFPIβ. An increase in TNF-α levels was also observed in HCC1500 with TFPIα upregulated, while no effect was observed in cells with upregulated TFPIβ. Furthermore, increased Akt phosphorylation was observed after downregulation of TFPIα and TFPIβ in SUM102 cells.

In conclusion, downregulation of TFPIα might have reduced cell growth of after three days in culture. Down-and upregulation of TFPIα and TFPIβ might have reduced and induced apoptosis, respectively, and thus contribute with additional evidence of TFPI isoforms role in apoptosis. In addition, the PI3-Kinase-Akt pathway may be involved in TFPIα and TFPIβ regulated apoptosis and TFPIα may induce apoptosis through TNF-α.

Abbreviations

BM	Basement membrane
cDNA	Complementary DNA
Cyt c	Cytochrome c
ddNTPs	Dideoxynucleotide triphosphates
DISC	Death-inducing signalling complex
dNTPs	Deoxynucleotide triphosphates
dsRNA	Double stranded RNA
ECM	Extracellular matrix
ER	Estrogen receptor
E.coli	*Escherichia coli*
F	Factor
FBS	Fetal bovine serum
GF	Growth factor
GFP	Green fluorescent protein
GPI	Glycosyl phosphatidylinositol
HER2	Human epidermal growth factor receptor 2
HUVECs	Human umbilical vein endothelial cells
IAP	Inhibitors of apoptosis
mRNA	Messenger RNA
MsCs	Mesengial cells
MOMP	Mitochondrial outer membrane permeabilization
NF-κB	Nuclear factor kappa B
t-PA	Tissue-type plasminogen activator
PAI-1	Plasminogen activator inhibitor-1
PBS	Phosphate buffered saline
PCR	Polymerase chain reaction
PARP	Poly (ADP-ribose) polymerase
PDK1	Phosphoinositide-dependent protein kinase 1
PI3	Phosphoinositide-3
PMM1	Phosphomannomutase 1

PR	Progesterone receptor
qRT-PCR	Quantitative reverse transcriptase polymerase chain reaction
RISC	RNA-induced silencing complex
RNAi	RNA interference
RT	Reverse transcriptase
rTFPI	Recombinant TFPI (exogenously added)
RQ	Relative quantity
shRNA	Short hairpin RNA
siRNA	Small interference RNA
TBST	Tris-Buffered Saline
TBS-T	TBS with Tween
TF	Tissue factor
TFPI	Tissue factor pathway inhibitor
TMP	Tetramethylbenzidine
TNF-α	Tumor necrosis factor-α
VEGF	Vascular endothelial growth factor
VTE	Venous thromboembolism

Table of contents

1. Introduction

1.1 Cancer – a genetic disease

Cancer is a genetic disease where accumulation of genomic alterations results in uncontrolled growth of cells, which eventually invade the neighbouring tissue and may spread throughout the body. Human cells possess several control systems that protect the body against the potential hazardous effects of genomic alterations. The development of cancer cells from normal cells is therefore suggested to be a multistep process. Each step involves an epigenetic or genetic change in a proto-oncogene, tumor suppressor gene or DNA maintenance gene. Proto-oncogenes are genes in which a gain-of-function mutation leads to cancer development, while tumor suppressor genes normally protects against cancer and are often inactivated in cancer by loss-of-function mutations. Mutations in the DNA maintenance genes result in genomic instability (Alberts et al. 2008; Hanahan & Weinberg 2000; Vogelstein & Kinzler 2004).

1.1.1 The hallmarks of cancer

In 2000, the following six changes in cell physiology were suggested by Hanahan and Weinberg to be essential for the development of a cancerous cell; self-sufficiency in growth signals, insensibility to growth-inhibitory signals, evasion of apoptosis, limitless replicative potential, sustained angiogenesis and tissue invasion and metastasis. All of these changes are driven by genomic instability and possibly tumor induced inflammation (Hanahan & Weinberg 2000) (Figure 1.1.1). In addition to these six hallmarks, evasion of immune destruction and reprogramming of energy metabolism have recently been suggested to also be essential for cancer development (Hanahan & Weinberg 2011).

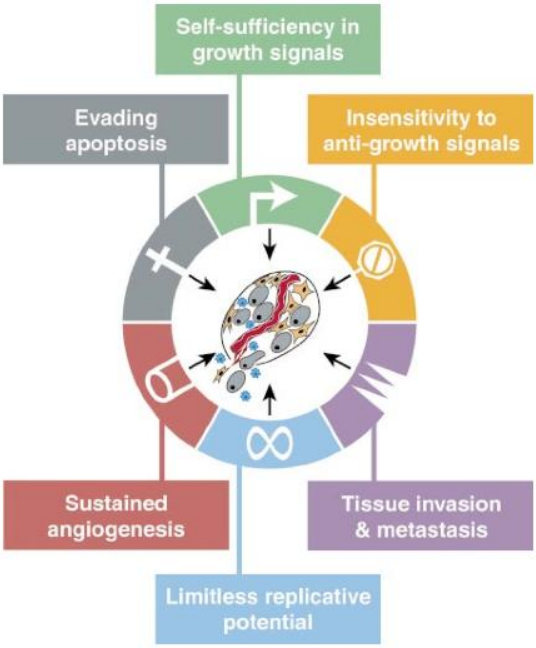

Figure 1.1.1. The six hallmarks of cancer. The six hallmarks of cancer proposed to be essential for growth of cancerous cells (Adapted from Hanahan and Weinberg 2002).

Self-sufficiency in growth signals and insensibility to growth-inhibitory signals

To maintain normal tissue homeostasis, both growth-stimulating and growth-inhibitory signalling molecules present in the extracellular environment control cell proliferation. These signals bind to and activate transmembrane receptors on the surface of cells. These receptors further activate intracellular signalling pathways, which eventually leads to a change in cell behaviour (Alberts et al. 2008). Cancer cells often gain the ability to grow independent of external growth signals by expressing their own growth factors (GF), such as platelet-derived growth factor (Henriksen et al. 1993). Furthermore, overexpression of transmembrane GF receptors, such as epidermal GF receptor, has been found in many cancer cells (Korc et al. 1986). Cancer cells have also been reported to have mutations in the downstream signalling molecules that transduce the growth signals further inside the cell (Bos 1989). Similarly, cancer cells often gain the ability to be unresponsive to anti-growth signals by altering the activity or expression of anti-growth receptors or downstream signalling molecules, such as transforming GF receptor β and the retinoblastoma protein (Iolascon et al. 2000; Zhang et al. 1994).

Evasion of apoptosis

Apoptosis is a normal process where the cell commits suicide by activating pathways leading to controlled death of the cell. During apoptosis the cell shrinks and condenses, the nuclear envelope dissolves, the nuclear chromatin is fragmented and the cytoskeleton collapses. In the end, the cell dissolves into small membrane-enclosed fragments called apoptotic bodies, which are phagocytized by neighbour cells, such as macrophages. This process is used to remove diseased or abnormal cells, but also to maintain normal tissue homeostasis (Kerr et al. 1972; Majno & Joris 1995; Rath & Aggarwal 1999). Cancer cells, however, gain the ability to evade this process (Hanahan & Weinberg 2000). Intracellular signalling pathways activated by stress stimuli, such as DNA damage, depend upon a functional p53 protein to transmit signals and elicit an apoptotic response, and this protein is thus often inactivated in cancer cells. In fact, mutations in the *TP53* gene are detected in more than 50% of all human cancers (Soussi & Beroud 2001). An inactive receptor resembling the FAS death receptor has also been found overexpressed in many lung and colon cancers. This receptor binds the Fas death ligand and thereby inhibits the ligand from binding to the true Fas death receptor, thus preventing apoptosis (Pitti et al. 1998).

Limitless replicative potential and sustained angiogenesis

The ends of the chromosomes, called telomeres, normally protect the chromosomal DNA from degradation and recombination, however they become shorter each time a cell divides. Eventually, this process results in termination of replication and cell death. Cancer cells gain limitless replicative potential often by overexpressing the telomerase enzyme, a protein that maintains the length of the telomeres (Blasco 2005). Furthermore, cancer cells demand increased supply of oxygen and nutrients to survive and grow into large tumors. This is achieved through formation of new blood vessels from pre-existing blood vessels, in a process called angiogenesis (Baeriswyl & Christofori 2009). Different pro- and anti-angiogenic signalling molecules regulate this process and cancer cells often gain sustained angiogenesis by overexpressing and/or downregulating these molecules (Bergers & Benjamin 2003). For example, increased expression of the pro-angiogenic molecule vascular endothelial GF (VEGF) has been demonstrated in pancreatic cancer cells (Itakura et al. 2000).

Tissue invasion and metastasis

At some point, certain cancer cells will detach from the primary tumor, invade the adjacent tissue and vessels, spread with the circulation to other parts of the body, leave the vessel and then form new, secondary tumors (metastases) at distant sites (Alberts et al. 2008; Bacac & Stamenkovic 2008). This complex process, called metastasis, is dependent on all the five physiological changes mentioned above and is involved in more than 90% of cancer-related deaths (Hanahan & Weinberg 2000). Tissue invasion and metastasis engage changes in the activity of molecules that facilitate cell-cell adhesion, such as the E-cadherin protein, which is inactivated in almost all developing human epithelial cancers (Christofori & Semb 1999). Furthermore, changes in expression of integrin proteins that adheres cells to the extracellular matrix (ECM) are observed in many types of cancer cells (Mizejewski 1999). Cancer cells have also been found to increase expression of proteinases that degrade the basement membrane and the ECM, such as matrix metalloproteinases (Coussens & Werb 1996).

Reprogramming of energy metabolism and evasion of immune destruction

Cells with a high proliferation rate must produce high amounts of macromolecules, such as proteins and nucleic acids, and at the same time produce energy in form of ATP. Cancer cells have been found to gain this ability by increasing the uptake of glucose and limiting their energy metabolism to glycolysis, which produces many intermediates used in the production of macromolecules (Jones & Thompson 2009). Based on these findings, reprogramming of energy metabolism is suggested to be an emerging hallmark of cancer. Furthermore, cells in the immune system normally monitor, detect and destroy newly developing cancer cells in the tissue environment. Thus, for normal cells to develop into large tumors they need to overcome this immune system barrier. Evasion of immune destruction is therefore suggested to be another emerging hallmark of cancer (Hanahan & Weinberg 2011).

1.2 Cell signalling

1.2.1 Apoptotic pathways

In vertebrates, there are two pathways that lead to apoptosis: the extrinsic pathway (death receptor pathway) and the intrinsic pathway (mitochondrial pathway) (Tait & Green 2010). The extrinsic pathway is activated when extracellular signalling molecules (ligands), such as tumor necrosis factor-α (TNF-α), bind to death receptors, like the TNF receptor 1 on the surface of cells (Kaufmann & Hengartner 2001) (Figure 1.2.1, right). The activation of death receptors results in recruitment of adaptor proteins and initiator procaspases- 8 or 10 to the plasma membrane, forming a death – inducing signalling complex (DISC). In the DISC, the initiator procaspases are autoactivated and then cleaves and activates executioner procaspase-3 that further triggers the apoptotic effects (Alberts et al. 2008; Lawen 2003). For example, caspase-3 has been shown to cleave and inactivate poly (ADP-ribose) polymerase (PARP), a protein involved in the DNA repair system (Decker et al. 2000; Nicholson et al. 1995). In addition to induction of apoptosis, ligand-dependent activation of certain death receptors may also lead to activation of other intracellular pathways that cause other types of effects. For example, binding of TNF-α to the TNF receptor 1 activates both apoptotic and anti-apoptotic pathways, such as the nuclear factor – κB (NF-κB) pathway (Rath & Aggarwal 1999).

The intrinsic apoptotic pathway can be activated inside the cell when exposed to stress such as low levels of oxygen and nutrients, or damage to the DNA (Figure 1.2.1 left). A family of proteins, called the Bcl-2 family, regulate the intrinsic pathway of apoptosis and consists of both anti- and pro-apoptotic proteins. When exposed to stress stimuli, the cell activates or generates pro-apoptotic proteins called BH3-only proteins. These proteins bind and inhibit anti-apoptotic Bcl-2 proteins, leading to activation and aggregation of pro-apoptotic BH123 proteins (Bax and Bak) in the outer mitochondrial membrane. Aggregation of the BH123 proteins leads to mitochondrial outer membrane permeabilization (MOMP) and release of cytochrome c (cyt c) and other proteins from the mitochondrial intermembrane space into the cytoplasm (Alberts et al. 2008; Tsujimoto 1998). In the cytoplasm, cyt c binds to and change conformation of an adaptor protein called Apaf1, which assemble into a large multi-protein complex called the apoptosome. In the apoptosome, the adaptor proteins recruit

initiator procaspases-9 to the apoptosome, which results in autoactivation of the procaspases-9, followed by activation of the executioner procaspases -3 and 7 (Kim, H. E. et al. 2005). Anti-inhibitors of apoptosis (anti-IAPs), such as SMAC and OMI, are proteins that also are released into the cytosol together with cyt c. These proteins promote apoptosis by binding to IAPs that normally inhibit activated executioner caspases. In some cells, the extrinsic pathway also activates the intrinsic pathway for proper amplification of the apoptotic signal and cell death. The BH3-only protein Bid is involved in this process (Tait & Green 2010).

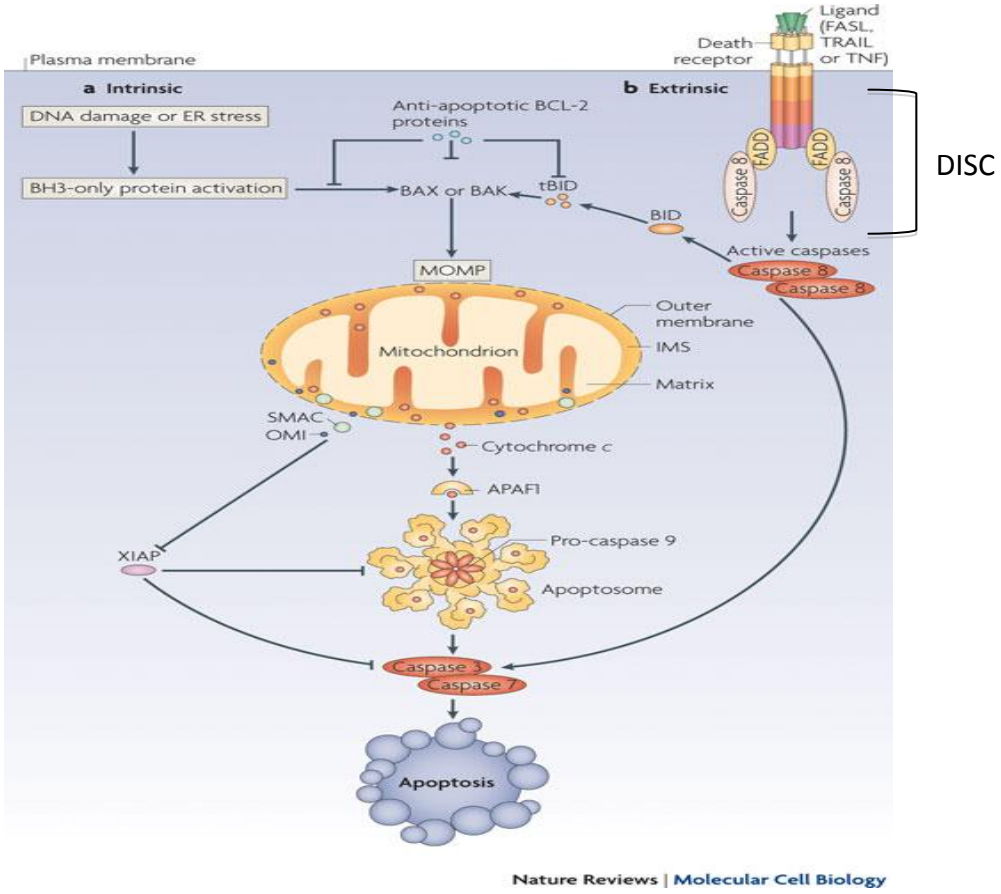

Figure 1.2.1. Induction of apoptosis. Induction of apoptosis trough the intrinsic (left) and the extrinsic (right) pathways (Modified from Tait & Green 2010).

1.2.2 PI3-Kinase-Akt pathway

The phosphoinositide-3 (PI3)-Kinase-Akt pathway is activated when cells are stimulated to grow and survive by extracellular signalling molecules, and is important in the development of many human tumors (Garcia-Echeverria & Sellers 2008). The extracellular signalling molecules, such as the epidermal GF, bind to transmembrane receptors, typically receptor tyrosine kinases leading to activation of the intracellular signalling protein PI3-Kinase (Figure 1.2.2) (Alberts et al. 2008). Active PI3-Kinase phosphorylates the phosphatidylinositol-4,5-bisphosphate (PIP2) to phosphatidyl-inositol-3,4,5-trisphosphate (PIP3), which leads to recruitment of Akt to the plasma membrane together with the phosphoinositide-dependent protein kinase 1 (PDK1) (Vara et al. 2004). At the plasma membrane, PDK1 and PDK2 (TORC2), phosphorylates and activates Akt, which then leaves the plasma membrane and phosphorylates its intracellular target proteins. One target protein is the pro-apoptotic BH3-only protein Bad that normally binds and inhibits Bcl-2 anti-apoptotic proteins in the cytoplasm. Bad is inactivated when phosphorylated by Akt, leading to the release and action of the Bcl-2 proteins that inhibit apoptosis (Cantley 2002).

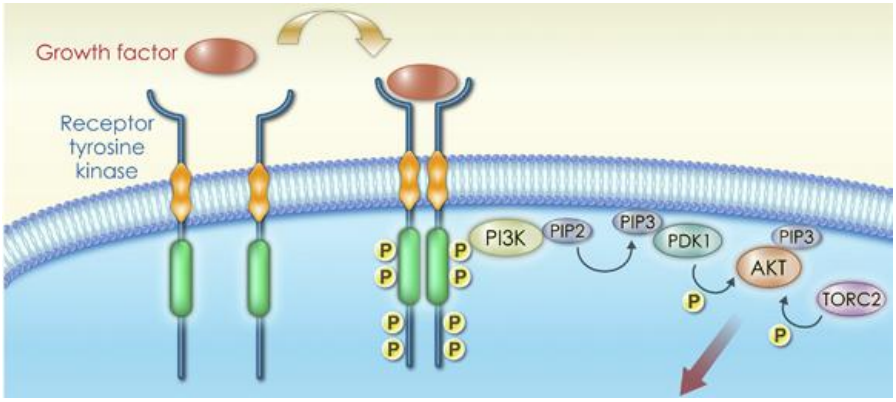

Figure 1.2.2. The PI3-Kinase-Akt pathway. A growth factor signalling molecule binds to a receptor tyrosine kinase receptor, leading to activation of PI3-Kinase, PIP3 formation and recruitment of PDK1 and Akt to the membrane. PDK1 and TORC2 then phosphorylates and activates Akt, which then leaves the membrane and acts on its target proteins (From Garcia-Echeverria and Sellers 2008).

1.3 Blood coagulation

Blood coagulation is the process where blood flow from an injured blood vessel is terminated when a blood clot is formed at the site of injury. Both coagulation activators and inhibitors regulate the blood coagulation process to avoid disruption of the normal blood flow (Gomez & McVey 2006).

1.3.1 The cell based model of tissue factor initiated blood coagulation

Upon vessel injury, factor VII (FVII) in the circulation is exposed to the transmembrane receptor tissue factor (TF) expressed by extravascular cells (Gomez & McVey 2006). Binding between TF and FVII initiates the blood coagulation and leads to the formation of TF-FVIIa complexes, which then activate factor IX (FIX) and factor X (FX) to FIXa and FXa, respectively. FXa cleaves and activates prothrombin to thrombin, however, only limited amounts of thrombin are generated because FXa only gains full activity after binding its activated cofactor factor Va (FVa). The small amounts of thrombin present are nevertheless capable of activating FV, in addition to factor VIII (FVIII) and factor XI (FXI), leading to formation of more thrombin in positive feedback loops. The FVIIIa-FIXa and FXa-FVa complexes then direct the generation of explosive amounts of thrombin, and thereby cleavage of fibrinogen to fibrin monomers (Figure 1.3.1). Moreover, thrombin also activates platelets, which release pro-coagulant factors and express phospholipids, thus providing negatively charged surfaces that the FVIIIa-FIXa and FXa-FVa complexes may bind to and form procoagulant complexes. Furthermore, activated platelets adhere and aggregate at the injured site, and together with polymerized fibrin establish a blood clot that reduces the blood flow (Gomez & McVey 2006; Smith 2009).

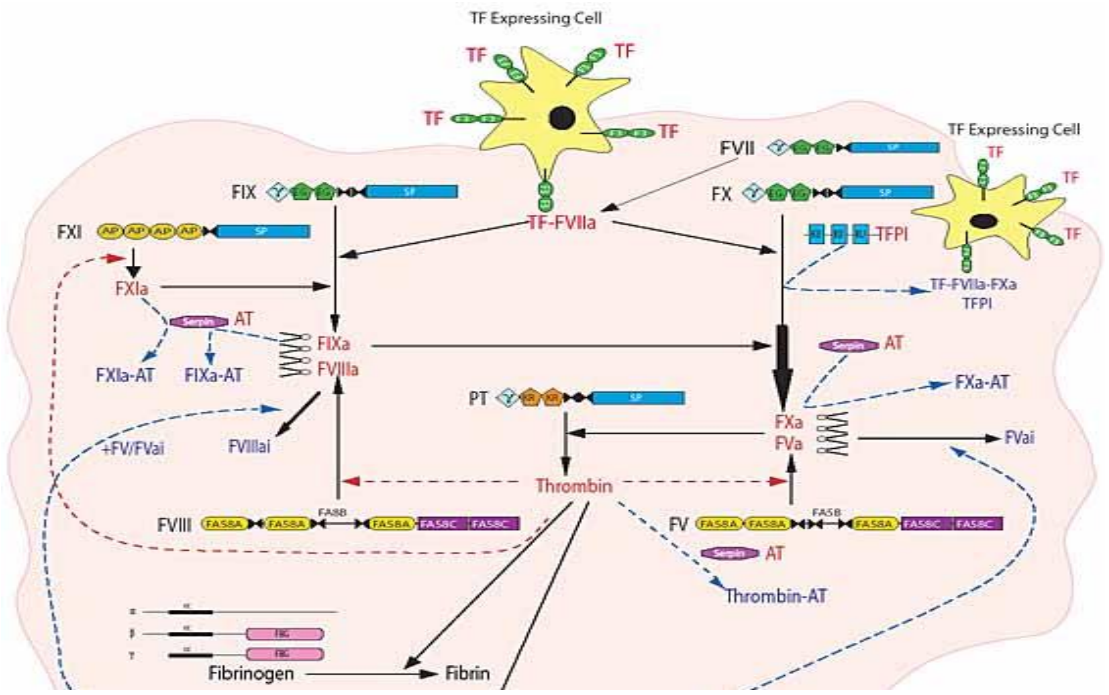

Figure 1.3.1 Tissue factor initiated blood coagulation. The pathway initiates when TF expressed at the surface of extravascular cells binds and activates FVII to FVIIa, which then further activates FX and FIX leading to formation of small amounts of thrombin. These small amounts result in activation of FV, FVIII and FXI, eventually leading to formation of explosive amounts of thrombin and a fibrin clot. (Modified from Gomez and McVey 2006).

1.3.2 Inhibitors of the coagulation pathway

Several inhibitors of the blood coagulation pathway exist to prevent uncontrolled thrombin formation, which may otherwise lead to development of thrombosis and other blood clotting disorders (Esmon 2000). The four known coagulation inhibitors have different targets in the coagulation pathway, and use different mechanisms (Spronk et al. 2003). Tissue factor pathway inhibitor (TFPI) binds and inhibits FXa and the TF-VIIa complex, and its activity is enhanced by protein S (Wood, J. P. et al. 2014) . Protein C is a plasma protein that is activated by a thrombin-thrombomodulin complex and the endothelial cell protein C receptor (Taylor et al. 2001), and together with its cofactor protein S cleaves and inactivates FVIIIa and FVa (Esmon 1989). Antithrombin binds and inactivates several protease enzymes in the coagulation pathway, such as thrombin, FIXa and Xa, and its activity is enhanced by heparin-like glycosaminoglycans at the surface of endothelial cells (Spronk et al. 2003).

1.3.3 Blood coagulation and cancer

The connection between blood coagulation and cancer is well established. A systematic study published in 2008 showed that 10% of patients diagnosed with VTE will develop cancer within 12 months (Carrier et al. 2008). Oppositely, cancer patients have a higher risk of developing VTE compared to healthy individuals. However, the risk varies for different types of cancer. The highest rates of VTE have been found in patients with pancreatic (8,1%), kidney (5,6%), ovary (5,6%), lung (5,1%) and stomach (4,9%) cancer, while breast cancer is among the types of cancer with the lowest rate of VTE (2,3%) (Khorana et al. 2007). In addition, patients with metastatic cancer are more prone to VTE than patients with localized cancer (Chew et al. 2006).

Tumor cells have been found to induce coagulation themselves by expressing high levels of procoagulant proteins like TF and cancer procoagulant, an activator of FX (Rickles et al. 2001; Shoji et al. 1998). The tumor cells also interact with host cells and manipulate them to induce blood coagulation, either by direct cell-cell contact via adhesion molecules or indirectly through secretion of cytokines, such as VEGF, interleukin-1β and TNF-α (Figure 1.3.3 left). Direct and indirect interaction between tumor cells and endothelial cells results in decreased expression of tissue-type plasminogen activator (t-PA), an activator of fibrinolysis, and increased expression of PA inhibitor -1 and TF by endothelial cells. Hence, the normally anti-coagulant endothelium is converted to a pro-coagulant endothelium. Furthermore, activated macrophages and monocytes have been observed to surround growing tumors. These tumor-associated cells also express high levels of TF on their surface, either induced by the tumor cells or by the tumor inflammatory response (Rickles & Falanga 2001; Shoji et al. 1998).

TF has been found in several studies to promote cancer cell growth, invasion, metastasis, adhesion and angiogenesis (Amarzguioui et al. 2006; Ott et al. 1998; Poon et al. 2003; Yu et al. 2005). Initiation of blood coagulation by TF results in the formation of thrombin and fibrin, which both have been found to indirectly induce angiogenesis by stimulating expression of interleukin-8 and VEGF. In addition, thrombin also promote cancer cell growth, adhesion, invasion and metastasis by binding and activating protease-activating-

receptor-1 (PAR-1) and by activating platelets (Figure 1.3.3 right) (Lima & Monteiro 2013; Mosesson 2005; Rickles & Falanga 2001; Wojtukiewicz et al. 1993; Wysoczynski et al. 2010). In addition to these effects, the TF-FVIIa complex mediates coagulation independent intracellular signalling and activation of PAR-2, which have been shown to induce cancer cell growth, invasion, and migration (Lima & Monteiro 2013; Ott et al. 2005; van den Berg et al. 2012).

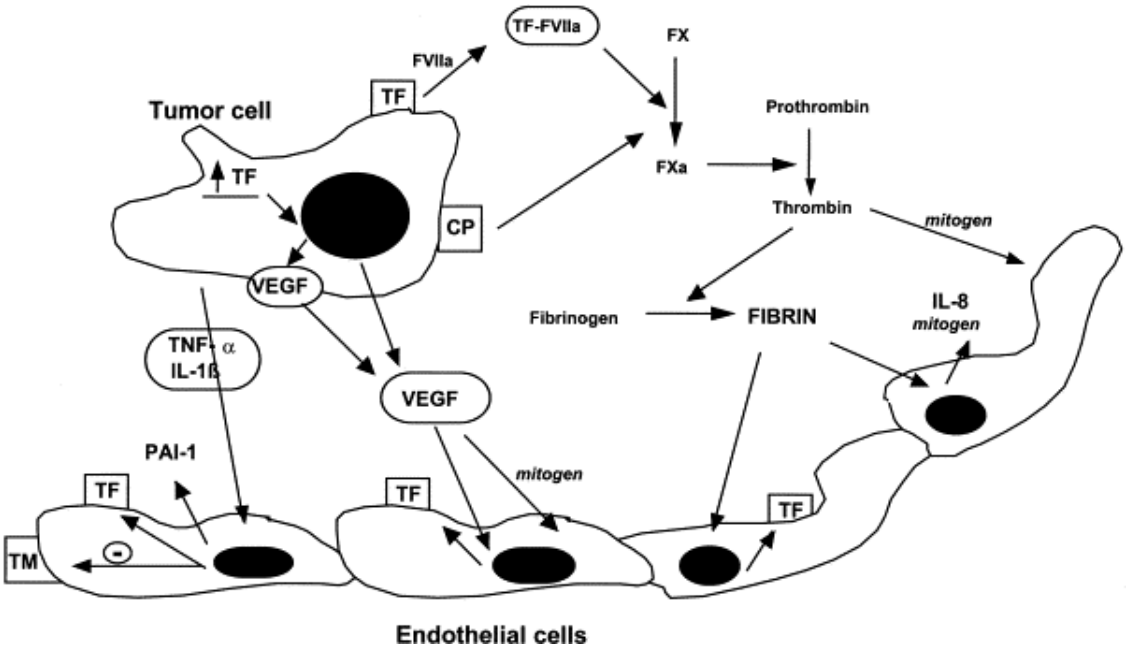

Figure 1.3.3. The connection between blood coagulation and cancer. Tumor cells express TF and cancer proagulant that induce blood coagulation. They also stimulate neighbouring cells to express TF and PA inhibitor-1 by secreting VEGF, TNF-α and interleukin-1β cytokines (left). This leads to formation of thrombin and fibrin, which further stimulates cancer cell growth, angiogenesis, adhesion, metastasis and invasion (right). (From Rickles and Falanga 2001).

1.4 Tissue Factor Pathway Inhibitor (TFPI)

1.4.1 Structure and biology

The human TFPI gene is located on chromosome 2, spans 90kb and consists of ten exons spaced with nine introns. Three isoforms of human TFPI, produced by alternative splicing, have been identified: TFPIα, TFPIβ and TFPIδ (Broze & Girard 2013) (Figure 1.4.1.1). The full length TFPIα isoform consists of a negatively charged N-terminal domain, a positively charged C-terminal domain and three sequential Kunitz-type inhibitor domains, each encoded by separate exons (Girard et al. 1991). TFPIβ consists of the same N-terminal and the first two Kunitz domains, but lacks the third Kunitz domain and has a different C-terminal domain compared to TFPIα (Chang et al. 1999). The sequence of the TFPIδ isoform is found in humans and chimpanzees and is listed in the NCBI GeneBank database. This sequence encodes the two first Kunitz domains, but has a unique C-terminal end with 12 amino acids. The TFPIδ isoform is not further characterized (Maroney et al. 2010).

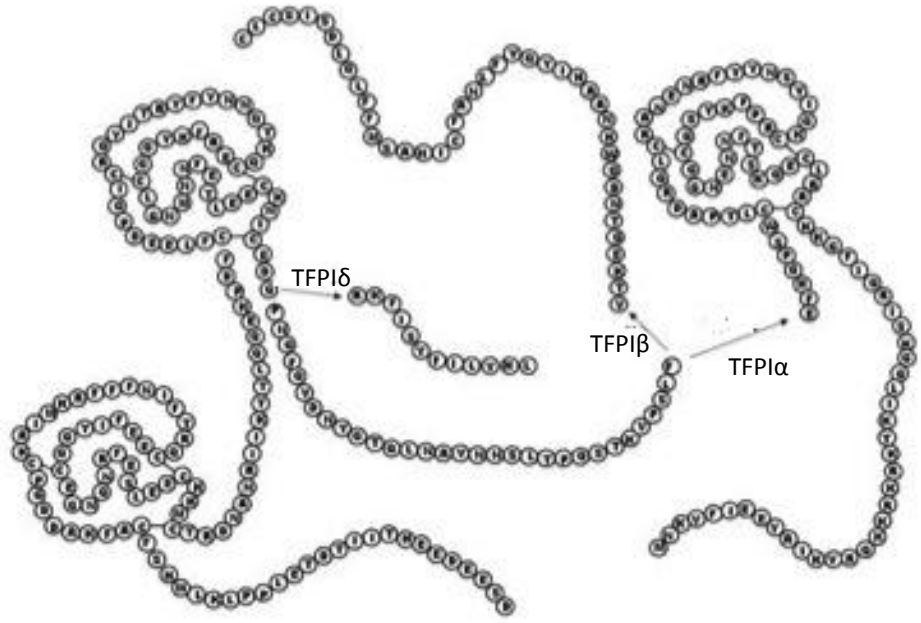

Figure 1.4.1.1. Protein structure of the alternatively spliced TFPI isoforms in humans. TFPIα consist of a N-terminal, C-terminal and three Kunitz domains in between. TFPIβ and TFPIδ lack the third Kunitz domain and have different C-terminals. (From Maroney et al. 2010).

Both TFPIα and TFPIβ have a N-terminal signal sequence that directs them into the endoplasmic reticulum (Maroney & Mast 2008), where they are post-translationally modified with the addition of O-linked and N-linked oligosaccharides (Piro & Broze 2005). In the endoplasmic reticulum, TFPIα is either indirectly bound to a glycosyl phosphatidylinositol (GPI) anchor with a co-receptor or stays soluble (Maroney et al. 2006). TFPIα binds to the co-receptor with its third Kunitz domain and the C-terminal end (Piro & Broze 2004) (Figure 1.4.1.2 left). TFPIβ is attached to the endoplasmic reticulum membrane by the GPI anchor, which binds to a GPI anchor attachment signal in the TFPIβ protein sequence (Maroney & Mast 2008; Zhang et al. 2003) (Figure 1.4.1.2 right). From the endoplasmic reticulum, the proteins are further transported via Golgi to the cell membrane, where soluble TFPIα is secreted and GPI-bound TFPIα and TFPIβ remains attached to the cell (Maroney et al. 2006; Mayor & Riezman 2004). Some TFPIα is also present in intracellular stores that are releasable by heparin (Stavik et al. 2013; Zhang et al. 2003).

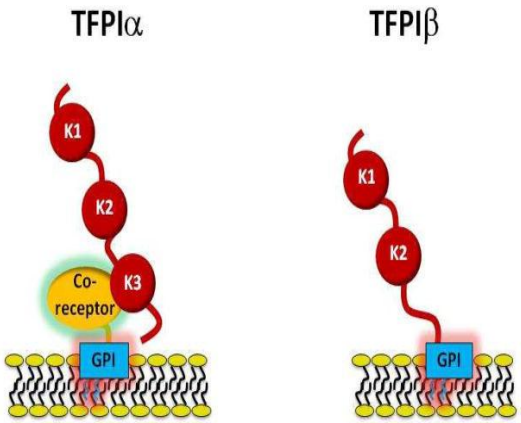

Figure 1.4.1.2. Binding of TFPI to the cell surface. TFPIα is attached to the cell surface indirectly through a GPI-linked co-receptor. TFPIβ is attached to the cell surface directly through a GPI anchor. (From Broze and Girard 2013).

The main source of TFPI in humans are endothelial cells and megakaryocytes (Bajaj et al. 1990). In plasma, the TFPIα isoform can be found in full length or as C-terminal truncated forms often bound to different lipoproteins, such as the low-density lipoproteins, via the third Kunitz domain (Broze et al. 1994). In human plasma, 10% of the total TFPI is free full length TFPIα, 10% is free C-terminal truncated TFPIα and 80% is C-terminal truncated TFPI bound to lipoproteins (Broze & Girard 2013).

1.4.2 TFPI and blood coagulation

As it name implies, TFPI is an inhibitor of TF induced blood coagulation. TFPI binds and inhibits both FXa and the TF-FVIIa complex, which are involved in the initiation phase of the coagulation cascade. TFPI inhibition of TF-FVIIa is dependent on factor FXa, and may either bind to a preformed FXa-TF-VIIa complex in a one step reaction or to FXa and then to TF-VIIa in a two-step reaction, both resulting in a quaternary inhibitory complex (Figure 1.4.2) (Wood, J. P. et al. 2014). TFPI binds to the TF-FVIIa complex with the first Kunitz domain and to FXa with the second Kunitz domain (Broze et al. 1990). In addition, optimal inhibition of FXa and TF-VIIa by TFPIα has been shown to involve all three Kunitz domains and the C-terminal end (Cunningham et al. 2002; Higuchi et al. 1992; Peraramelli et al. 2013; Wesselschmidt et al. 1992). Protein S has been found to enhance TFPIα inhibition of FXa, probably by localizing TFPIα to membrane surfaces (Hackeng et al. 2006; Ndonwi et al. 2010; Wood, Jeremy P et al. 2014). Furthermore, TFPIβ, which lacks the third Kunitz domain and the C-terminal end of TFPIα, has also been shown to inhibit both FXa and TF-FVIIa, and probably involves the GPI anchor (Piro & Broze 2005; Wood, J. P. et al. 2014).

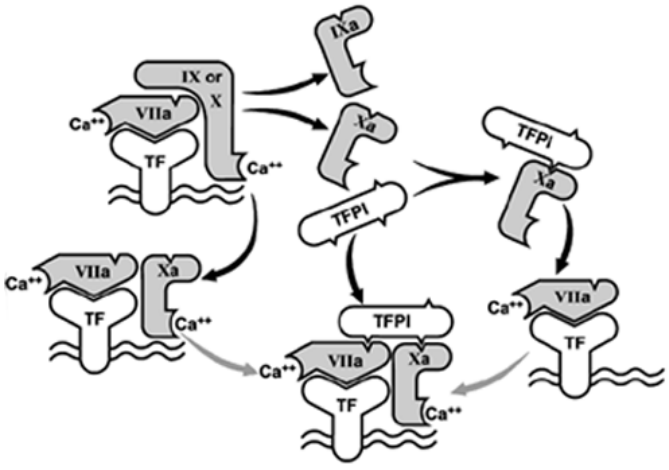

Figure 1.4.2. Inhibition of FXa and TF-VIIa by TFPI. Two models for TF-VIIa inhibition are proposed; 1) TFPI binds to a preformed FXa-FVIIa-TF complex (left) or 2) TFPI binds FXa and then the FVIIa-TF complex (right). TFPI binds to FXa with its second Kunitz domain and the FVIIa-TF complex with its first Kunitz domain. (From Broze 2003).

1.4.3. Non-hemostatic properties of TFPI

TFPI and cell growth

In 1997, the first report on an effect of TFPI on cell growth was discovered by Kamikubo and co-workers who observed that full length human recombinant TFPI (rTFPI) inhibited proliferation in human smooth muscle cells (SMCs). The effect was suggested to be dependent on the C-terminal end of TFPI, since no difference in proliferation was seen with human rTFPI lacking the C-terminal end (Kamikubo et al. 1997). Full length rTFPI has also been reported to inhibit proliferation in human umbilical vein endothelial cells (HUVECs). Both the C-terminal end and the third Kunitz domain were shown to be involved, but the effect was suggested to be independent of TF. However, the effect was not detectable in melanoma, lung carcinoma or rat glioma cells (Hembrough et al. 2001). Hembrough and co-workers supported these findings, as they observed that a C-terminal TFPI peptide inhibited endothelial cell proliferation, but not tumor cell proliferation (Hembrough et al. 2004). Other studies have reported that full length rTFPI inhibited proliferation in rat mesengial cells (MsCs) (Liang et al. 2009). Moreover, Stavik and co-workers showed that overexpression of TFPIα and TFPIβ reduced proliferation in the breast cancer cell line SK-BR-3, while downregulation of TFPI in SUM102 breast cancer cells had no observable effect on the cell proliferation (Stavik et al. 2010; Stavik et al. 2011).

TFPI and apoptosis

In 1998, Hamuro and co-workers made the first discovery of TFPI and its effect on apoptosis. They found that full length human rTFPI induced apoptosis in HUVECs. They also observed that abolition of the coagulation inhibitory effect of TFPI did not affect the apoptotic action, indicating that the apoptotic effect of TFPI is independent of its coagulation inhibitory effect (Hamuro et al. 1998). Furthermore, Lin and co-workers found that full length rTFPI induced apoptosis in cultured rat MsCs via the third Kunitz domain and the C-terminal end. The effect was shown to be independent of TF and mediated by inhibiting the PI3-Kinase-Akt pathway (Lin et al. 2007). Another study showed that overexpressed TFPI induced apoptosis in human vascular SMCs and involved proteins in both the extrinsic and intrinsic apoptotic pathway, such as caspase-8, caspase-9, caspase-3 and cyt c (Dong et al. 2011). Studies performed in rat vascular SMCs showed that virus mediated overexpression of human TFPI

induced apoptosis by inhibiting the JAK-2/STAT-3 pathway, which affected the expression of the downstream signalling molecules, such as the anti-apoptotic protein Bcl-2 and the cell cycle promoter protein cyclin-D1 (Fu et al. 2012). In 2010, Stavik and co-workers made the first report on TFPI-induced apoptosis in breast cancer cells as they observed that overexpression of TFPIα or TFPIβ increased apoptosis, while downregulation of TFPI decreased apoptosis. Many proteins were found to be involved, such as the death receptor ligand TNF-α and the NF-κB protein. Moreover, overexpression of TFPI (α+β) and TFPIα resulted in increased expression of TF and PAR-1/2 indicating that TF signalling may have a role in TFPI mediated apoptosis in breast cancer cells (Stavik et al. 2010). In hamster ovary cancer cells, TFPI has been shown to induce apoptosis, as demonstrated by activation of the NF-κB pathway and increased PARP cleavage. The effect was independent of caspase-3 (Skretting et al. 2012).

TFPI and cancer development

Patients with solid tumors have been reported to express higher levels of plasma TFPI and to have higher TFPI activity than healthy individuals (Iversen et al. 1998). In addition, both TFPIα and TFPIβ have been found expressed in different breast cancer cells, with TFPIα representing the most dominant isoform (Stavik et al. 2013). Furthermore, a study from 2002 showed that full length TFPI injected into mice reduced lung metastasis (Amirkhosravi et al. 2002). Hembrough and co-workers reported that full length human r-TFPI inhibited both primary and metastatic growth in mice, independent of the hemostatic system (Hembrough et al. 2003). Another study showed that a C-terminal TFPI peptide inhibited angiogenesis both in endothelial cells and *in vivo* in mice (Hembrough et al. 2004). Moreover, Di and co-workers reported that full length rTFPI inhibited migration of human gastric cancer cells (Di et al. 2010). Furthermore, a study by Stavik *et al.* showed that downregulation of total TFPI (α+β) or TFPIβ in breast cancer cells induced cancer cell adhesion, migration and invasion (Stavik et al. 2011). In addition, breast cancer cells with high endogenous TFPI expression have shown to form tumors with reduced sizes compared to cells with either downregulated total TFPI (α+β) or TFPIβ (Tinholt et al. 2012). All the above mentioned studies indicate that TFPI plays a role in cancer development.

1.5 Knock down and overexpression models

1.5.1 Knock down of target genes using RNA interference (RNAi)

RNA interference (RNAi) is a process where short RNA molecules inhibit gene expression in a sequence specific manner (Agrawal et al. 2003). The process is induced in cells by the presence of large double stranded RNA (dsRNA) molecules of various origins. Such large dsRNA molecules attract an RNAse called Dicer that cleaves the dsRNA molecules into shorter dsRNA molecules of 21-23 nucleotides (nt) (Figure 1.5.1 right). These are called small interfering RNAs (siRNAs) (Carthew & Sontheimer 2009; Watson et al. 2008; Wilson & Doudna 2013). The siRNAs associate with a ribonuclease protein from the family of Argonaute and other proteins to form a ribonucleoprotein complex, called RNA-induced silencing complex (RISC) (Wilson & Doudna 2013). In the RISC, one of the siRNA strands are removed (the passenger strand), while the other strand (the guide strand) directs the RISC to complementary messenger RNA (mRNA) transcripts (Watson et al. 2008). Argounaute in the RISC then cleaves the complementary mRNA with its endonuclease activity (Agrawal et al. 2003; Dominska & Dykxhoorn 2010)

Researchers have, since RNAi was discovered, exploited this process to study gene function (Agrawal et al. 2003). The most common method is to transfect cells with synthetic 21nt siRNAs that are complementary to target mRNA transcripts, and later analyse the effects of the inhibition of gene expression. These siRNAs are rapidly degraded in cells and such transfection is thus called transient transfection (Rao et al. 2009). An alternative method is to transfect cells with plasmid vectors cloned with DNA inserts that are transcribed into short hairpin RNAs (shRNAs). The transcribed shRNA are recognized and cleaved by Dicer in the cytoplasm to produce the shorter siRNA molecules (Sui et al. 2002; Watson et al. 2008). The shRNA plasmids may integrate into the host cell genome and are thus often used to make stable cell lines which continuously downregulates the target gene. Stable cell lines are made by transiently transfecting cells with an shRNA plasmid containing an antibiotic resistance gene and then further use the appropriate antibiotic to select cells with integrated plasmid in their genome (Recillas-Targa 2006; Taxman et al. 2010).

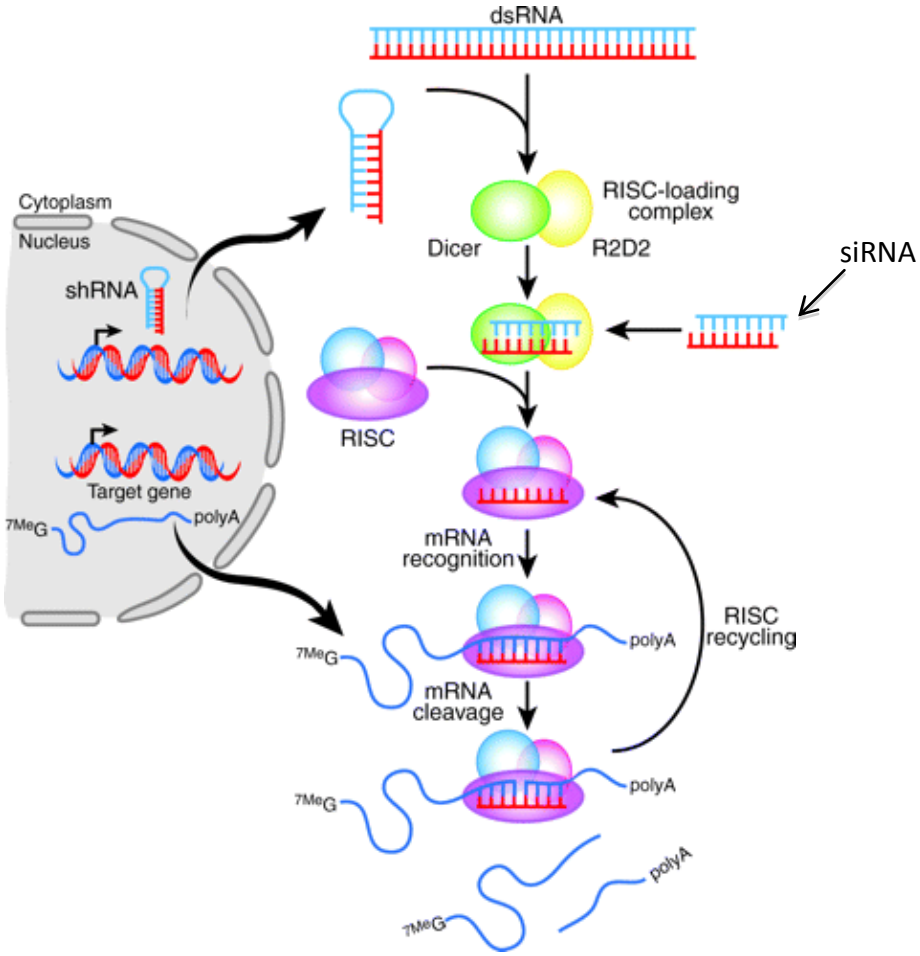

Figure 1.5.1 RNA interference. Large dsRNA or shRNA molecules, transcribed from plasmids in the nucleus, are cleaved by Dicer into the smaller siRNA molecules. These siRNAs associate with proteins to form the RISC, where the passenger strand of the siRNAs is removed and the guide strand directs the RISC to complementary mRNA transcripts. Argounate in the RISC then cleaves the mRNA. (Modified from Dominska & Dykxhoorn 2010).

1.5.2 Overexpression of target genes in eukaryotic cells using expression vectors

Overexpression of target genes with expression vectors, usually plasmids, is another method used to assess gene functions in eukaryotic cells. The complementary DNA (cDNA) of the target genes is cloned into the plasmid vectors, before transfected into eukaryotic cells. The target gene is then transcribed and translated to produce high amounts of protein (Watson et al. 2008). In similar with shRNA plasmids, these plasmids can also integrate into the host genome and be used to make stable cell lines that continuously overexpress the target gene (Recillas-Targa 2006).

In this thesis, four plasmid expression constructs were used; TFPIα plasmid, TFPIβ plasmid, empty vector control plasmid and a pMAX green fluorescent protein (GFP) plasmid. TFPIα and TFPIβ cDNA inserts have in previous experiments been cloned into the pcDNA3.1/V5-His-TOPO vector (Figure 1.5.2) (Stavik et al. 2010). This vector contains a constitutive CMV promoter upstream of the cDNA insert that ensures high expression of the cloned genes (TFPI in this thesis) in eukaryotic cells. In addition, the vector contains two antibiotic resistance genes; *ampR* and *neoR*. The ampicillin resistance gene can be used for selection of transformed prokaryotic cells, while the neomycin resistance gene can be used for selecting stable eukaryotic cells. The GFP plasmid expresses a green fluorescent protein when transfected into eukaryote cells, which can be detected and visualized using UV-light. The GFP plasmid was used in this thesis to optimize plasmid transfection in the HCC1500 cells because negligible research had been done with these cells.

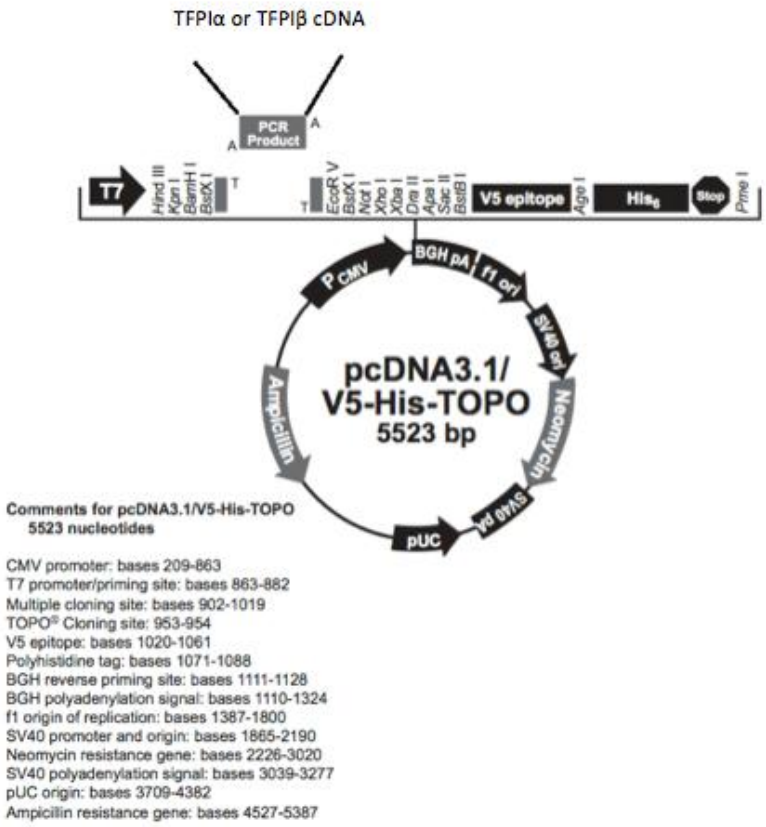

Figure 1.5.2 The pcDNA3.1/V5-His-TOPO vector. Schematic map of the pcDNA3.1/V5-His-TOPO vector. The position of the TFPIα and TFPIβ cDNA inserts are indicated. (Modified from: http://www.lifetechnologies.com/order/catalog/product/K480001).

1.6 Breast cancer

Breast cancer is the most frequent cancer in women (25% of all cancers) and the second most frequent cancer after lung cancer when both genders are considered. In fact, 1,7 million new incidents were reported worldwide in 2012 (Ferlay et al. 2012). Although the incidence of breast cancer is high, the survival rate is also among the highest of all cancers. Developing countries have higher survival rates than developing countries, much due to early detection with screening programmes and better treatment facilities (Parkin et al. 2005).

Breast cancer represents a heterogeneous group of tumors, with both intertumor and intratumor phenotypic diversity. Breast tumors are often classified into different subtypes based on their gene expression profiles. Five different subtypes of breast cancers are known today: luminal-A, luminal-B, basal-like, human epidermal growth factor receptor 2 (HER2) and normal-like. Different subtypes of breast cancer are treated with different strategies, and are associated with different survival rates (Polyak 2011). The basal-like subtype has been found to have the lowest survival rate (Perou et al. 2000; Sørlie et al. 2001). In addition, the tumors are often classified based on the expression of estrogen receptor (ER), progesterone receptor (PR) and HER2. Tumors that do not express either of these receptors are classified as triple negative (Rao et al. 2014). Furthermore, the cancer cells within the same tumor often show differences related to invasiveness, metastasis, angiogenesis, motility, proliferation and metabolism. This intra-tumor heterogeneity may be caused by differences in genomic instability and/or the differentiation of cancer stem cells (Marusyk & Polyak 2010).

1.6.1 Selected breast cancer cells

Breast cancer cell lines were selected as experimental cell models in this thesis because the research group already was using these cells, in addition to studying the connection between cancer and hemostasis at the genetic-, transcriptional and translational level in breast cancer patients (OsloII).

The SUM102 and HCC1500 breast cancer cell lines were used in this study, in addition to the HEK293T human endothelial kidney cell line (their suppliers are listed in under Materials in section 2.4). The HEK293T cell line was used for siRNA screening experiments because this cell line is easy to work with and easily transfected. The SUM102 breast cancer cell line had previously been used in the research group and was known to have high TFPI expression. Therefore, the SUM102 cells were used to downregulate TFPIα or TFPIβ in this thesis. This cell line was derived from an invasive ductal carcinoma and was characterized as basal-B, triple negative and *TP53* wild type (Kao et al. 2009). The characteristics of the breast cancer cell lines used in this thesis are listed in Table 1.6.2. The HCC1550 breast cancer cell line was used to upregulate TFPIα or TFPIβ in this thesis. This cell line was selected after searching for a candidate breast cancer cell line with low TFPI expression, but otherwise identical characteristica as SUM102 regarding subtype, hormone receptor status and *TP53* mutational status. In 2006, Neve *et al.* conducted a gene expression study of 51 breast cancer cell lines where the HCC1500 cell line was classified as triple negative and basal-B (Neve et al. 2006). This cell line was further shown in the Gobo (*GOBO*) and IARC TP53 databases (*IARC TP53 Database*) to have low TFPI expression and to be *TP53* wild type, respectively, and was thus concluded to be a good candidate cell line.

Table 1.6.1 Characteristica of the breast cancer cell lines SUM102 and HCC1500.

Cell line	**Subtype**	**Tumor type**	**Hormone receptor status***	***TP53* mutational status**	**TFPI expression**
SUM102	Basal-B	Invasive ductal carcinoma	Triple negative	Wild type	High
HCC1500	Basal-B	Ductal carcinoma	Triple negative	Wild type	Low

*Expression status of progesterone receptor, estrogen receptor and HER-2.

1.7 Aims of the thesis

Several studies have indicated that TFPI has a role in cancer biology. More knowledge of the effects of TFPI on cancer development and the molecular mechanisms involved, could potentially give rise to new cancer treatment strategies. The effects of downregulated total TFPI (α+β) and only TFPIβ on different aspects of breast cancer cell development have been analysed in the research group previously. However, until now, downregulation of only the TFPIα isoform had not yet been accomplished. In order to investigate the separate effects of TFPIα and TFPIβ on cancer cell development and to investigate some of the molecular mechanisms behind these effects, the following specific aims to be addressed in this thesis were:

1. To select siRNA oligonucleotides that efficiently knock down only the TFPIα isoform
2. To use the selected TFPIα specific siRNAs, and already in-house TFPIβ specific siRNAs to knock down TFPIα and TFPIβ, separately, in triple negative and *TP53* wild type breast cancer cells
3. To overexpress TFPIα and TFPIβ with plasmid constructs in triple negative and *TP53* wild type breast cancer cells
4. To analyse the effect of knock down and overexpression of TFPIα or TFPIβ on cell growth and induction of apoptosis in the breast cancer cells
5. To study some molecular mechanisms responsible for the effect of TFPIα and TFPIβ on apoptosis in the breast cancer cells

2. Materials

2.1 Reagents and chemicals

Table 2.1 Reagents and chemicals.

Reagent/chemical	Supplier	Catalogue number
2-mercaptoethanol	Merck, Darmstadt, Germany	8.05740.0250
2-propanol	Merck, Darmstadt, Germany	1.09634.2500
Albumine, from Bovine Serum (BSA)	Sigma- Aldrich, St.louis, USA	A7906-1006
Bluejuice TM Gel Loading Buffer 10X	Invitrogen, Carlsbad, CA, USA	10816015
Bovine Pituitary Extract	Invitrogen, Carlsbad, CA, USA	13028-014
Bromphenolblue 2%	Sigma-Aldrich, St.louis, USA	B0126
Dimethyl Sulphoxide (DMSO) Hybri-Max®	Sigma-Aldrich, St.louis, USA	D260
Dithiotreitol (DTT) 1M	Thermo Scientific, Rockford, USA	R0861
DMEM	Lonza, Verviers, Belgium	BE12-604F
Dulbecco`s PBS (1X)	PAA, GmbH, Pasching, Austria	H15-002
FastDigest® Bstx1 restriction enzyme	Fermentas, Vilnius, Lithuania	FD1024
FastDigest ® buffer 10X	Fermentas, Vilnius, Lithuania	B64
Fetal Bovine Serum Gold (FBS)	PAA, Pasching, Austria	A15-151
GelRed Nucleic Acid Gel Stain in water	VWR, Oslo, Norway	730-2958
GeneRuler 1Kb DNA ladder	Fermentas, Vilnius, Lithuania	5M0311
Geneticin G-418 Sulphate	Gibco, Auckland, New Zealand	11811-031
Glycerol 99%	Sigma-Aldrich, St.louis, USA	G5516
Glycine	Biorad, CA, USA	161-0718
Hydrochloric acid, 37% A.C.S reagent	Sigma-Aldrich, St.louis, USA	25814-8
HuMEC basal free Medium	Invitrogen, Carlsbad, CA, USA	12753-018
HuMEC supplements	Invitrogen, Carlsbad, CA, USA	12754-06
Lipofectamine® 2000 Reagent	Invitrogen, Carlsbad, CA, USA	11668-019
Magermilchpulver	Applichem GmbH, Darmstadt, Germany	A0830
Methanol	Merck, Darmstadt, Germany	I671909313
OPTI-MEM® Reduced Serum Medium	Invitrogen, Carlsbad, CA, USA	31985-062
Phenylmethanesulfonylflouride (PMSF)	Sigma-Aldrich, St.louis, USA	A6279
Phosphatase Inhibitor Cocktail 2 (PIC2)	Sigma-Aldrich, St.louis, USA	P5726
pMAX GFP ®	Lonza, Verviers, Belgium	VDF-1012

Precision Plus Protein™ Dual Color Standards	BioRad, CA, USA	161-0734
Reagent A100	ChemoMetec A/S, Allerød, Denmark	910-0003
Reagent B	ChemoMetec A/S, Allerød, Denmark	910-0002
RIPA buffer	Sigma-Aldrich, St.louis, USA	R0278
RPMI 1640	Lonza, Vervieres, Belgium	BE12702F
SDS	BioRad, CA, USA	161-0301
SeaKem® LE Agarose	Lonza, Rockland, USA	5004
S.O.C Medium	Invitrogen, Carlsbad, CA, USA	15544-034
Sodium Chloride	Merck, Darmstadt, Germany	1.06404.5000
Sodium deodyl sulphate (SDS) 10%	Biorad, CA, USA	147268S
Sulphuric-acid, 95-98%, A.C.S Reagent	Sigma-Aldrich, St.louis, USA	25810-5
TaqMan (R) Gene Expression Master Mix	Applied Biosystems, CA, USA	4369016
TBE Electrophoresis buffer 10X	Fermentas, Vilnius, Lithuania	B52
TransIT-X2 Dynamic Delivery System	Mirus Bio LLC, Wisconsin, USA	MIR6025
Transit®-2020 Transfection Reagent	Mirus Bio LLC, Wisconsin, USA	MIR5400
Trizma® base	Sigma-Aldrich, St.louis, USA	TI503
Trypan Blue Stain 0,4%	Invitrogen, Carslbad, CA, USA	T10282
Trypsin EDTA	Lonza, Vervieres, Belgium	BE17-002
TWEEN® 20	Sigma-Aldrich, St.louis, USA	PI379
Versene (EDTA)	Lonza, Verviers, Belgium	BE17-711E

2.2 Kits

Table 2.2 Kits

Kit	Supplier	Catalogue number
Amersham ECL prime kit	GE health care, Buckinghampshire, UK	RPN2232
Asserachrom® TOTAL TFPI Kit	Diagnistica Stago, Asneries, France	00261
BigDye Terminator v.3.1 Cycle Sequencing Kit	Applied Biosystems, CA, USA	4337465
Cell death detection ELISA plus	Roche Applied Science, IN, USA	11774425001
EndoFree® plasmid Giga Kit (5)	QIAGEN, Valencia, CA, USA	12391
High Capacity cDNA revers transcription kit	Applied Biosystems, CA, USA	4368813
PIERCE® BCA Protein Assay Kit	Thermo Scientific, Rockford, USA	23227
RNAaqueous® Phenol Free Total RNA Isolation Kit	Invitrogen, Carlsbad, CA, USA	AM1912
TNF-α human ELISA	Demeditec Diagnostics GmbH, Kiel, USA	DE75111

2.3 Instruments and equipment

Table 2.3 Instruments and equipment.

Instrument/equipment	Supplier
ABI 3730 DNA Analyzer	Applied Biosystems
ABI PRISM 7900HT Sequence Detection System (SDS)	Applied Biosystems
Benchmark Microplate Reader	BioRad
Countess Automated Cell Counter	Invitrogen
Countess Cell Counting Chamber Slides	Invitrogen
Image quant LAS 4000	GE health care
Laminar Floow Hood (LFH)	Kojair Tech Oy
Mini-protean® TGX gels	BioRad
NanoDrop® ND-1000 Spectrophotometer	NanoDrop Technologies
Nikon Eclipse TE 300 microscope	Nikon
NucleoCasette	ChemoMetec A/S
NucleoCounter NC-100	ChemoMetec A/S
Nunc™ Cell Culture Treated Flasks with Filter Caps (25cm^2, 75cm^2, 175cm^2)	Thermo Scientific

Nunc™ Cell-Culture Treated Multidishes (6-well and 12-well)	Thermo Scientific
Omega Lum G Imaging System	Aplegen
Precise Tris-glycine gels 10%	Thermo Scientific
Protran Nitrocellulose Transfer Membrane	Whatman GmbH
Steri-Cycle CO_2 incubator	Thermo Scientific
Thermal Cycler 2720	Applied Biosystems

2.4 Cells

Table 2.4 Cells

Cell type	**Supplier**	**Catalogue number**
One Shot® TOP10 Chemically Competent Cells, *E.coli*	Invitrogen, Carlsbad, CA, USA	C4040-03
HCC1500	American Type Culture Collection (//www.atcc.org/)	CRL-2329
SUM102	University of Michigan, USA (//www.cancer.med.umich.edu/breast_cell/Production/index.html)	
HEK293T	American Type Culture Collection (//www.atcc.org/)	CRL-3216

2.5 Antibodies

Table 2.5.1 Primary and secondary antibodies for western blotting

	Antibody	Supplier	Catalogue number	Dilution
Primary antibodies	PARP antibody, Rabbit	Cell signalling	9542	1:500
	Actin, Goat IGg	Santa Cruz Biotechnology	SC-1616	1:1000
	Caspase-8, Rabbit IGg	Cell signalling	4790	1:1000
	Anti α-Tubulin, Mouse IGg	Sigma Aldrich	T5168	1:1000
	Phospho-Akt (PI3 Kinase), Rabbit	Cell signalling	9271	1:1000
Secondary antibodies	Polyclonal Rabbit Anti-Goat Immunoglobin /HRP	DAKO	P0449	1:10000
	Polyclonal Goat Anti- Rabbit Immunoglobin /HRP	DAKO	P0448	1:1000
	Polyclonal Goat Anti-Mouse Immunoglobin /HRP	DAKO	P0447	1:1000

Table 2.5.2. Blocking antibodies and inhibitors

Antibody/inhibitor	Target	Supplier	Catalogue number
LY294002	Akt	Cell signalling	9901
PD98059	NF-κB	Cell signalling	9900
PAR-2 Antibody (SAM11)	PAR-2	Santa Cruz Biotechnology	SC-13504
Anti-human Tissue Factor Antibody, IGg1	TF	American Diagnostica	ADG4509
Human TNF –α Antibody, Mouse IGg1 (Clone 28401)	TNF-α	R&D Systems	MAB610
Negative Control, Mouse IGg1	-	DAKO	X0931

2.6 TaqMan assays

Table 2.6 TaqMan assays

Assay	Primer/ probe*	Sequence 5´-3´
PMM1 assay	PMM1-Forward primer	CCGGCTCGCCAGAAAATT
	PMM1-Reverse primer	CGATCTGCACTCTACTTCGTAGCT
	PMM1-Probe	ACCCTGAGGTGGCCGCCTTCC
TFPIα assay	TFPIα-Forward primer	AAGAATGTCTGAGGGCATGTAAA
	TFPIα-Reverse primer	CTGCTTCTTTCTTTTTCTTTTGGTTT
	TFPIα-Probe	AGGGTTTCAAAAGAATATCAAAAGGAGGCC
TFPIβ assay	TFPIβ-Forward primer	CAAGGTTCCCAGCCTTTTTGT
	TFPIβ-Reverse primer	CAAAGGCATCACGTATACATATA
	TFPIβ-Probe	TCCAACCATCATTTGTTCCTTCTTTTGT
Total TFPI assay	Total TFPI-Forward primer	ACACACAATTATCACAGATACGGAGTT
	Total TFPI-Reverse primer	GCCATCATCCGCCTTGAA
	Total TFPI-Probe	CCACCACTGAAACTTATGCATTCATTTTGTGC

*Each primer and probe obtained from Eurogentec

2.7 Sequencing primers

Table 2.7 Sequencing primers

Primer	Supplier	Sequence 5´- 3´
T7 primer (forward)	Invitrogen, Carlsbad, CA, USA	TAATACGACTCACTATAGGG
BGH Reverse primer	Invitrogen, Carlsbad, CA, USA	TAGAAGGCACAGTCGAGG

2.8 siRNA oligonucleotides

Table 2.8 siRNA oligonucleotides

siRNA	**Supplier**	**Sense 5 ´- 3´**	**mRNA target position (Accession no: NM_006287(α), NM_001032281 (β))**
1A	Eurogentec	CAGAUUCUACUACAAUUCAtt	692-710
2A	Eurogentec	AUAUUCUUUGGAUGAAACCtt	807-825
3A	Eurofins	GAGAACAGAUUCUACUACAAUUCAGUC	688-714
4A	Eurofins	AGAACAGAUUCUACUACAAUUCAGUC	689-715
5A	Eurofins	CAGAUUCUACUACAAUUCAGUCAUUGG	693-719
6A	Eurofins	CCAAUGAGAACAGAUUCUACUACAAUU	683-709
7B	Dharmacon	GGAAGAAUGCGGCUCAUAUUU	655-675
9B	Dharmacon	GAAGAAUGCGGCUCAUAUUUU	656-676
Silencer® NegativeControl siRNA #5	Ambion, AM4642		

2.10 Solutions

Loading buffer (Western blot):

1,5mL Trizma base

6,0mL 10% SDS

1,0mL 2% Bromphenolblue

1,5mL 99% Glycerol

1/10 1M DTT

10X Running buffer (Western blot):

30g Trizma base

144g Glycine

10g 10% SDS

MilliQ water to 1L (pH 8,3)

Tris Glycine buffer (Western blot):

3g Trizma base

14,4g Glycine

800mL MilliQ water

200mL Methanol

10X Tris-Buffered Saline (TBS) buffer (Western blot):

24,23g Trizma

80,06g Sodium Chloride

MilliQ water to 1L (pH 7,6)

1X TBS with Tween (TBS-T) buffer (Western blot):

100mL 10X TBS buffer

900mL MilliQ water

1mL TWEEN

5% Bovine serum albumin (BSA) (Western blot):

5g Albumin, from bovine serum

100mL TBS

Stripping solution (Western Blot):

7,57g Trizma

20g SDS

MilliQ water to 1L (pH 6,8)

→ Autoclaved

Secondary antibody solution:

4,8mL 1X TBS-T

200µL 5% Magermilchpulver in TBS-T

Antibody

1,5% agarose gel

0,75g SeaKem® LE Agarose

50mL 1X TBE electrophoresis buffer

5µl GelRed

RIPA lysis buffer with inhibitors.

1mL RIPA buffer

2µL Apronitin

10µL Phosphatase Inhibitor Cocktail 2

6µL 100µM PMSF

3. Methods

3.1 Microbiological techniques

3.1.1 Transformation of competent *Escherichia coli (E.coli)*

One Shot®TOP10 Chemical Competent *Escherichia coli (E.coli)* bacterial cells were transformed with TFPIα and TFPIβ plasmids and an empty vector plasmid (described in section 1.5.2), according to the manufacturer's protocol. The chemically competent cells have been treated with calcium chloride that promotes DNA plasmid binding to the cell membrane, and the plasmids enters the cell when pores in the membrane opens up after heat shock. In short, the *E.coli* cells were mixed with the plasmid (1µg), heat shocked and incubated in SOC-medium, before the cell suspensions were spread (10µL) on LB agar plates with 100µg/mL ampicillin and incubated over night.

3.1.2 Cultivation of transformed *E.coli*

The following day, transformed *E.*coli cells were cultivated to amplify the amount of plasmid before isolation. Single colonies were picked from each plate and pre-cultured in separate tubes with 8mL LB medium with ampicillin (100µg/mL) for six hours (37 °C and 300 rpm). The cell suspension with the most sufficient growth was transferred to 2,5L LB medium with ampicillin and further cultured for 16 hours (37 °C and 210 rpm).

3.2 DNA and RNA techniques

3.2.1 Nucleic acid isolation and quantification

Plasmid DNA isolation from transformed E.coli

TFPIα and TFPIβ plasmid DNA were isolated from the transformed *E.coli* cultures using the EndoFree® plasmid Giga Kit, according to the manufacturer's protocol. In short, the transformed and cultivated cells were harvested, resuspended and lysed, and lysate supernatant with plasmid DNA was filtered out from precipitated genomic DNA, proteins and cell debris. Contaminants in the supernatant were washed out with a DNA binding

column, before the plasmid DNA was eluted, precipitated with 2-propanol, washed with 70% ethanol and resuspended in TE buffer. The isolated plasmids were stored at -20°C.

Total RNA isolation

Total RNA was isolated from cell lysates using the RNAaqueous® Phenol Free Total RNA Isolation kit, according to the manufacturer`s protocol. In short, the cell lysates were diluted with 64% ethanol buffer and drawn through RNA binding filters (centrifuging for 30 sec at 13 000 rpm), and contaminants were washed out in three consecutive washing steps. The tubes were then centrifuged to remove traces of washing solution and RNA was eluted twice with Elution Solution. The isolated RNA samples were stored at -80˚C.

RNA and DNA quantification

Isolated RNA and DNA were quantified using a NanoDrop® ND-1000 Spectrophotometer, according to the manufacturer's instructions. Nucleic acids absorb UV light at 260nm, while proteins absorb at 280nm. The RNA and DNA concentrations were therefore determined at OD_{260}. OD_{260}/OD_{280} ratios were used as estimates of the purity of the RNA and DNA samples, where ratios of 2,0 and 1,8 indicate pure RNA and DNA samples, respectively and lower ratios indicate phenol and/or protein contamination.

3.2.2 Restriction enzyme digestion

Isolated TFPIα and TFPIβ plasmid DNA was digested with the restriction enzyme to examine if the plasmids contained the correct cDNA inserts. The restriction enzyme *BstXI* was chosen since the vector contains two *BstXI* cleaving sites flanking each site of the cDNA inserts (Figure 1.5.2). A digestion reaction was prepared as described in Table 3.2.2. The reaction was centrifuged for a few seconds, incubated for 15 min at 37 °C and placed on ice until gel electrophoresis was carried out.

Table 3.2.2. Reagents and volumes used for restriction enzyme digestion of plasmid DNA.

Reagent	**Volume (µL)**
Nuclease-Free water	15
10X FastDigest® buffer	2
Plasmid	2,5-2,9 (1µg)
Fast digest Bstx1 restriction enzyme	1
Total	**20**

3.2.3 Agarose gel electrophoresis

Agarose gel electrophoresis is a technique used to separate DNA molecules based on size. The negatively charged DNA molecules migrate towards the positive pole in an electric field and are size separated since smaller molecules migrates faster through the gel pores, than do the longer molecules (Watson et al. 2008). Agarose gel electrophoresis of digested plasmid DNA was applied to verify the sizes of the resulting fragments. The gel electrophoresis was performed with a 1,5% agarose gel containing GelRed, placed in a tub filled with TBE buffer. 3µL 10X Loading Buffer was added to each sample and 20 µL of each sample and 10µL of a GeneRuler 1kB DNA ladder were applied to wells. The gel was run for one hour at 80 Volts and visualised with UV light and photographed using the Omega Lum G imaging system.

3.2.4 Sanger DNA sequencing

Isolated TFPIα and TFPIβ plasmids were DNA sequenced using the Sanger method to verify that no changes in the DNA sequence had occurred during isolation and amplification. In Sanger sequencing, DNA molecules with different lengths are synthesized from one single-stranded DNA template using DNA polymerase, primers, deoxynucleotide triphosphates (dNTPs) and dideoxy NTPs (ddNTPs). DNA polymerase extends the primers bound to the template DNA with dNTPs until the elongation terminates when a ddNTP is randomly incorporated into the growing chain, due to the lack of a 3´hydroxyl group. Each DNA molecule thereby ends with one of the four ddNTPs, each bound to a different fluorescent dye. The sequence is determined by size separating the molecules with capillaries while the colour of each molecule is detected with a fluorescent sensor (Watson et al. 2008).

The plasmids were sequenced using the BigDye Terminator v.3.1 Cycle Sequencing Kit, an ABI 3730 DNA Analyzer and one reverse and forward primer (listed in section 2.7). The sequencing reaction was prepared as described in Table 3.2.4. The two primers were used in separate reactions and the sequencing was performed with two replicates of each sample. The resulting sequences were compared with the reference DNA sequences for TFPIα (NM_006287, GeneBank) and TFPIβ (NM_001032281, GeneBank), using the BLASTN program (www.ncbi.nlm.nih.gov/BLAST/).

Table 3.2.4. Reagents and amount used for Sanger DNA sequencing

Reagent	**Amount**
Plasmid DNA	750ng
Primer (forward and reverse)	3,2pmoL
Bigdye® Terminator v.3.1 Ready Reaction mix	0,25µL
5X Sequencing buffer	2µL
Nuclease-Free water	xµL
Total	**10µL**

3.2.5 cDNA synthesis

To perform real time quantitative reverse transcriptase polymerase chain reaction (real-time qRT-PCR), RNA was reverse transcribed into single stranded cDNA. The cDNA synthesis was carried out using the High Capacity cDNA reverse transcription kit and the 2720 Thermal Cycler. cDNA is synthesized from RNA using the Reverse Transcriptase (RT) enzyme that extend the RT random primers, bound to RNA templates, with dNTPs.
The cDNA reaction was prepared as described in Table 3.2.5.1. Within each experiment, all reactions had the same RNA input (850-2800ng). The plate was sealed and centrifuged before put in the thermal cycler, which was pre-set to a program optimised for the High Capacity cDNA reverse transcription kit (Table 3.2.5.2).

Table 3.2.5.1 Reagents and volumes used for one cDNA reaction

Reagent	**Volume (µL)**
10X RT Buffer	5,0
25X dNTP Mix	2,0
10X RT Random Primers	5,0
MultiScribe™ Reverse Transcriptase	2,5
Nuclease-Free water	10,5
RNA	25
Total	**50**

Table 3.2.5.2. The thermal cycler program optimized for the High Capacity cDNA reverse transcription kit

	Step 1	**Step 2**	**Step 3**	**Step 4**
Temperature (°C)	25	37	85	4
Time (min)	10	120	5	∞

3.2.6 Real time qRT-PCR

Real time qRT-PCR was carried out on cDNA samples to measure and compare the mRNA expression of target genes. In qRT-PCR, each cDNA sample is exponentially amplified by running a series of PCR cycles, while a flourescent signal is measured after each cycle and shown in an amplification plot (Figure 3.2.6.B). All cDNA is copied once per cycle, due to Taq DNA polymerase that uses dNTPs to extend two synthetic primers. A fluorescent nucleotide probe designed to anneal to target cDNA between the primers is used to detect the amplification of cDNA. The probe contains two fluorescent molecules, where one emits light (reporter) and the other absorbs this light (quencher), due to close proximity to the reporter. When the DNA polymerase reaches the probe, it's 5´- 3´exonuclease activity cleaves the probe, and the reporter becomes separated from the quencher. The fluorescent light emitted by the reporter can now be detected (Figure 3.2.6.A). This light is proportional to the amount of target cDNA in each sample and thereby also the target gene mRNA expression.

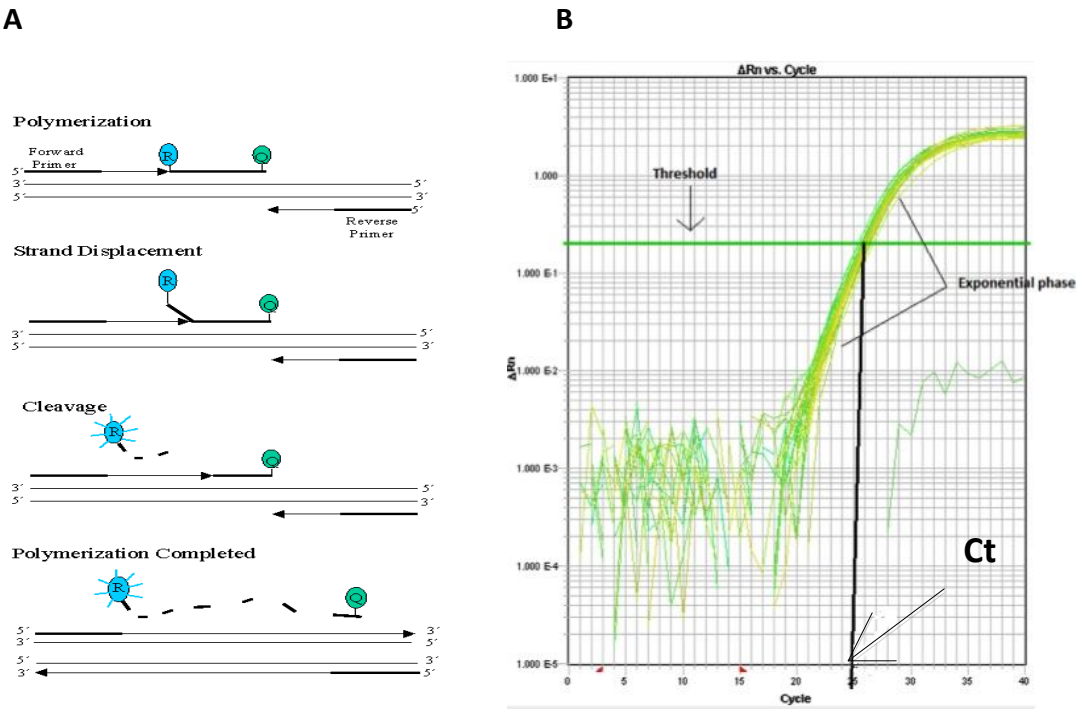

Figure 3.2.6. (A) Real time qRT-PCR principle. The probe is bound to target cDNA between the two primers. When the probe is cleaved by the Taq polymerase, the reporter is separated from the quencher, which results in emission of fluorescent light from the reporter (Figure from Applied Biosystems)**.** (B) Amplification plot for endogenous control PMM1. The horizontal green line is the manually set threshold and Ct is the cycle where the amplification curves reach the threshold in the exponential phase.

An endogenous control was used to correct for variations in cDNA input and/or revers transcriptase efficiency. The endogenous control should have equal expression in all samples, such as a housekeeping gene. Phosphomannomutase 1(PMM1) was chosen as the endogenous control in this thesis because it is unaffected by up- or downregulation of TFPI (previously tested).

mRNA expression of the target gene was calculated using the comparative cycle threshold (Ct) method. Ct is the PCR-cycle in which the amplification curve reaches a threshold, manually set at the exponential phase (Figure 3.2.6.B). The relative quantity (RQ) of target gene mRNA in each sample compared to the calibrator (negative control siRNA or empty control vector) was calculated using the formulas below. RQ values > 1 means that the target gene is overexpressed while values < 1 means that the target gene is downregulated, compared to the calibrator.

ΔCt = Ct target gene – Ct endogenous control

ΔΔCt = ΔCt test sample – ΔCt calibrator sample

$RQ = 2^{-\Delta\Delta Ct}$

Four self-designed TaqMan assays were used in this thesis, containing one probe and one reverse and forward primer (listed in section 2.6). The final reaction mix contained 350nM probe and 900nM of each reverse and forward primer. The real time qRT-PCR reactions were run in triplicates on a 384-well plate, each prepared (on 96-well plates) as described in Table 3.2.6.1. Within the same experiment, all cDNA samples were equally diluted (6,0 – 17,0ng/µL). One non -template control containing nuclease free water instead of cDNA was included. The plate was sealed and centrifuged (2 min, 1500x g) before placed in the ABI PRISM 7900HT Sequence Detection System, which was set to run the program stated in Table 3.2.6.2.

Table 3.2.6.1 Reagents and volume used for one real-time qRT-PCR reaction.

Reagent	**Volume (µL)**
Assay (20X)	0,5
Taqman® Gene Expression Master mix (2X)	5,0
cDNA	4,5
Total	***10***

Table 3.2.6.2. The ABI PRISM 7900HT Sequence Detection System Program

	Step 1	**Step 2**	**Step 3 (40 cycles)**	
Cycle	-	-	**Part 1**	**Part 2**
Temperature (°C)	50	95	95	60
Time (min)	2	10	0,25	1

To apply the comparative Ct method for calculation of relative gene expression, it is important that the PCR efficiency of the target assay and endogenous control assay is

similar. The efficiency was assessed by making a five-fold dilution series of one cDNA sample and running real-time qRT-PCR on the standards with each assay.

3.3 Mammalian cell techniques

3.3.1 Cell culturing

All cells were cultured in Nunc™ Cell Culture Treated Flasks, in a Steri-Cycle $C0_2$ incubator at 37 °C with 5% $C0_2$. The cells, which all are adherent, have different requirements for growth and were therefore cultured in specific media with supplements (Table 3.3.1). Fetal Bovine Serum Gold (FBS) with 10% DMSO was used to store the cells long- term in liquid N_2. All cell work was carried out in a laminar flow hood using strict aseptic conditions. The cells were visualized with a Nikon Eclipse TE 300 microscope.

Table 3.3.1. The specific cell media, supplements and splitting ratio for each cell line

Cell line	Medium	Supplements	Splitting ratio
HEK293T	DMEM	10% FBS	1:5
SUM102	HuMEC basal free Medium	HuMEC supplements and 5% Bovine Pituitary Extract (+5% FBS for splitting)	1:4
HCC1500	RPMI 1640	10% FBS	1:2

The cells were split when they reached 80-90% confluence using the splitting ratios in Table 3.4.1. The medium was removed from the culturing flask and the cells were washed with Phosphate Buffered Saline (PBS) before detached using Trypsin EDTA. Media (with FBS for Trypsin inactivation) was then added before the cell suspension was transferred to a new flask with fresh medium.

3.3.2 Cell quantification

The cells were counted using a NucleCounter NC-100 according to the manufacturer's instructions. In short, cell suspensions were mixed with a membrane lysing solution (Reagent A) and a buffer for stabilization (Reagent B) before loaded into a NucleoCassette and put in the Nucleocounter. The Nucleocassette contains propidium iodide, which is a fluorescent dye that stains the nuclei of cells by binding the DNA and thus allows for cell quantification.

3.3.3 Transient transfection

Screening of siRNA oligonucleotides for TFPIα downregulation in HEK293T cells

The efficiencies of selected siRNA oligonucleotides (siRNAs) against TFPIα were tested in HEK293T cells. The Silencer® Negative control siRNA#5 was used as a negative control in all siRNA transfection experiments in this thesis. The cells were transiently transfected with the siRNAs using the Lipofectamine® 2000 Reagent, according to the manufacturer's protocol. The Lipofectamine reagent consists of positively charged lipids that form circular lipid bilayers, called liposomes, which enclose the sIRNAs. The positively charged liposomes fuse with the negatively charged plasma membrane and thus transfer the siRNAs across the membrane and into the cytoplasm (Dalby et al. 2004).

Cells ($2{,}5x10^5$) were seeded in 12-well Nunc™ Cell-Culture Treated Multidishes the day before transfection. The next day, cells were transfected with siRNAs using 200pmol siRNA and 5,0µL Lipofectamine (40:1 ratio), diluted in OPTI-MEM® Reduced Serum and incubated for five min. Media was removed from the cells before the transfection mix and fresh media was added. Media was removed and replaced with fresh media 4-6 hours after transfection due to Lipofectamine toxicity. The cells were incubated for 24h before cells were harvested for RNA isolation (described in section 3.3.4).

Optimization of TFPIα downregulation with siRNA oligonucleotides in SUM102 cells

SUM102 cells were transiently transfected with the most efficient TFPIα siRNA oligonucleotides (siRNA-3A, 5A and 6A) to find optimal transfection conditions for downregulation of TFPIα. Cells ($3{,}0x10^5$) were seeded in 12-well dishes the day before

transfection. Cells were transfected as described above, except that different siRNA: Lipofectamine transfection ratios were tested; 40:1 and 10:1 (30pmol siRNA: 3µL Lipofectamine). The cells were harvested for RNA isolation 24h after transfection as described in section 3.3.4.

Downregulation of TFPIα and TFPIβ with siRNA oligonucleotides in SUM102 cells

SUM102 cells were transiently transfected with TFPIα (siRNA-3A and 6A) and TFPIβ (siRNA-7B and 9B) siRNA oligonucleotides to downregulate the expression of TFPIα and TFPIβ, separately. $3{,}5x10^5$ cells were seeded out in 6-well dishes the day before transfection. The cells were transfected as described in the siRNA screening section, except using the 10:1 transfection ratio described above. Media was harvested and cells were harvested for protein and RNA isolation 24-120 hours after transfection (described in section 3.3.4).

Optimization of plasmid transfection in HCC1500 cells

Before transfection with the TFPIα and TFPIβ overexpressing plasmids, the HCC1500 cells were transiently transfected with a pMAX green fluorescent protein (GFP) plasmid to find optimal transfection conditions for plasmids. Two transfection reagents, TransIT-2020 and Lipofectamine 2000, were tested and two plasmid DNA: TransIT-2020 ratios; 1:3 and 1:1,5 (1µg plasmid DNA: 3 and 1,5µL TransIT-2020). Cells ($3{,}5x10^5$) were seeded in 12-well dishes the day before transfection. The next day, cells were transfected with GFP plasmid, where transfection with Lipofectamine 2000 was carried out similar to siRNA transfection described in the screening section, except using a 1:3 transfection ratio. When transfected with the TransIT-2020 reagent, the GFP plasmid was diluted in OptiMem, mixed with TransIT-2020 and incubated for 15-30 min (then carried out as described in the screening section). The amount of total and fluorescent cells, 48-120 hours after transfection, was determined using the Image J software.

Overexpression of TFPIα and TFPIβ with plasmid constructs in HCC1500 cells

HCC1500 cells were transiently transfected with TFPIα and TFPIβ plasmids to overexpress TFPIα and TFPIβ. The empty vector plasmid was used as a negative control (described in

section 1.5.2). The cells ($3,0x10^5$) were seeded in 12-well dishes one day before they were transfected by using the TransIT-2020 reagent and the 1:1,5 transfection ratio, as described in the previous section. Media was harvested and cells were harvested for protein and RNA isolation 144 hours after transfection (as described in section 3.3.4).

3.3.4 Harvest of media and cells

When harvesting media, it was collected and stored at -20 °C. Cells harvested for RNA isolation were washed once with cold PBS and lysed in 300-600µL Lysis/binding buffer. Cells harvested for protein were washed three times with cold PBS (cells in suspension centrifuged for 16 sec at 14 500 rpm) and lysed in 50-300µL RIPA buffer with inhibitors for 5 min on ice. The resulting protein and RNA cell lysates were stored at -20 °C and -80 °C, respectively. Before use in the protein techniques, the protein cell lysates and media samples were vortexed and centrifuged for 60 seconds at 15 000 rpm.

3.3.5 Stable cell lines

To create cell lines with stable TFPIα and TFPIβ overexpression, HCC1500 cells were transfected with TFPIα and TFPIβ plasmids as described in the plasmid optimization section. When introduced into cells, the plasmids are incorporated into the genome and are thereby transferred to the next generations when the cells are dividing. 48 hours after transfection, selection media with 500µg/mL geneticin (G418) was added to the cells for several weeks.

3.4 Protein techniques

3.4.1 Total protein quantification

Total protein in cell lysates was quantified using the PIERCE® BCA Protein Assay Kit. Total protein was detected and quantified with a bicinchoninic acid (BCA) working reagent, where Cu^{2+}(green) molecules are reduced to Cu^{1+} (purple) in the presence of proteins. Cu^{1+} bound to BCA in chelate complexes absorbs UV light at 570nm proportional to the amount of protein in the samples.

A 2X Albumin standard dilution series was made, ranging from 0-2 mg/mL. 5µL of each cell lysate (preparation described in section 3.3.4), one blank sample (RIPA with inhibitor) and five standards were added in triplicates in a 96-well plate. 200µL BCA working reagent (reagent A+B in a 1:50 ratio) was added and the plate was mixed for 30 sec and incubated at 37 °C for 30 min. Finally, the absorbance was measured at 570nm using a Benchmark Microplate reader. The concentration of total protein was determined from the standard curve using the Microplate manager 5.2 software.

3.4.2 Enzyme-linked immunosorbent assay (ELISA)

ELISA is a method used for detecting and quantifying specific analytes in a solution. The analyte is usually detected and quantified using two specific antibodies that binds the analyte at different sites, making an ELISA sandwich. The antibody on the top of the sandwich is enzyme-linked and when incubated with a substrate, produces a product that has a specific colour and absorbs light at a specific wavelength. This absorption is proportional to amount of enzyme product and thereby also amount of analyte (Lea 2008).

Total TFPI ELISA

Total TFPI in media and cell lysates (prepared as described in 3.3.4) was quantified using the Asserachrom® TOTAL TFPI kit, according to the manufacturer's protocol. The kit contains microplates with wells pre-coated to the first human TFPI specific antibody. The test samples and the second human TFPI antibody, conjugated to a peroxidase enzyme, were added together to these pre-coated microwells. The ortho-Phenylenedimine substrate was added to the microwells and the absorbance of the resulting colour was measured at 490nm, 30 min after terminating the resulting colour reaction with H_2SO_4. The Benchmark Microplate reader was used to measure the absorbance and the concentration of total TFPI in each test sample was determined from the standard curve using the Microplate manager 5.2 software.

TNF-α ELISA

TNF-α antigen in cell media (prepared as described in section 3.3.4) was quantified using the TNF-α human ELISA kit, according to the manufacturer's protocol. The kit contains a microplate with wells pre-coated with the first TNF-α specific antibody. The samples and the second TNF-α specific antibody, conjugated to a peroxidase enzyme, were added to the pre-coated wells in two separate steps, with two hours incubation in between. The Tetramethylbenzidine (TMB) chromogen substrate was added to the wells and the absorbance was measured at 450nm, 10 min after terminating the color reaction with a TMB stop solution. The absorbance was measured using the Benchmark Microplate reader and the concentration of TNF-α antigen in each sample was determined from the standard curve using the Microplate manager 5.2 software.

3.4.3 Western blotting

Western blotting is a technique used to detect and semi-quantify proteins. The technique is based on three steps: separation of proteins by size with gel-electrophoresis, transfer of separated proteins to a membrane (blotting) and detection of target protein with a primary and secondary antibody. The primary antibody binds the specific target protein of interest and is bound by a labelled secondary antibody, which is used together with a detection system to visualize the target protein.

Gel-electrophoresis

The cell lysates were prepared as described in 3.3.4. Total protein (5-15µg) was mixed with loading buffer in a 2:1 ratio. Samples were boiled for 5 min at 97 °C before loading the gel (Mini-protean® TGX gels and Precise Tris-glycine gels 10%), placed in a tank with 1X Running buffer. A Precision Plus Protein™ Dual Color Standard was used as ladder. The proteins were separated according to size by gel-electrophoresis for 40-45 min at 185 Volts.

Blotting

The gel was sandwiched together with a Protran Nitrocellulose Transfer Membrane between filterpaper and blotting pads, all soaked in Tris Glycin Buffer (blotting buffer). The sandwich was put in a tank filled with blotting buffer and an ice-block and the proteins were

electrotransferred by wet blotting to the membrane for 20 min at 110 Volts and constant magnetic stirring.

Detection of target protein

The membrane was blocked in 5% BSA for one hour to prevent unspecific antibody binding to unoccupied membrane sites. Then, it was washed with TBST (3X5 min) and incubated with a target specific primary antibody over night at 4 °C, or one hour at room temperature. The membrane was washed in TBST (3X10 min) to remove unbound primary antibody before incubated with a horseradish peroxidase (HRP) conjugated secondary antibody for one hour (all antibodies are listed in section 2.5.1). The washing step was repeated before the Amersham ECL prime detection system was used to visualize the target protein. The ECL prime solution contains Luminol that is oxidized by HRP conjugated to the secondary antibody and thereby emits light (chemiluminescence) proportional to the amount of protein on the membrane. The Image quant LAS 4000 imager was used for visualization and the Image QuantTL software was used to quantify the amount of target protein on the membrane.

To detect another specific target protein, the membrane was washed in TBST (3X10 min) and blocked with 5% BSA for 30 min, before incubated with a new primary and secondary antibody. The membrane was stripped for all bound antibodies by incubating it with 45mL stripping solution and 350µL 2-merkaptoethanol for 30 minutes at 55 °C, and then washed with TBST (3X5 min) before blocked with 5% BSA for one hour. The membrane was stored in plastic at -20°C.

3.5 Functional assays

3.5.1 Apoptosis

Western blotting

Western blotting (described in section 3.4.3) was used as a technique to analyse the effect of down- and upregulation of TFPIα and TFPIβ on apoptosis. PARP and caspase-8 were used as apoptotic markers and actin and α-tubulin were used as loading controls (the specific

antibodies used to detect these proteins are listed in section 2.5.1). PARP is a part of the DNA repair system and is a target of caspase-3 in the death receptor pathway. Caspase-8 is an initiator caspase that cleaves and activates other caspases, including caspase-3. Actin and α-tubulin were used as controls for protein loading.

DNA fragmentation assay

The effect of down- and upregulation of TFPIα and TFPIβ on apoptosis was also studied by measuring the amount of DNA fragmentation in the cells using the Cell death detection ELISA plus kit. The method was conducted as described in the manufacterer´s protocol, except for preparation of the cell lysate samples, which was performed as described in section 3.3.4. In this ELISA kit, two antibodies targeting different compartments of mono- and oligonucleosomes are used to measure amount of DNA fragmentation. The test samples and a mixed solution of the two antibodies (immunoreagent) were added in separate steps to microwells pre-coated with streptavidin. One antibody in the immunoreagent binds to the histone proteins in the nucleosomes and also binds to the streptavidin in the wells with its biotin molecules. The second antibody binds to the DNA in the nucleosomes and is conjugated to a HRP enzyme. After incubation, the ATBS solution (substrate) was added to the wells and the absorbance was measured after 8 min, at 405nm with the Benchmark microplate reader. After 18 min the ATBS stop solution was added and the absorbance was measured again.

Inhibition of Akt, NF-κB, TF, PAR-2 and TNF-α proteins

Akt, NF-κB, TF, PAR-2 and TNF-α proteins were inhibited in SUM102 cells with TFPIα and TFPIβ downregulated to study whether these proteins were involved in the apoptotic effect of TFPI. Transfected cells were incubated in two hours with 650µL fresh media containing blocking antibodies (10 µg/mL) or specific inhibitors (20mM) targeting the different proteins (listed in section 2.5.2). Negative Control antibody (10 µg/mL) was used as control for the blocking antibodies, while DMSO (20mM) was used as control for the specific inhibitors. After incubation, the cells were harvested for RNA isolation and protein (as described in section 3.3.4). The inhibition effect on apoptosis was analysed with Western blotting, using PARP and caspase-8 as apoptotic markers.

3.5.2 Cell growth

The effect of TFPIα and TFPIβ downregulation on SUM102 cell growth was studied by counting the amount of living cells and measuring the amount of total protein. The counting was performed with a Countess Automated Cell Counter following the manufacturer's protocol. 6-120 hours after transfection of SUM102 cells, the media was collected and the cells were detached with 500µL Trypsin EDTA. The collected media was added to the detached cells and the cell suspension was mixed with Trypan Blue Stain before loaded into the Countess Cell Chamber Counting slides and counted with the cell counter (in triplicates). Trypan blue is able to pass trough the membrane of dead cells and stain them. Living cells appear white because the trypan blue are not able to pass through their membranes. After counting, the cells were harvested for RNA isolation and protein (described in 3.3.4) and amount of total protein in the protein cell lysates was quantified as described in section 3.4.1.

3.5.3 Signalling

The effect of TFPIα and TFPIβ downregulation on the activity of the PI3-Kinase-Akt signalling pathway was studied by performing stimulation experiments and analysing the effect on Akt phosphorylation with Western blotting. Transfected SUM102 cells were starved for 5,5 hours in media without supplements before the cells were detached with 500µL Versene EDTA and centrifuged at 14 5000 rpm in 16 sec. $1{,}0x10^6$ cells were then washed with 500µL PBS to remove the starvation media before the cells were stimulated in media with 10% FBS for 0, 5 and 10 min. After stimulation, the washing step was repeated twice and the cells were harvested for RNA isolation and protein described in section 3.3.4.

3.6 Statistical analysis

In this thesis, the student t-test was used to compare data between treated samples and control samples in the cell growth assay, DNA fragmentation assay and Western blotting. In this thesis, the datasets were assumed to be normally distributed and independent of each other, and therefore an unpaired t-test was used. A probability value of $P \leq 0{,}05$ was considered significant and was denoted with *.

4. Results

4.1 Validation of TaqMan assays

4.1.1 PCR efficiency

To use the comparative Ct method for calculation of relative mRNA expression of target genes (described in section 3.2.6), the target (TFPI)- and endogenous control (PMM1) assays need to have high and similar PCR efficiency. To evaluate the PCR efficiencies, the assays were run with a five-fold dilution series of a cDNA sample (Figure 4.1.1 A, B and C). The slopes of the resulting standard-curves were converted to assay efficiencies using the formula below.

$$\text{Efficiency (\%)} = 10^{(-1/\text{slope})} - 1 * 100\%$$

All assay used in this thesis showed efficiencies between 94-97%, (Table 4.1.1), thus fulfilling the 90-105% amplification efficiency required for optimized assays. Furthermore, the PCR efficiency similarity between the TFPI target assays and the PMM1 endogenous control was evaluated by calculating the difference between their slope values (ΔSlope). The ΔSlope for each target assay should be less than 0,1. This was shown for all of the TFPI target assays (Table 4.1.1). The comparative Ct method could thus be used for calculating the relative TFPI mRNA expression using PMM1 as the endogenous control in this thesis. Moreover, all of the assay standard-curves had R^2 values of 0,99, which fulfilled the criterion of R^2 ≥ 0,980 for good linearity of PCR standard-curves.

A

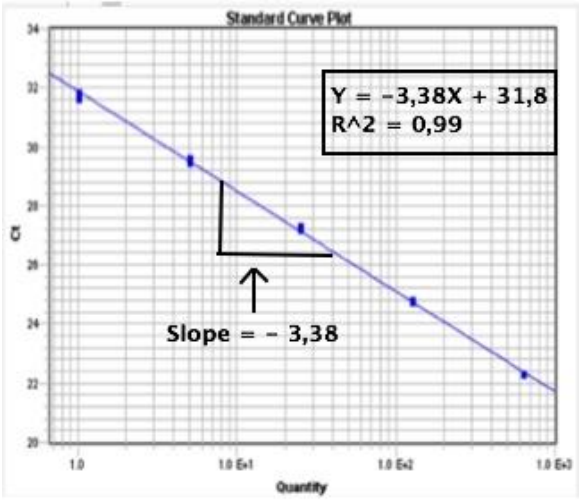

B

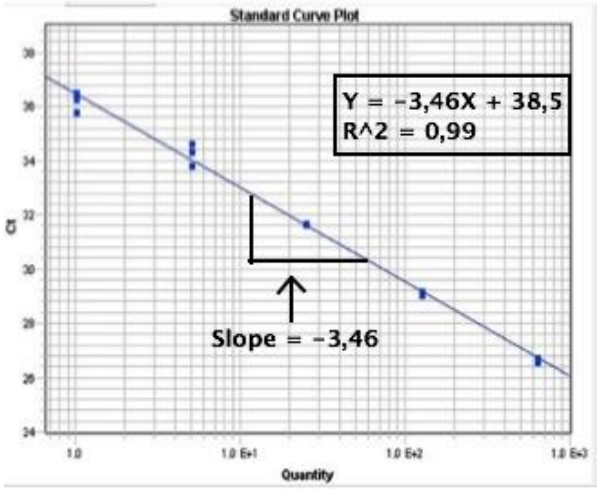

C

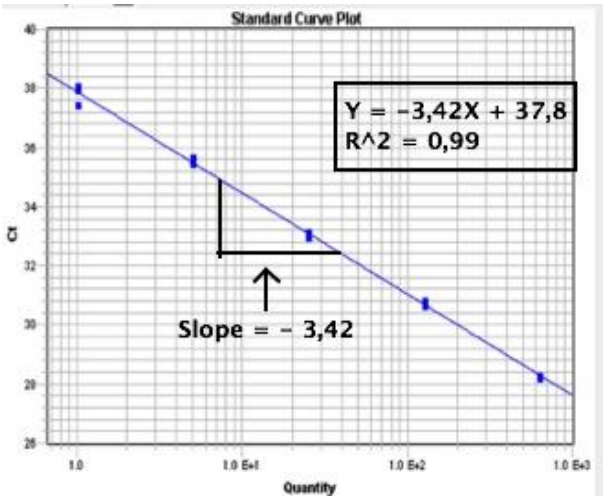

Figure 4.1.1. Standard-curves for the TaqMan assays. (A) PMM1 assay, (B) TFPIα assay and (C) TFPIβ assay. The standard-curve slope is indicated and the Ct values and log quantity is shown on the Y and X- axis, respectively.

Table 4.1.1 TaqMan assay PCR efficiency and ΔSlope for each target assay and the PMM1 endogenous assay.

Assay	Efficiency	ΔSlope*
PMM1	97%	-
TFPIα	94%	-0,08
TFPIβ	96%	-0,04

*ΔSlope = slope of TFPI target assay – slope of PMM1 endogenous control assay.

4.1.2 Specificity

To assess the specificity of the TFPIα and TFPIβ TaqMan assays used in qRT-PCR, TFPIα and TFPIβ were upregulated with plasmids in HCC1500 cells (as described in the plasmid optimization section) and the TFPIα and TFPIβ mRNA expression was measured. Cells transfected with the TFPIα plasmid showed high TFPIα mRNA expression, while no difference in TFPIα mRNA expression was observed in cells transfected with TFPIβ plasmid, compared to the control (Figure 4.1.2A). Similarly, high TFPIβ expression was seen in cells transfected with the TFPIβ plasmid and no difference in TFPIβ expression was observed for cells transfected with the TFPIα plasmid (Figure 4.1.2B). The TFPIα and TFPIβ assays were thereby shown to be target specific.

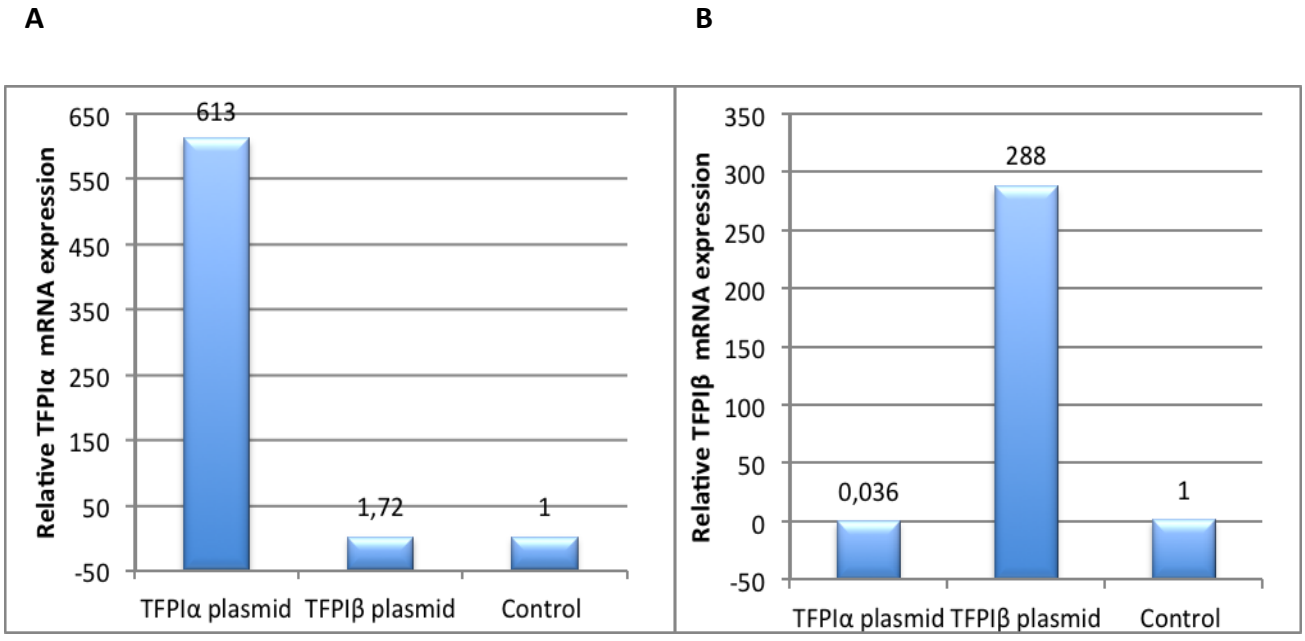

Figure 4.1.2. Relative TFPI mRNA expression in HCC1500 cells with TFPIα and TFPIβ upregulated. The cells were transfected with TFPIα, TFPIβ or control plasmids and harvested after 144 hours. Expression levels were measured with real-time qPCR and normalized against the endogenous control PMM1 and the control. (A) Relative TFPIα mRNA expression measured using the TFPIα assay. (B) Relative TFPIβ expression measured using the TFPIβ assay. Values of one experiment are shown.

4.2 Downregulation of TFPIα and TFPIβ

4.2.1 Selection of siRNA oligonucleotides against TFPI

siRNA oligonucleotides (siRNAs) were used in this thesis to downregulate the expression of TFPIα and TFPIβ, separately. Total TFPI (α+β) and only TFPIβ have previously been effectively downregulated, but not TFPIα alone. Therefore four new siRNAs against TFPIα, siRNA-3A-6A, were selected and tested in this thesis, along with two in-house siRNAs, siRNA-1A and 2A. siRNA-1A and 2A were both obtained from Eurogentec as 21nt dsRNA molecules. siRNA-1A was originally adopted from a previous study (Piro & Broze 2004). siRNA-3A, 4A, 5A and 6A were all selected after using a siRNA self-design tool program provided by Eurofins. This program designed suitable siRNAs by using the Genebank TFPIα mRNA sequence (RefSeq: NM_006287) as a reference, and the specified TFPIα specific sequence (nucleotides 628 to 1210 from start point). The four siRNAs ranked with the highest predicted efficiency score were selected and ordered as blunt-end 27nt dsRNA molecules. Moreover, two in-house TFPIβ siRNAs, siRNA-7B and siRNA-9B, were used to downregulate the TFPIβ isoform (already optimized). The described siRNA oligonucleotides are listed in section 2.8.

4.2.2 Screening of siRNA oligonucleotides for TFPIα downregulation in HEK293T cells

The downregulation efficiency and specificity of the two in–house siRNAs (siRNA-1A and 2A) and the four new selected siRNAs (siRNA3A-6A) against TFPIα (described above) were tested in HEK293T cells. Transfection with siRNA-1A and 2A reduced the relative TFPIα mRNA expression with only 13% and 20%, respectively, compared to the control. All four new siRNAs showed high downregulation efficiencies, where siRNA-3A, 5A and 6A were most efficient, with a 76%, 65% and 80% reduction in relative TFPIα mRNA expression, respectively (Figure 4.2.2). The relative TFPIβ mRNA expression was unaffected in all cases, meaning that all the siRNAs were TFPIα specific.

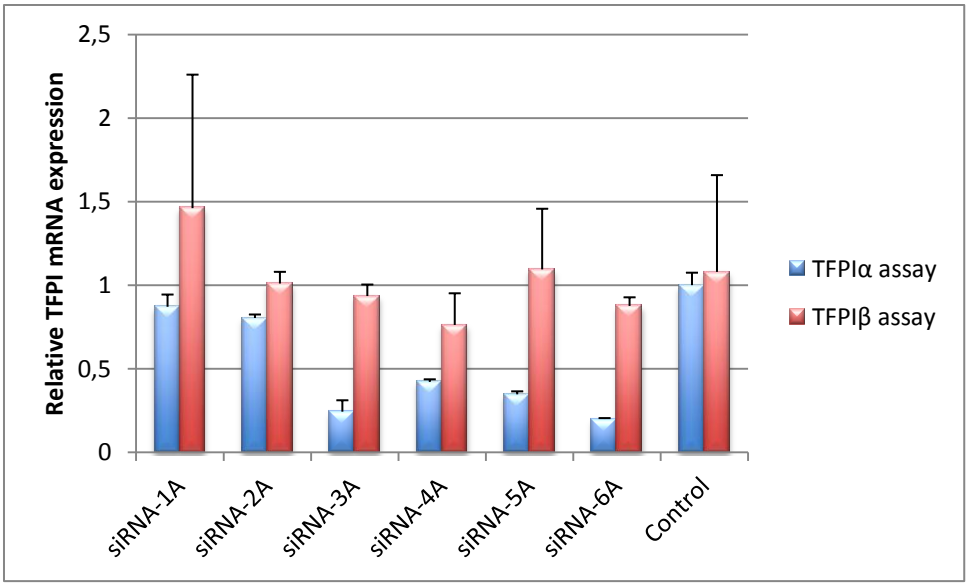

Figure 4.2.2. Relative TFPIα and TFPIβ mRNA expression in HEK293T cells transfected with siRNAs against TFPIα. The cells were transfected with siRNA-1A-6A and control siRNA using the Lipofectamine 2000 reagent (200pmol siRNA: 5µL Lipofectamine). The cells were harvested after 24h and the TFPIα and TFPIβ mRNA expression was measured with real-time qRT-PCR and normalized against endogenous control PMM1 and the control. Mean values (n=2) + SD of one experiment are shown.

4.2.3 Optimization of TFPIα downregulation in SUM102 cells

After screening of the TFPIα specific siRNAs in HEK293T cells, downregulation of TFPIα was optimized in the SUM102 breast cancer cells. The most efficient siRNAs, siRNA-3A, 5A and 6A, (shown in Figure 4.2.2) were tested with two different siRNA: Lipofectamine ratios; 40:1 and 10:1. The 10:1 ratio showed similar or better transfection efficiency for all three siRNAs, compared to the 40:1 ratio. siRNA-3A and 6A with a downregulation efficiency of 36% and 65%, respectively, were used in further transfection experiments.

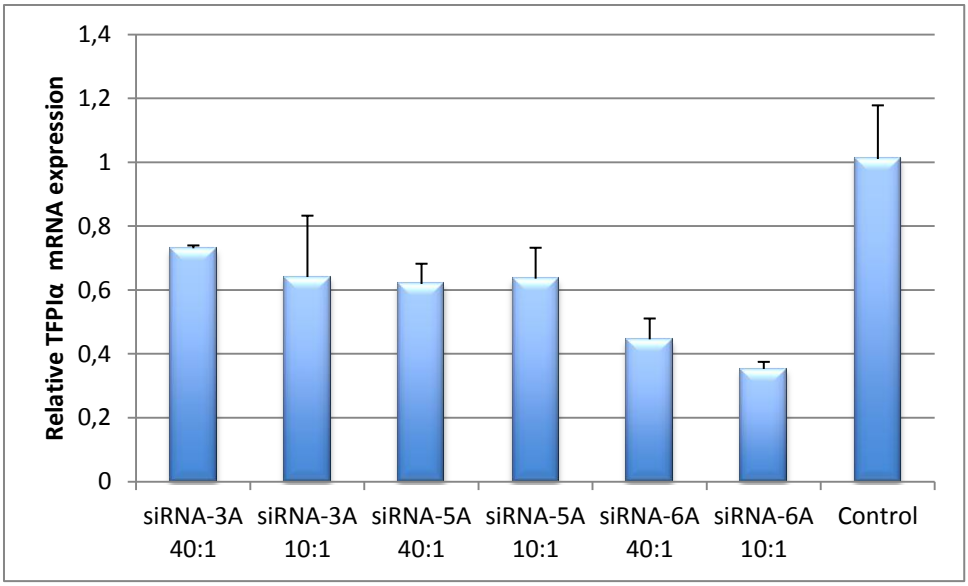

Figure 4.2.3. **Relative TFPIα mRNA expression in SUM102 cells with TFPIα downregulated**. The cells were transfected with siRNA-3A, 5A and 6A and control siRNA using 10:1 (30pmol siRNA: 3µL Lipofectamine) and 40:1 (200pmol: 5µL Lipofectamine) transfection ratios. The cells were harvested after 24h and the TFPIα mRNA expression was measured with real-time qRT-PCR and normalized against endogenous control PMM1 and the control. Mean values (n≥2) +SD of two experiments are shown.

4.2.4 Downregulation of TFPIα and TFPIβ with siRNAs in SUM102 cells

Relative TFPI mRNA expression

After optimizing the TFPIα siRNAs, the SUM102 cells were transfected with siRNA-3A and 6A and 7B and 9B to downregulate TFPIα and TFPIβ, respectively. The TFPIβ specific siRNAs had been optimized previously. To find the time point with most efficient downregulation, the TFPIα and TFPIβ mRNA expression was measured 24-120h after transfection. Transfection with siRNA-3A displayed only a 25% reduction in relative mRNA expression after 24h. However, from 48h the downregulation was more effective and stable up to 120h, with a 44% and 39% reduction, respectively. Transfection with siRNA-6A resulted in relative reduction of TFPIα mRNA expression between 38%-58%. The expression was most efficient and relatively stable from 48-120h, with some exception at 72h (Figure 4.2.4.1). siRNA-7B and 9B were equally efficient in downregulating TFPIβ (except at 96h) and showed highest efficiency at 24, 48 and 96h. The relative TFPIβ mRNA expression was reduced between 49%-71% and 50% -70%, respectively, for siRNA-7B and 9B (Figure 4.2.4.2)

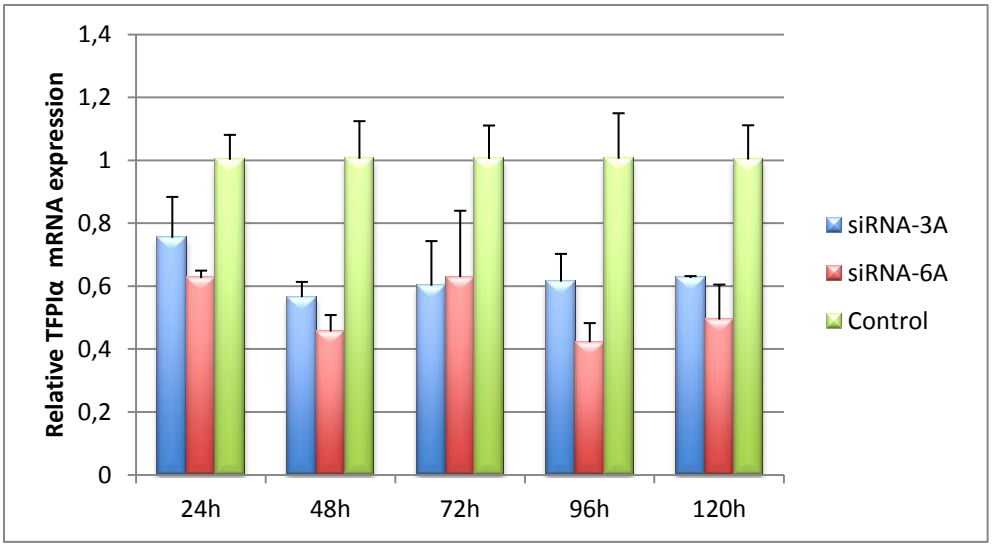

Figure 4.2.4.1. Relative TFPIα mRNA expression in SUM102 cells with downregulated TFPIα. The cells were transfected with siRNA-3A, 6A and control siRNA and harvested 24-120h after transfection. The mRNA expression was measured with real-time qRT-PCR and normalized against the endogenous control PMM1 and the negative control. Mean values (n≥3) +SD of three experiments are shown.

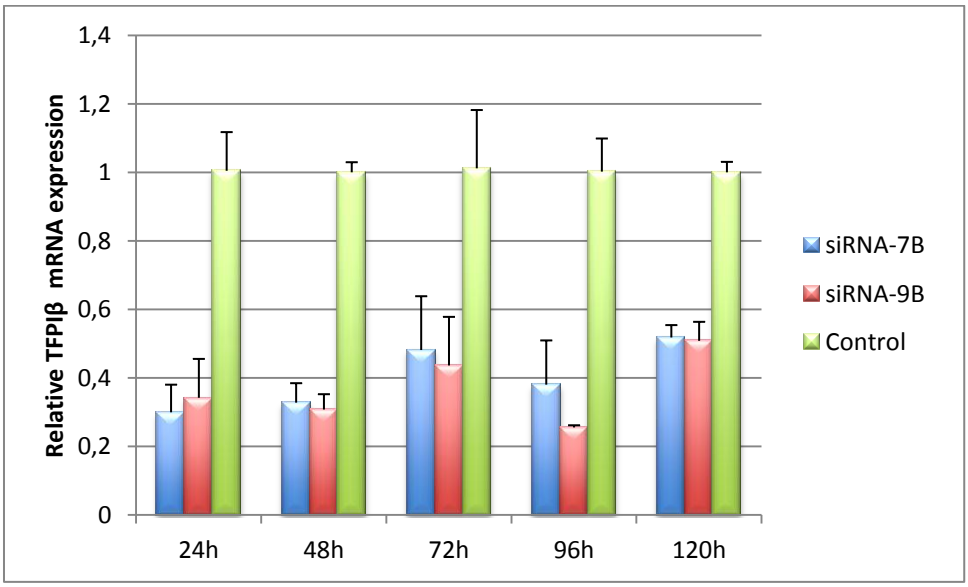

Figure 4.2.4.2. Relative TFPIβ mRNA expression in SUM102 cells with downregulated TFPIβ. The cells were transfected with siRNA-7B, 9B and control siRNA and harvested 24-120h after transfection. The mRNA expression was measured with real-time qRT-PCR and normalized against the endogenous control PMM1 and the negative control. Mean values (n≥3) +SD of three experiments are shown.

Total TFPI protein expression

To confirm TFPI knock down at the protein level, total TFPI protein levels were measured (described in section 3.4.2) in cell media and lysates harvested 48-120h after the SUM102 cells were transfected with siRNA-3A, 6A, 7B and 9B. Theoretically, both TFPIα and TFPIβ are measurable in the cell lysate, while only the TFPIα isoform may be secreted and is therefore measurable in the cell media. Transfection with siRNA-3A and 6A showed a 33% and 55% reduction in total TFPIα levels in cell media, respectively, at 72h and a 24% and 33% reduction at 96h, compared to the control (Figure 4.2.4.3). Only negligible differences were observed at 48h and at 120h the downregulation effect was abolished. Furthermore, cells transfected with siRNA-7B showed a 20%, 11% and 11% reduction in total TFPI levels in cell lysates at 72, 96 and 120h, respectively, compared to the control. No difference was observed at 48h. For siRNA-9B, a 15%, 44% and 30% reduction in amount of total TFPI levels in cell lysates was observed at 48, 72 and 120h, respectively, compared to the control cells, while no difference was observed at 96h (Figure 4.2.4.4). Cells transfected with siRNA-3A showed no differences in TFPI levels after 72 or 96h, compared to the control.

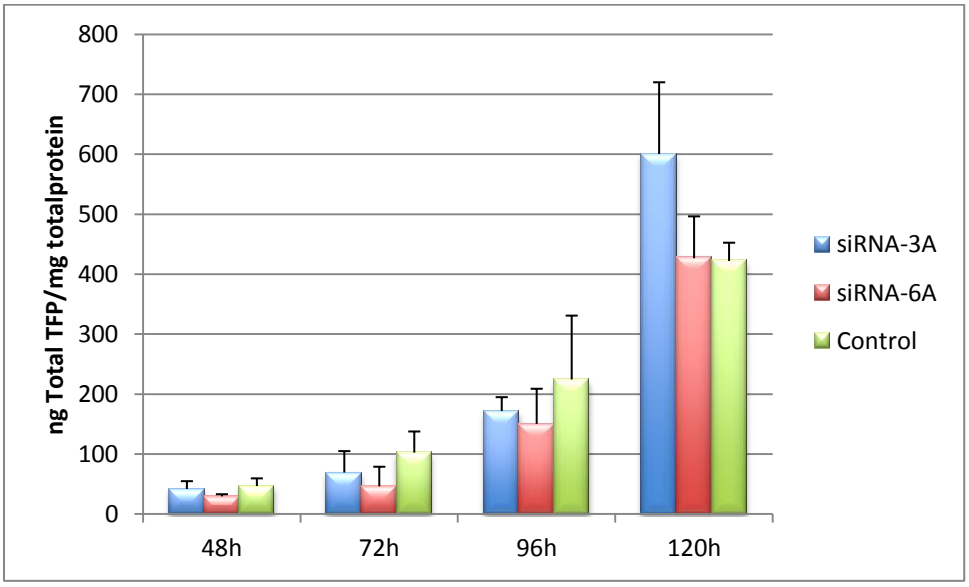

Figure 4.2.4.3. Total TFPI protein levels in cell media of SUM102 cells with downregulated TFPIα. The cells were transfected with siRNA-3A, 6A and control siRNA and harvested 48-120h after transfection. The results were corrected against cellular total protein. Mean values (n≥2) +SD of two experiments are shown.

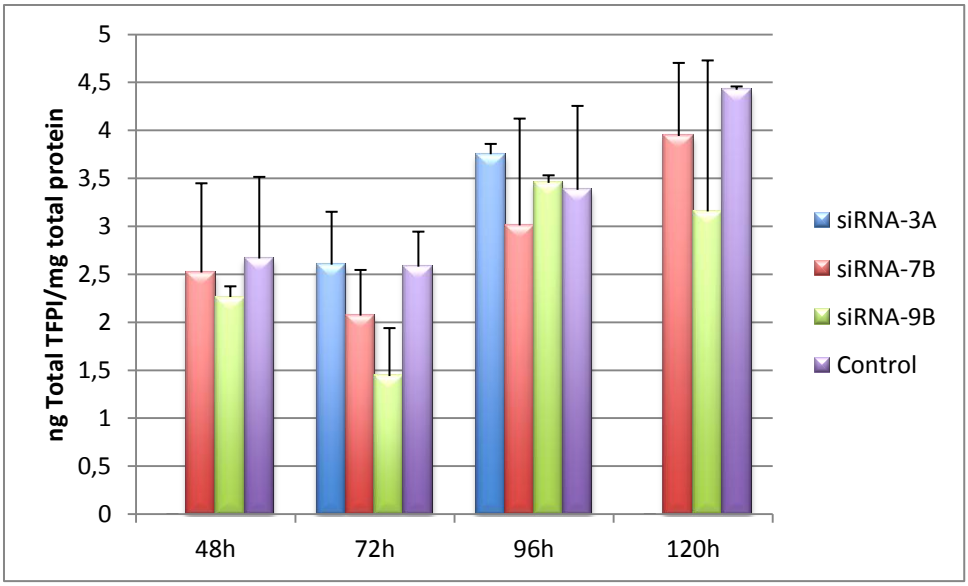

Figure 4.2.4.4. Total TFPI protein levels in cell lysate of SUM102 cells with downregulated TFPIα and TFPIβ. The cells were transfected with siRNA-3A, 7B, 9B and control siRNA and harvested 48-120h after transfection. The results were corrected against cellular total protein. Mean values (n≥2) +SD of two experiments are shown.

4.3 Overexpression of TFPIα and TFPIβ

4.3.1 Characterization of TFPIα and TFPIβ plasmids

The plasmids with TFPIα and TFPIβ cDNA were digested with *BstXI* (described in section 3.2.2) to analyse the presence of correct cDNA inserts. Agarose gel electrophoresis (described in section 3.2.3) was run to verify the fragment sizes. Two small bands of 956bp (lane 4, Figure 4.3.1) and 846bp (lane 5, Figure 4.3.1) appeared on the agarose gel, which correspond to the expected sizes of the TFPIα and TFPIβ cDNA inserts, respectively. The restriction enzyme digestion thus indicated that the TFPIα and TFPIβ plasmids contained the correct cDNA inserts. The upper two bands in lane 2-5 correspond to undigested relaxed- and supercoiled plasmid, and the upper third band in lane 4 and 5 correspond to the linearized plasmids. The TFPIα and TFPIβ plasmids were also Sanger DNA sequenced to analyse for DNA sequence changes that could have occurred during plasmid isolation (described in section 3.2.4). Sequence analysis showed that the cDNA inserts did not have any sequence dissimilarities compared to the TFPIα (NM_006287, GeneBank) and TFPIβ (NM_001032281, GeneBank reference mRNA sequences (data not shown).

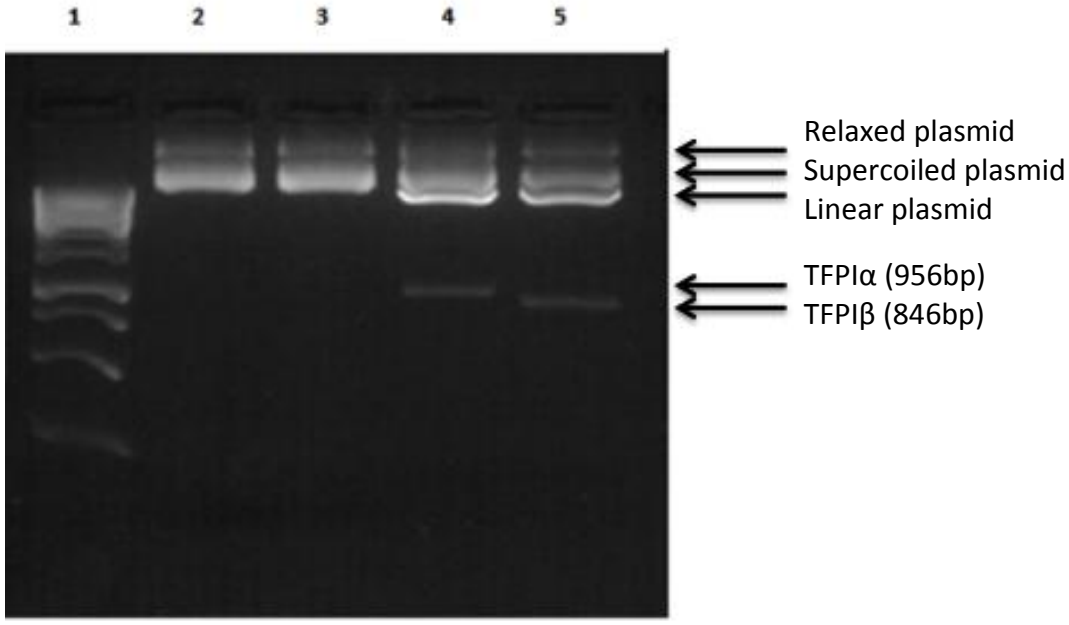

Figure 4.3.1 Agarose gel electrophoresis of *BstXI* digested TFPIα and TFPIβ plasmids. The GeneRuler 1Kb DNA ladder is shown in lane 1. Lane 2 and 3 show undigested TFPIα and TFPIβ plasmids, respectively, and lane 4 and 5 show digested TFPIα and TFPIβ plasmids, respectively. Relaxed, supercoiled and linearized plasmid, and the TFPIα and TFPIβ cDNA inserts are indicated.

4.3.2 Optimization of plasmid transfection in HCC1500 cells

HCC1500 cells were transfected with GFP plasmid to find optimal plasmid transfection conditions in these cells, before transfecting with TFPIα and TFPIβ plasmids. Two different transfection reagents, Lipofectamine 2000 and TransIT-2020, were tested. Transfection with TransIT-2020 was performed with two different plasmid DNA: TransIT-2020 ratios; 1:3 and 1:1,5 (described in plasmid optimization section). The transfection efficiency was determined by amount of fluorescent cells, which was measured 48-120h after transfection.

For Lipofectamine 2000, the amount of fluorescent cells was highest at 48h with 7,5% fluorescent cells, and thereafter decreased in a time dependent manner (Figure 4.3.2B). Transfection with TransIT-2020 showed relatively stable amount of fluorescent cells, especially at the 1:1,5 ratio with values ranging between 8,5-9,3%. The transfection of HCC1500 cells was most efficient when using the TransIT-2020 reagent with the 1:1,5 ratio showing 2,5 and 2 times more fluorescent cells at 120h compared to Lipofectamine 2000

and the 1:3 ratio, respectively (Figure 4.2.3.A and B). The TransIT-2020 reagent with the 1:1,5 ratio was therefore used in further transfection experiments.

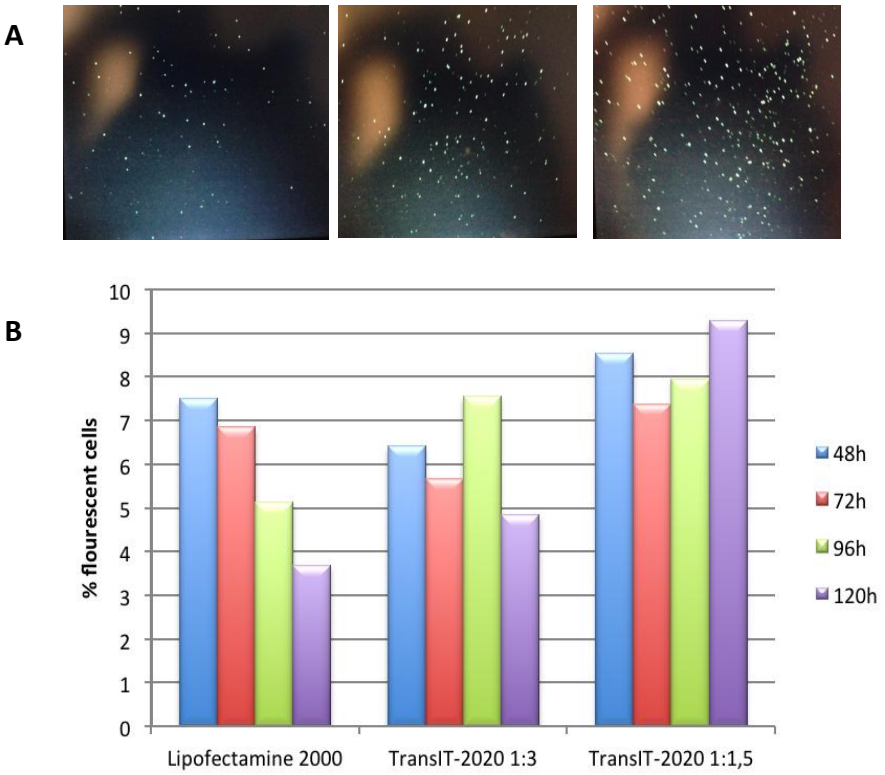

Figure 4.3.2. **Amount of fluorescent cells (%) 48-120 hours after transfection with GFP plasmid**. The HCC1500 cells were transfected with GFP plasmid using the Lipofectamine 2000 or the TransIT-2020 transfection reagent. For TransIT-2020, 1:3 and 1:1,5 transfection ratios were used (µg plasmid: µL TransIT-2020). (A) Pictures were taken of transfected cells at each time point. Pictures taken at 120h of transfected cells are shown for the corresponding reagents. (B) Amount of fluorescent cells was determined using Image J and correlated to total amount of cells. Cells with only media and transfection reagent (no plasmid) was used as a control. Values of one experiment are shown.

4.3.3 Overexpression of TFPIα and TFPIβ with plasmids in HCC1500 cells

After optimization of plasmid transfection, HCC1500 cells were transfected with TFPIα and TFPIβ plasmids to overexpress TFPIα and TFPIβ, respectively, before the expression was measured at the mRNA and protein level. TFPIα was measured in the cell media, while TFPIβ was measured in the cell lysate. Overexpression of TFPIα and TFPIβ resulted in a 613- and 288-fold increase in relative TFPIα and TFPIβ mRNA expression, respectively, (Figure 4.3.3A) and a 15- and 6-fold increase in total TFPI protein levels, respectively, compared to the control (Figure 4.3.3.B).

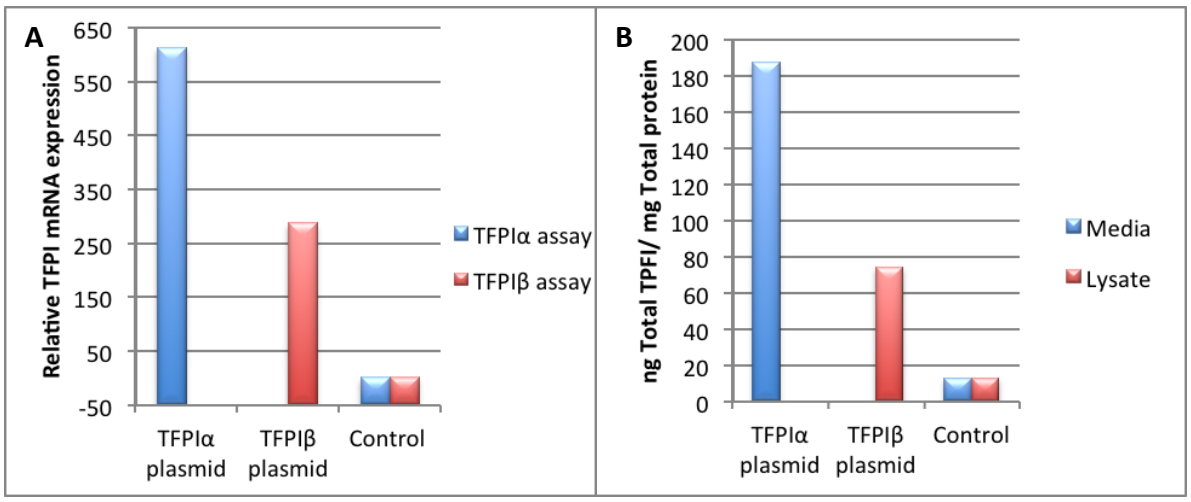

Figure 4.3.3. Transient overexpression of TFPIα and TFPIβ in HCC1500 cells. The cells were transfected with TFPIα, TFPIβ and control plasmid using the TransIT-2020 (1:1,5 ratio) transfection reagent and harvested 144h after transfection. (A) Relative TFPIα and TFPIβ mRNA expression was measured by real-time qRT-PCR and normalized against the PMM1 endogenous control and the control (B) Total TFPI antigen levels in cell media and lysate were measured and corrected against cellular total protein. Values of one experiment are shown.

4.4 Effect of TFPIα and TFPIβ downregulation on cell growth

To study the effects of downregulation of TFPIα and TFPIβ, separately, on cell growth, SUM102 cells were transfected with siRNA-6A, 7B and control siRNA and the amount of living cells and total protein was determined between 6-120h after transfection.

Downregulation of TFPIα showed no difference in amount of living cells at 6, 24 or 48h, compared to the control. However, a significant difference in amount of cells was observed at 72, 96 and 120h, with 26%, 21% and 31% less living cells, respectively, compared to the control (Figure 4.4A). Cells with TFPIβ downregulated showed no difference compared to control cells at any time point. Furthermore, when measuring the amount of total protein in the cell lysates, cells with TFPIα downregulated showed 29%, 33% and 48% significant less total protein at 48, 72 and 96h, respectively, compared to control cells. In addition, some differences were observed at 24 and 120h (Figure 4.4B). Cells with TFPIβ downregulated showed equal amounts of total protein as control cells at 6, 24 and 48h. However, some

differences (not significant) occurred at 72, 96 and 120h, especially at 96h with 31% less total protein, compared to control cells.

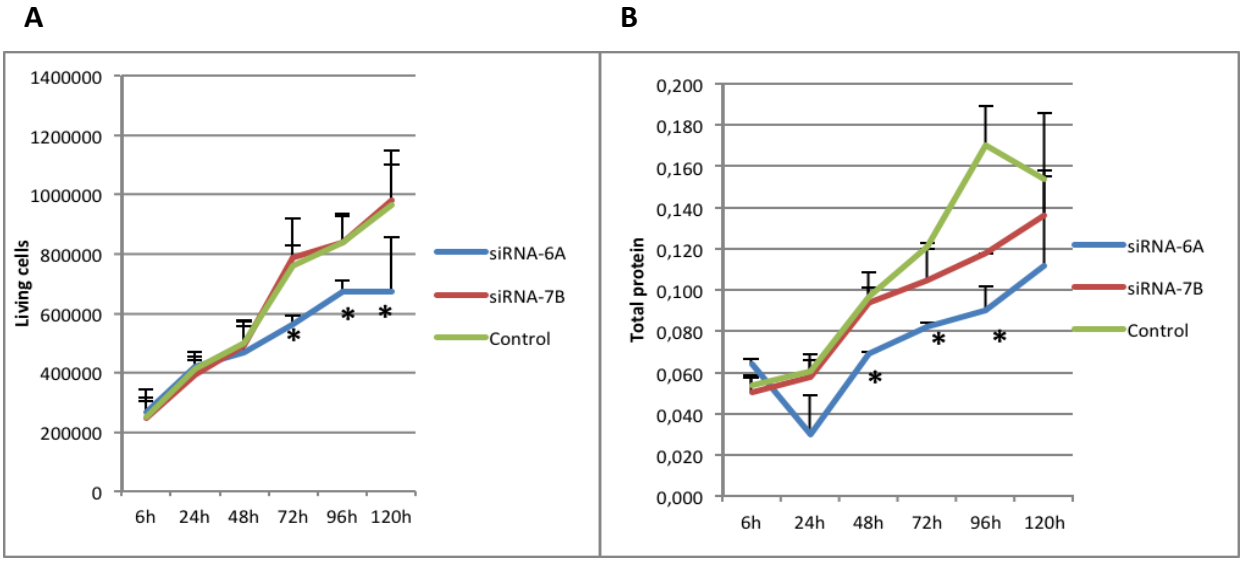

Figure 4.4. Effect of downregulation of TFPIα or TFPIβ on the growth of SUM102 cells. Cells were transfected with siRNA-6A, 7B and control siRNA and incubated for 6, 24, 48, 72, 96 and 120h (A) Amount of living cells at each time point (B) Amount of total protein (mg) in cell lysates at each time point. Mean values (n=2) + SD of one experiment is shown.

4.5. Apoptosis

4.5.1 Effect of TFPIα and TFPIβ downregulation on apoptosis in SUM102 cells

Western blotting was used as a technique to analyse the effect of downregulation of TFPIα and TFPIβ on apoptosis, using PARP and caspase-8 as apoptotic markers. PARP is a protein that is a part of the DNA repair system and is cleaved by caspase-3 late in the apoptotic pathway. Caspase-8 is a protein involved in the early phase of the apoptotic pathway and cleaves and activates other caspases, including caspase-3. The apoptotic effect was also analysed using an apoptosis assay that measures amount of DNA fragmentation.

At 96h, downregulation of TFPIα and TFPIβ in SUM102 cells resulted in a significant 40% and 34% reduction of cleaved PARP, respectively, compared to the control (Figure 4.5.1.A and B). At 72 hours, an 18% reduction in amount of cleaved PARP was observed in cells with TFPIα

downregulated. No difference was observed at 120 hours in both cell samples. No effect on total PARP was observed. Neither did TFPIα or TFPIβ downregulation affect levels of total caspase-8 at any time point, and cleaved caspase-8 was too low to be detected. Furthermore, downregulation of TFPIα or TFPIβ resulted in a significant 25% and 30% reduction in DNA fragmentation, respectively, at 96 hours compared to the control. At 120 hours, no difference was observed (Figure 4.5.1C).

Since downregulation of TFPIα and TFPIβ resulted in a decrease in apoptosis, relevant proteins were investigated for their involvement in the effect on apoptosis. Previous studies have indicated that Akt, NF-κB and TNF-α proteins are involved in TFPI regulated apoptosis. In addition, the effect of TFPI on apoptosis has been suggested to be independent of TF. To further analyse the involvement of these proteins, SUM102 cells with TFPIα or TFPIβ downregulated were treated with inhibitors targeting the Akt, NF-κB, TNF-α, TF or PAR-2 proteins (as described in section 3.5.1). The effect on apoptosis was then analysed by Western blotting, with caspase-8 and PARP as apoptotic markers. No differences in amount of total PARP or total caspase-8 were observed in TFPI downregulated cells, untreated or treated with inhibitors (data not shown). Furthermore, the cleaved PARP fragment was not detected with Western blotting in these samples.

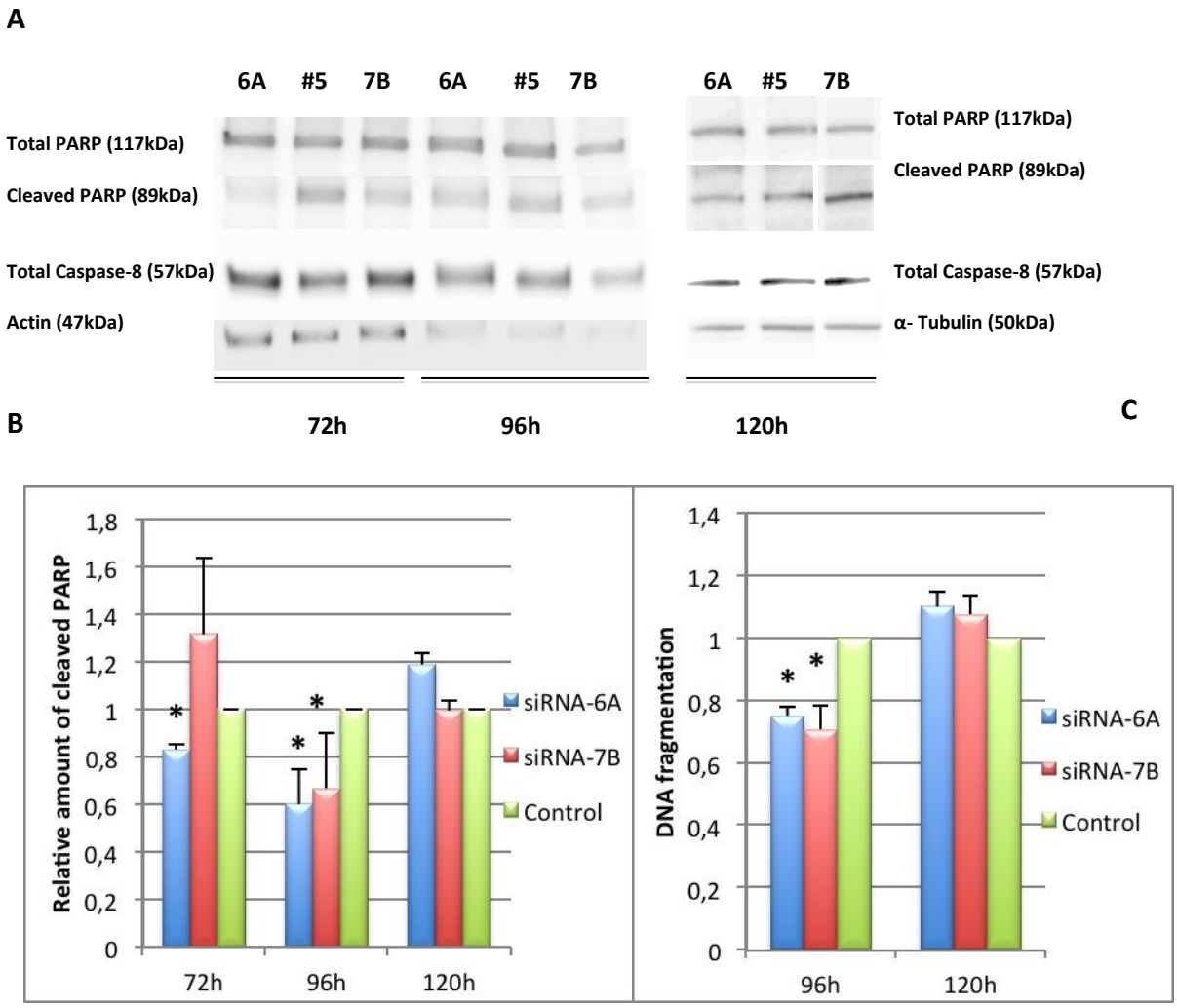

Figure 4.5.1. Effect of downregulation of TFPIα or TFPIβ in SUM102 cells on apoptosis. The cells were transfected with siRNA-6A, siRNA-7B or control siRNA and cells harvested after 72, 96 and 120h. (A) Western blot analysis of amount of total PARP, cleaved PARP and total caspase-8, with actin or α- tubulin as loading control. One representative experiment of X ≥ 2 experiments is shown for each time point. (B) Quantification of relative amount of cleaved PARP, using the Image QuantTL software. The values were corrected against actin or a-tubulin and the control. Mean values (n ≥2) + SD of one experiment are shown (C) Amount of DNA fragmentation was measured in fresh cell lysates and the values were subtracted from the background and corrected against the control. Mean values (n=2) + SD of one experiment are shown.

4.5.2 Effect of TFPIα and TFPIβ overexpression on apoptosis in HCC1500 cells

To verify that the effects on apoptosis were TFPI specific, similar experiments were performed with TFPIα or TFPIβ overexpression in HCC1500 cells.

Overexpression of TFPIα and TFPIβ resulted in a 23% and 7% reduction in amount of total PARP and a 42% and 7% reduction in amount of cleaved PARP, respectively, compared to the control (Figure 4.5.2A and B). Amount of total caspase-8 was also reduced with 53% and 12% in cells with TFPIα or TFPIβ overexpressed, respectively. Furthermore, overexpressed TFPIβ increased DNA fragmentation with 15%, while no effect was seen with TFPIα (Figure 4.5.2C).

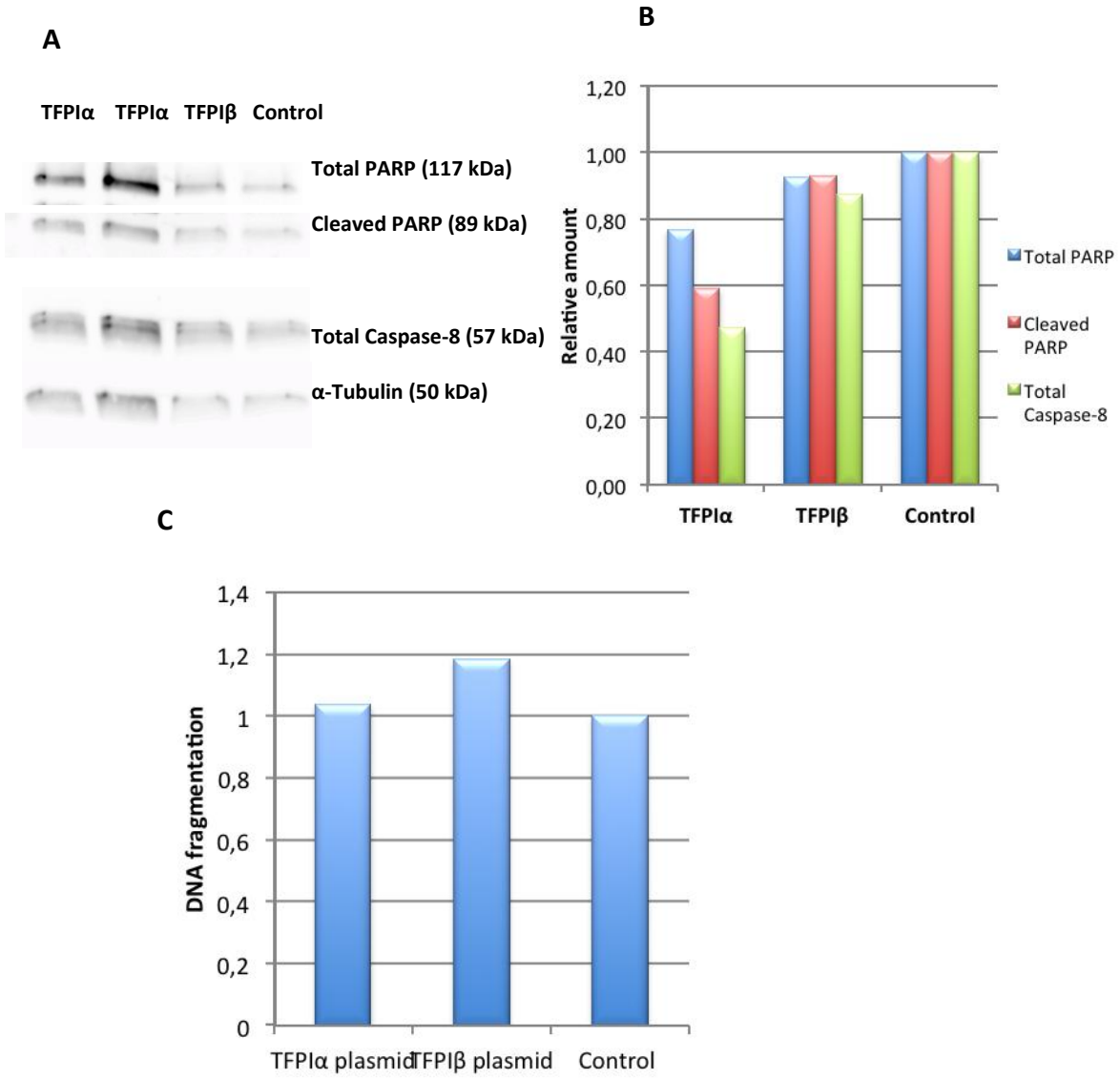

Figure 4.5.2. Effect of TFPIα and TFPIβ overexpression on apoptosis in HCC1500 cells. The cells were transfected with TFPIα, TFPIβ or control plasmid and harvested after 144h. (A) Western blot analysis of amount of total PARP, cleaved PARP and total Caspase-8 with α-tubulin as loading control. (B) Quantification of relative amount of total PARP, cleaved PARP and total caspase-8, using the Image QuantTL software. The values were corrected against α-tubulin and the control. (C) Amount of DNA fragmentations was measured in fresh cell lysates and the values were subtracted from the background and corrected against the control. Values of one experiment are shown.

4.6 Effect of TFPIα and TFPIβ on TNF-α levels

In earlier studies, TFPI was observed to have an affect on TNF-α levels in the SK-BR-3 breast cancer cell line. To analyse this effect further, HCC1500 and SUM102 cells were up- and downregulation with TFPIα and TFPIβ, respectively and TNF-α levels were measured in the cell media. Upregulation of TFPIα in HCC1500 cells resulted in a 2,7-fold increase in TNF-α antigen levels, while no difference was found in HCC1500 cells with TFPIβ upregulated (Figure 4.6). TNF-α antigen levels were not detectable (below lowest standard) in SUM102 cells with TFPIα and TFPIβ downregulated and cells with control siRNA.

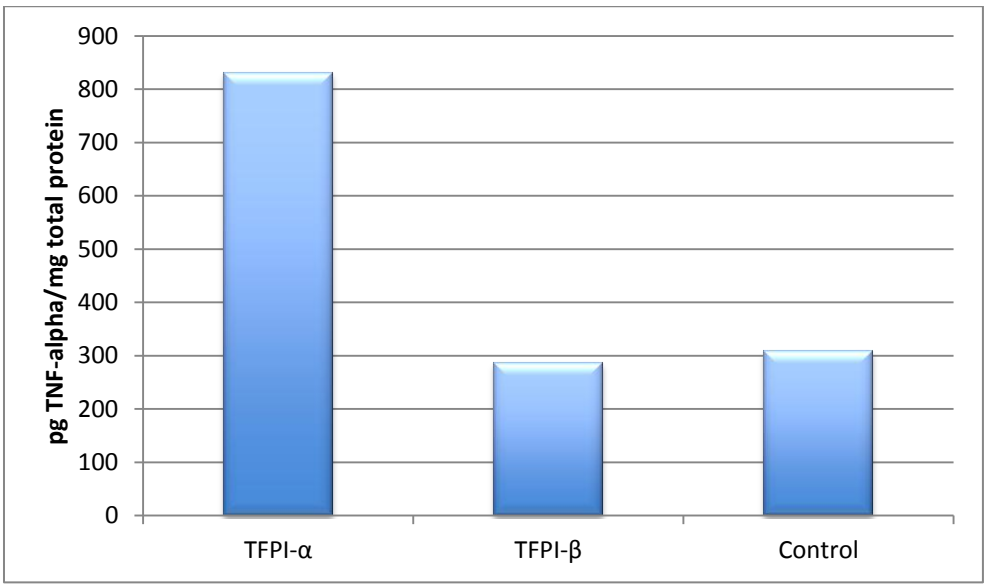

Figure 4.6.TNF-α antigen levels in TFPIα and TFPIβ upregulated HCC1500 cells .The cells were transfected with TFPIα, TFPIβ and control plasmid and harvested after 144h. Amount of TNF-α antigen levels in the cell media was measured and corrected against cellular total protein. Values of one experiment are shown.

4.7 Effect of TFPIα and TFPIβ downregulation on Akt phosphorylation in SUM102 cells

TFPI has earlier been shown to induce apoptosis by inhibiting the PI3-Kinse-Akt pathway. To further investigate the involvement of this pathway, the phosphorylation status of Akt was analysed in SUM102 cells with TFPIα and TFPIβ downregulated. The effect was studied with Western blotting using the p-Akt antibody. Negligible p-Akt was detected in both dowregulated samples stimulated for 0 min, showing that the stimulation was successful

(Figure 4.7A). Although not significant (high standard deviations), downregulation of TFPIα resulted in a 1,34- and 1,72-fold increase of Akt phosphorylation at 5 and 10 min, respectively. No difference was seen in cells with TFPIβ downregulated at 5min, while a significant 1,35-fold increase of Akt phosphorylation was shown at 10 min (Figure 4.7B).

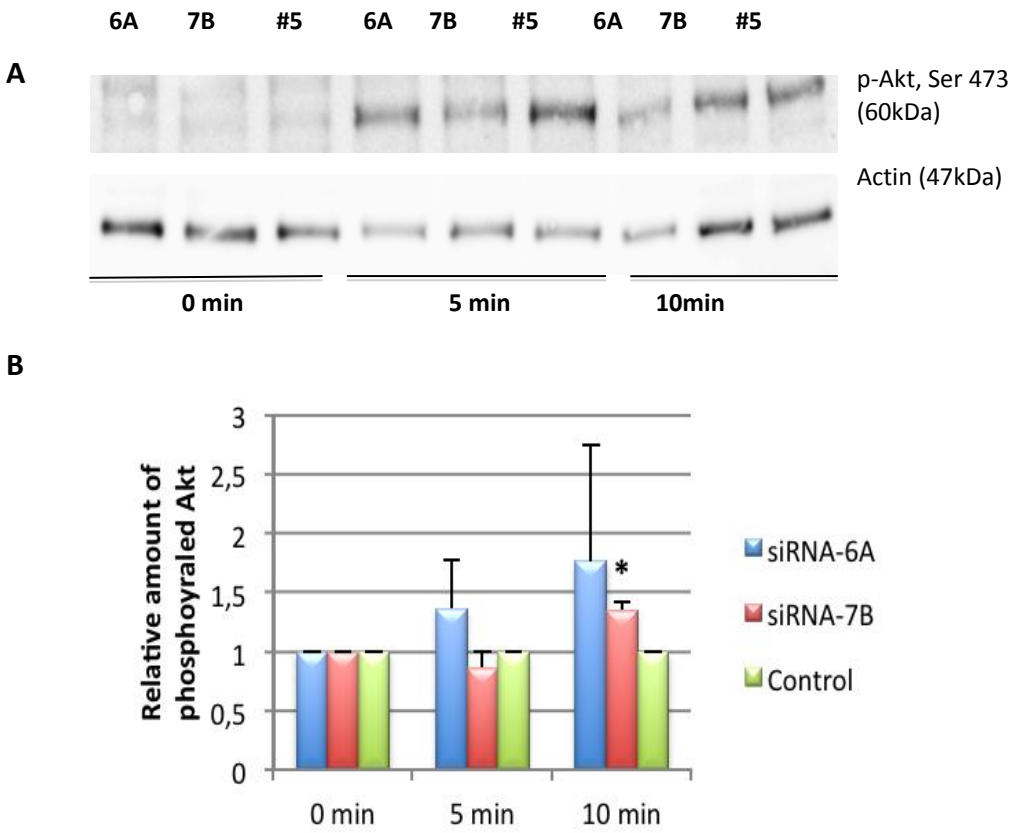

Figure 4.7 The effect of TFPIα and TFPIβ downregulation on Akt phosphorylation in SUM102 cells. The cells were transfected with siRNA-6A, 7B or control siRNA and stimulated with serum for 0, 5 and 10min, 96h after transfection (A) Western blot analysis of amount of phosphorylated Akt, with Actin as a loading control. One representative experiment of two is shown (B) Quantification of relative amount of phosphorylated Akt, using the Image QuantTL software. The values were corrected against Actin, the control and the corresponding 0min values. Mean values (n = 2) +SD of two experiments are shown.

5. Discussion

Patients with cancer have a higher risk of developing thrombotic diseases and visa versa (Mandalà et al. 2003; Varki 2007). TF is indicated to be the link between these diseases, which is mainly known for its role in initiating blood coagulation by binding and activating FVII (Gomez & McVey 2006; Rickles & Falanga 2001). TFPI inhibits TF initiated blood coagulation by binding to FXa and the TF-FVIIa complex (Broze et al. 1990). TFPIα and TFPIβ have been found expressed in different types of tumor derived breast cancer cells, with TFPIα as the dominant isoform (Stavik et al. 2013). Furthermore, recent studies reported that TFPIα and TFPIβ have anti-tumor effects in breast cancer cells (Stavik et al. 2010; Stavik et al. 2011). These results indicate that TFPI plays a role in cancer biology. An understanding of the molecular mechanism underlying these effects of TFPI may lead to increased knowledge of the connection between blood coagulation and cancer, and could potentially give rise to individual therapy for cancer patients.

The main aims of this study were to select siRNA oligonucleotides that efficiently downregulated TFPIα, to efficiently down- and upregulate TFPIα and TFPIβ, separately, in triple negative and *TP53* wild type breast cancer cells, to analyse the effects of these manipulations of TFPIα and TFPIβ expression on growth and apoptosis, and to study some potential molecular mechanisms responsible the effect of TFPIα and TFPIβ on apoptosis.

5.1 Downregulation of TFPIα and TFPIβ

5.1.1. Screening and optimization of selected TFPIα siRNA oligonucleotides

Total TFPI (α+β) and TFPIβ have in previous studies been effectively downregulated (Stavik et al. 2010; Stavik et al. 2011), but not TFPIα alone. To selectively downregulate TFPIα, four new TFPIα specific siRNAs and two in-house siRNAs were tested for their efficiency and specificity in HEK293T cells. All the four new siRNAs showed high TFPIα knock down efficiencies. Since all the new 27nt blunt-end TFPIα siRNAs showed higher efficiency than the two in-house 21nt siRNAs, it might be indicated that 27nt siRNAs are more efficient than 21nt siRNAs. This is in correspondence with Kim *et al.* who reported that 27nt long dsRNA

molecules were more effective than 21nt molecules, probably because these larger molecules are cleaved by Dicer when introduced in to the cell and the resulting siRNAs are then directly linked to the natural RISC formation in cells (Kim, D. H. et al. 2005). Although not efficient in this thesis, an earlier study has shown that a shRNA with the same sequence as one of the in-house siRNAs, downregulated the TFPIα mRNA expression in ECV304 endothelium-like human cells with high efficiency (Piro & Broze 2004). This indicates that different cells and conditions may have large impact on the efficiencies of siRNAs. In addition, since Piro and Broze used stable cell lines, in contrast to transient cells in this thesis, the use of different cell models may have influenced these results (discussed further in section 5.5)

The three siRNAs that showed the highest efficiency in the HEK293T cells were further tested and the transfection conditions were optimized in the SUM102 breast cancer cells. Two of these three siRNAs were selected for use in further experiments. However, the TFPIα knock down was generally less efficient in the SUM102 cells compared to the HEK293T cells, confirming that knock down efficiency may be cell type dependent.

5.2.2 The TFPIα and TFPIβ knock down cell model

TFPIα and TFPIβ was knocked down in SUM102 cells with siRNAs and the expression was measured at the mRNA and the protein level. The two 21nt siRNAs used to dowregulate TFPIβ had previously been selected and optimized. TFPIα and TFPIβ was efficiently downregulated at the mRNA level between 48-120h for TFPIα and between 24-96h for TFPIβ. TFPIα was less downregulated than TFPIβ at almost all time points. The effect of TFPIα downregulation at the protein level in cell media was most efficient between 72-96h, while the effect was abolished after 120h. Furthermore, in cells with TFPIβ downregulated the effect was measured in the cell lysate since TFPIβ is not secreted, and at 72h the downregulation was most efficient. No difference in TFPIα protein levels was detectable in the cell lysate. Collectively, it was demonstrated that the TFPI knock down effect was not as efficient at the protein level compared to the mRNA level, neither for TFPIα nor TFPIβ.

In this thesis, amount of total TFPI in the cell lysate (control samples) was 40-fold lower compared to amount of TFPI in the cell media. Similarly, a recent study found that the amount of total TFPI in the cell lysate of SUM102 cells was about 5-fold lower compared to the amount of TFPIα in the cell media (Stavik et al. 2013). The minor TFPIβ downregulation at the protein level in this thesis may therefore be explained by the low endogenous expression of TFPIβ in these cells, hence making it difficult to detect even lower amounts of TFPIβ after downregulation. The same study by Stavik and co-workers showed that there are low amounts of TFPIα in the cell lysate because this isoform is mostly secreted in the cell media. The low downregulation of TFPIα in the cell lysate may therefore also be due to the originally low amounts of this isoform in the lysate. The downregulation effect at the protein level for TFPIα in cell media was reflected by the moderate downregulation at the mRNA level.

The TFPIα and TFPIβ knock down model may be very useful in functional experiments for studying the effect of the TFPI isoforms on different cancer cell properties. However, since the TFPI downregulation was not optimal, the isoform specific effects of TFPIα and TFPIβ may be difficult to observe due to high background from untransfected cells. The model may therefore be most applicable in initial studies to indicate possible effects, while other models may be used later to confirm the effects. For further functional studies, the most efficient TFPIα siRNAs are currently in progress of being cloned as shRNAs in plasmid vectors. These shRNA plasmids will be transfected into SUM102 cells to make stable cell lines with constant expression of the shRNAs and thereby stable TFPIα downregulation.

5.3 Overexpression of TFPIα and TFPIβ

In this thesis, TFPIα and TFPIβ was overexpressed in the HCC1500 breast cancer cells. The HCC1500 cell line was characterized in this thesis as basal-B and triple negative (not expressing ER, PR or HER2) based on a study done by Neve and co-workers in 2006 (Neve et al. 2006). However, later another study was found where this cell line was characterized as luminal and to have expression of ER and PR (Kao et al. 2009). Possible reasons for why these two studies are inconsistent may be that they used different arrays to analyse the

gene expression, or that they used different gene markers when doing the cluster analysis. The researchers that established the HCC1500 cell line characterized it as ER and PR positive (Gazdar et al. 1998), which indicates that the HCC1500 cells may not be as similar to the SUM102 cells as originally assumed. In addition, unlike the SUM102 cell line, the HCC1500 cell line is not considered invasive.

5.3.1 The TFPIα and TFPIβ overexpression model

Optimization of plasmid transfection in the HCC1500 cells with the GFP plasmid showed that the TransIT-2020 reagent was the most efficient transfection reagent and that the GFP expression was stable from 48 to 120h. This was probably due to the surprisingly slow proliferation of these cells, resulting in plasmid concentrations remaining relatively high within the cells.

Transfection of HCC1500 cells with TFPIα and TFPIβ plasmids resulted in an efficient overexpression of both isoforms at both the mRNA level and protein level. The overexpression was 40- and 50- times higher at the mRNA level compared to the protein level for TFPIα and TFPIβ, respectively. Since both isoforms were efficiently overexpressed in the HCC1500 cells, the model could be used in further studies. However, this TFPI overexpression model may not be optimal for functional cell studies due to a low proliferation rate, which was experienced during the experimental work in this study. Several weeks were required to obtain enough cells to do one functional study. The model is thus perhaps more suited for investigating different molecular effects of the TFPIα and TFPIβ overexpression. For example, the model can be used to study the effect of TFPI upregulation on activity or levels of proteins involved in apoptosis, such as the TNF-α and caspase-8 proteins studied in this thesis. For further studies, stable HCC1500 cell lines with constant overexpression of TFPIα or TFPIβ are currently in progress in our lab.

TFPIα showed considerably higher upregulation than TFPIβ, both at the mRNA and the protein level. This could potentially have been due to low quality of the TFPIβ plasmid, such as the presence of contaminants, less supercoiled structure, or incorrect plasmid quantification. However, when analysing the plasmids with gel-electrophoresis, both the

TFPIα and the TFPIβ plasmid showed similar amounts of supercoiled structures. Furthermore, when isolating the plasmids, both plasmids showed optimal $OD^{260/280}$ values, thereby indicating that the plasmid solutions contained minimal protein and/or phenol contamination. Another reason for the observed difference in upregulation may be that TFPIα generally is more efficiently overexpressed in the HCC1500 cells than TFPIβ.

5.4 Functional studies of the effect of down- or upregulation of TFPIα and TFPIβ

5.4.1 Effect of TFPIα or TFPIβ downregulation on growth of SUM102 cells

Cancer cells often grow uncontrolled by being unresponsive to antigrowth signals and being self-sufficient in growth signals (Hanahan & Weinberg 2000). In this thesis, the effect of TFPIα or TFPIβ downregulation on cell growth in SUM102 breast cancer cells was evaluated with cell count or total protein quantification. Downregulation of TFPIα, somehow surprisingly, showed a significant decrease in number of living cells and amount of total protein 72h after transfection, compared to the control. Downregulation of TFPIβ showed no difference in growth, except for total protein at 96 hours. These results apparently indicated that downregulation of TFPIα inhibited the growth of SUM102 cells 72h after transfection, while downregulation of TFPIβ did not affect the growth.

The two methods of measuring the cell growth, cell count and total protein quantification, provided almost similar results. However, some differences occurred, demonstrating the importance of using several methods to determine cell growth. Alternative methods exist, like for example the WST-1 reagent that Stavik *et al.* used to measure the proliferation of SUM102 cells with total TFPI (α+β) downregulated. They did, however, not find any differences in cell growth properties (Stavik et al. 2010). This finding is in accordance with the TFPIβ growth experiment in this thesis, indicating that the result Stavik and co-workers obtained by downregulating TFPIα and TFPIβ together may have been caused by a masking effect of TFPIβ on the effect of TFPIα. Another possible reason for the different result with downregulated TFPIα in this thesis compared to downregulated total TFPI (α+β) in the study

by Stavik *et al.*, may be the use of different cell models (transient and stable cell lines) as further discussed in section 5.5. The effect of TFPIα downregulation on cell growth has never been studied before, and is therefore new information regarding effect of this isoform on breast cancer cell growth.

Although Stavik and co-workers did not find any effect on cell growth with downregulated TFPI, they observed that separate overexpression of TFPIα and TFPIβ inhibited the proliferation of the breast cancer cell line SK-BR-3 after 96 hours (Stavik et al. 2010). A possible reason for why this result is different from the result obtained with downregulated TFPIα and TFPIβ in this thesis may be the use of different cell lines (discussed in section 5.5). Moreover, other studies have found that full length rTFPI inhibited the growth of mesengial cells, endothelial cells, smooth muscle cells, melanomas, carcinomas and rat glioma cells (Hembrough et al. 2001; Kamikubo et al. 1997; Liang et al. 2009). However, since these studies applied rTFPI to the cells, their results are not directly comparable to the knockdown of endogenous TFPI in this thesis.

In addition to the points discussed above, another reason for the reduction in growth observed with downregulated TFPIα in this thesis, may be that the new 27nt blunt-end siRNAs used to downregulate TFPIα could have been toxic to the SUM102 cells. Larger and blunt-end siRNAs have indeed been reported in a study to be more toxic than the shorter siRNAs with nucleotide overhangs (Marques et al. 2006). In fact, in this thesis it was observed by microscopy that many cells died after 24 hours when transfected with the 27nt TFPIα siRNAs, compared to the 21nt TFPIβ siRNAs and the control siRNA. 27nt control siRNAs and TFPIβ siRNAs were also searched for, but nothing was found. In support of the point discussed in this section that the 27nt TFPIα specific siRNAs may have been toxic to the cells and thus caused cell death, the reduced cell growth observed with downregulated TFPIα was most likely not caused by apoptotic cell death, but perhaps by necrosis (see next section).

5.4.2. Effect of TFPIα or TFPIβ down- or upregulation on apoptosis

Evasion of apoptosis is another gained ability of cancer cells (Hanahan & Weinberg 2000). The effect of down- and upregulation of TFPIα or TFPIβ on apoptosis in SUM102 cells and

HCC1500 cells, respectively, was assessed in this thesis with Western blotting and a DNA fragmentation ELISA assay. PARP and caspase-8 were used as apoptotic markers in Western blotting. PARP is normally a part of the cellular DNA repair system, but is cleaved and inactivated by the executioner caspase-3 upon induction of apoptosis in a cell. Caspase-8 is an initiator caspase in the extrinsic pathway and is cleaved and autoactivated after a death inducing ligand binds to a death receptor at the surface of cells. After activation, it further cleaves and activates executioner caspases, such as caspase-3 (Decker et al. 2000; Lawen 2003).

Downregulation of TFPIα or TFPIβ significantly reduced the amount of cleaved PARP at 96 hours. Since PARP is normally cleaved by caspase-3 when apoptosis is induced in a cell (Nicholson et al. 1995), the observed reduction in the amount of cleaved PARP indicated that TFPIα and TFPIβ reduced the induction of apoptosis in the SUM102 cells. This result supports a pro-apoptotic effect of TFPIα and TFPIβ in SUM102 cells, which is in line with a study done with CHO-K1 ovary cells where overexpressed total TFPI (α+β) was observed to increase the amount of cleaved PARP (Skretting et al. 2012). On the other hand, as opposed to cleaved PARP, no differences were seen with either TFPI isoform on the amount of total PARP or total caspase-8. The effect on apoptosis in this thesis should therefore be interpreted with caution, as further discussed in section 5.5. Nevertheless, this thesis is the first known report to study the effect on apoptosis with separately downregulated TFPIα and TFPIβ.

Moreover, a possible reason for the lack of effects on total PARP and total caspase-8 may be that there exist many challenges with Western blotting as a quantitative method. First, this method is a multistep procedure and errors may occur in each of these steps (Taylor et al. 2013). Use of loading controls that are equally expressed in all cells and conditions should normally correct for some of these errors (normalization). However, it has been reported that the protein expression of the standardly used loading controls GAPDH, α-tubulin and actin, showed variation between different experimental conditions (Aldridge et al. 2008). In addition, the amount of protein necessary for detection of target proteins is often too high for the loading control proteins, resulting in saturated signals of the loading controls, which make them unsuitable for normalization of target proteins (Taylor et al. 2013). Secondly, to use Western blotting for relative quantification of target proteins many criteria should be

fulfilled, such as a broad dynamic range of detection, high signal intensity and sensitivity, and stable duration of protein signal (GE Healthcare 2014). Thirdly, determination of amount of protein using a quantification software is a partly manually controlled process that may provide inaccurate quantification of the proteins, especially with high background. In addition to these challenges with Western blotting, the cell lysates that were used in the experiments probably contained many untransfected cells due to the low downregulation efficiency, observed especially at the protein level. These untransfected cells may have provided high background, and thus contributed to the lack of observable effects with total PARP and caspase-8. Therefore, to obtain greater and more significant effects on apoptosis with Western blotting, the SUM102 cells could have been co-transfected with the TFPIα or TFPIβ siRNAs together with quantum dots. These quantum dots are fluorescent nanocrystals that complex with the siRNAs and can be used to sort out cells that are successfully transfected with flow cytometry (Chen et al. 2005). This pool of transfected cells may then be analysed with Western blotting without the background effect of transfected cells and thus make it easier to observe potential effects.

To measure apoptosis by a more sensitive method, the amount of DNA fragmentation was also assessed in this thesis. The results indicated that downregulation of TFPIα or TFPIβ in SUM102 cells reduced the fragmentation of DNA, supporting that both TFPIα and TFPIβ may have a pro-apoptotic effect in SUM102 cells. Similarly, Stavik and co-workers observed that downregulation of total TFPI (α+β) in SUM102 cells also decreased DNA fragmentation (Stavik et al. 2010). However, since the experiment was only performed once, cautions should be taken with this result, as discussed further in section 5.5.

Overexpressed TFPIα and TFPIβ in HCC1500 cells resulted in decreased amount of total PARP and total caspase-8, however, the effect with TFPIβ on total PARP and caspase-8 was less compelling. This result indicated that TFPIα induced apoptosis in HCC1500 cells. In agreement with this result, a study in human SMCs reported that full length rTFPI induced apoptosis by reducing the amount of total caspase-8 (Dong et al. 2011). On the other hand, Skretting and co-workers found that overexpression of TFPI in CHO-K1 ovary cells increased the amount of total PARP (Skretting et al. 2012). However, in that study they proposed that TFPI mostly induced apoptosis independent of caspase-3, by activating rather than

inactivating PARP. A possible reason for these different results with total PARP may be that TFPI induced apoptosis through different pathways in the CHO-K1 cell line and the SUM102 cell line. In addition to reduced amounts of total PARP and caspase-8, overexpression of TFPIα or TFPIβ also reduced the amount of cleaved PARP, which is comparable to that was observed with downregulated TFPIα and TFPIβ in SUM102 cells in this thesis. It is somewhat strange that a reduction of both total PARP and cleaved PARP was observed for upregulated TFPIα and TFPIβ in this thesis. Normally, only one of them is reduced and the other is increased. The challenges with Western blotting mentioned above may have affected these results. In addition, the experiment was only performed once and cautions should therefore be taken with these results (discussed in section 5.5)

In the HCC1500 cells with TFPIβ overexpressed, a slight increase in DNA fragmentation was observed, while no effect was observed with TFPIα. This result thus indicated that TFPIβ induced apoptosis in HCC1500 cells. The result with TFPIβ is in line with a study where overexpressed TFPIα and TFPIβ induced apoptosis in SK-BR-3 breast cancer cells (Stavik et al. 2010), and studies where full length rTFPI was reported to induce apoptosis in HUVECs and rat MsCs (Dong et al. 2011; Hamuro et al. 1998; Lin et al. 2007).

Taken together, the TFPIα or TFPIβ down- and upregulation in the SUM102 and HCC1500 cell lines, respectively, suggests that the effects on apoptosis are TFPI specific. However, as discussed in section 5.5, it may be complicated to compare results obtained in different cell lines. Moreover, both up-and downregulation of TFPIα and TFPIβ showed that both isoforms have pro-apoptotic effect. The pro-apoptotic effect of TFPIα has been suggested to be dependent on its third Kunitz domain and the C-terminal end (Lin et al. 2007). However, since TFPIβ do not posses these domains, the results in this thesis demonstrated that these domains may not explain all apoptotic effects of TFPI. TFPIβ has been suggested to mediate its effect through the GPI anchor, which have been reported to have signalling properties and to be associated with lipid rafts that functions as signalling transduction platforms (Trotter et al. 2000). Separately, downregulation of TFPIα or TFPIβ in SUM102 cells showed roughly the same effect on apoptosis, indicating that both of these isoforms have similar pro-apoptotic effects in these cells. On the other hand, overexpressed TFPIα reduced the amount of total PARP and caspase-8 more than TFPIβ in the HCC1500 cells, while

overexpressed TFPIβ increased the DNA fragmentation and TFPIα did not. It is thus challenging to conclude whether the TFPI isoforms have different functions and effects on apoptosis in the HCC1500 cells. The greater effect of TFPIα on caspase-8 and PARP may be due to TFPIα being more overexpressed than TFPIβ in the HCC1500 cells, however this cannot explain the DNA fragmentation result. Since the upregulation of the TFPI isoforms showed different effects on apoptosis with Western blotting and ELISA, it was demonstrated that several methods should be used for measuring apoptosis and that more than one experiment should be performed to obtain valuable results (further discussed in section 5.5).

5.4.3. Molecular mechanisms involved in the effect of TFPIα and TFPIβ on apoptosis

The Akt protein is a part of the PI3-Kinase-Akt pathway, which is activated upon stimulation with growth and survival (anti-apoptotic) signalling molecules (Kulik et al. 1997). Assessment of the phosphorylation status of Akt in TFPIα or TFPIβ downregulated cells in this thesis demonstrated that downregulation of TFPIβ significantly increased the phosphorylation of Akt. This result thus indicates that the PI3-Kinase-Akt pathway may be involved in TFPIβ regulated apoptosis. Although not significant, downregulation of TFPIα also showed increased Akt phosphorylation. These results are in line with another study that found that full length rTFPI reduced Akt phosphorylation in rat MsCs (Lin et al. 2007). In contrast, Stavik and co-workers found that downregulated TFPIβ in MDA-MB-231 breast cancer cells and downregulated total TFPI (α+β) in SUM102 cells had no effect on Akt phosphorylation (Stavik et al. 2011). These differences may be due to cell type specific differences (Further described in section 5.5).

TNF-α is a ligand that binds the TNF-α receptor and induces apoptosis through the extrinsic pathway (Alberts et al. 2008). Stavik and co-workers have previously found that overexpressed TFPIα increased the levels of TNF-α in SK-BR-3 cells, while TFPIβ had a negligible effect (Stavik et al. 2010). Comparably, in this thesis it was demonstrated that overexpressed TFPIα increased the amount of TNF-α in HCC1500 cells, while overexpressed TFPIβ showed no effect. These results thus indicate that the effect on apoptosis by TFPIα may be mediated through TNF-α, while the effect of TFPIβ may be mediated through other

mechanism(s). However, the TFPIα mRNA and protein expression levels in the HCC1500 cells were significantly higher than for TFPIβ, which could have influenced the results.

TF has been reported to stimulate cancer cell development both coagulation dependent through thrombin and PAR-1, and coagulation independent by binding to FVII and activating PAR-2 (Lima & Monteiro 2013; Ott et al. 2005; van den Berg et al. 2012). In addition, TF has been found to be expressed in different tumor derived breast cancer cells (Stavik et al. 2013). Moreover, recent studies have shown that expression of TF and PAR1/2 in breast cancer cells followed the expression of TFPI, indicating that the effect of TFPI on apoptosis might be dependent on TF (Stavik et al. 2010). On the other hand, studies in HUVECs and rat MsCs have reported that the effect of full length rTFPI on apoptosis was independent of TF (Hamuro et al. 1998; Lin et al. 2007). In addition to involvement of TF, TFPI was shown in CHO-K1 ovary cells and SK-BR-3 breast cancer cells to increase the activity of the NF-κB protein (Skretting et al. 2012; Stavik et al. 2010), where TNF-α was suggested to induce the activation of NF-κB in the SK-BR-3 cells (Stavik et al. 2010). These results thus indicate that also NF-κB might be involved in the TFPI regulated apoptotic effects.

To further elucidate the role of TF, PAR-2, NF-κB, Akt and TNF-α proteins in the effect of TFPI on apoptosis, SUM102 cells with TFPIα or TFPIβ downregulated were treated with different inhibitors targeting these five proteins. However, the time points and concentrations used in this thesis did not indicate any effects on caspase-8 or total PARP in untreated or inhibitor treated cells with TFPIα or TFPIβ downregulated. In addition, the cleaved PARP protein was not detectable with Western blotting in these experiments. A possible reason for the lack of effects may be that TFPIα and TFPIβ were not efficiently downregulated in the SUM102 cells in these experiments. In addition, as already mentioned I section 5.4.2, a background effect of untransfected cells and other challenges may have influenced the results.

5.5 Limitations

In this thesis, several limitations exist. First, the t-test that was used to compare two groups was based on few replicates, with only two biological replicates in some experiments. So few replicates can in reality not be used to calculate statistics. These analyses were therefore only used to point out some trends observed in this thesis. In addition, most of the functional studies in this thesis were only performed once, meaning that the results may only be used to indicate effects. Cautions should therefore be taken in drawing conclusions from the experiments with few data point. In general, at least three individual experiments, each with biological replicates, should be conducted to obtain trustworthy results.

In this thesis, transient TFPI down-and upregulation cell models were used, while the studies that this thesis was compared with for the most used stable cell models. There exist some challenges with comparing the TFPI effects in such different cell models. In stable cell lines, a TFPI specific shRNA or TFPI cDNA expression construct are inserted in to the cell genome and thereby express the TFPI shRNA or mRNA continuously as the cells replicate, and a continuous down- or upregulation of TFPI is maintained. In transient cells, however, the effect is lost after some time because the cells divide and the siRNAs or plasmids disappears (Würtele et al. 2003). Furthermore, the expression constructs used in stable cell models may be inserted into coding regions and thus potentially cause mutations, or may induce changes in the chromatin structure that can alter the gene expression. In worst case, such alterations to the host DNA may alternate the phenotype of some cells (Covarrubias et al. 1987; Remus et al. 1999; Würtele et al. 2003). Based on the difference between transient cells and stable cell lines, these two models may provide different effects of TFPI on cell growth and apoptosis, making it challenging to compare results obtained in the different cell models. Moreover, it is generally difficult to compare different cell experiments across different cell lines. Cell type specific properties may have distinct impacts on the effect of TFPI on apoptosis and cell growth.

6. Conclusions

In this thesis, the separate effects of TFPIα and TFPIβ isoforms on apoptosis and cell growth in breast cancer cells were investigated. In addition, were some potentially molecular mechanisms underlying the effects on apoptosis evaluated. The main conclusions in this thesis are:

- Four new TFPIα specific siRNAs were selected and all four showed high knock down efficiency in HEK293T cells. Out of the four siRNAs, the two most efficient siRNAs against TFPIα in the SUM102 cells were selected for further use.
- Transient transfection of SUM102 cells with two TFPIα and TFPIβ specific siRNAs resulted in an efficient downregulation of TFPIα and TFPIβ respectively, at the mRNA level, while the downregulation was less efficient at the protein level. Due to less efficient TFPIα and TFPIβ knock down at protein level, this downregulation cell model may be useful to indicate effects that may be further elucidated in other models.
- Transient transfection of HCC1500 cells with TFPIα and TFPIβ plasmids resulted in an efficient overexpression of both the TFPIα and the TFPIβ both at the mRNA level and the protein level. This cell model may therefore be applicable for studying the effects of TFPIα and TFPIβ upregulation at the molecular level, but not as good at the functional level, because of low growth rate of the HCC1500 cells.
- Cell count and total protein quantification indicated that downregulation of TFPIα may have inhibited growth of SUM102 cells 72 hours after transfection, while TFPIβ did not.
- Western blot quantification of cleaved PARP, total PARP and total caspase-8 and measurment of DNA fragmentation indicated that down- and upregulation of TFPIα and TFPIβ reduced and induced apoptosis, respectively, in breast cancer cells.
- TNF-α antigen quantification indicated that TNF-α might be involved in TFPIα mediated apoptosis in HCC1550 cells, while TFPIβ might use another mechanism.
- Assessment of Akt phosphorylation indicated that the PI3-Kinase-Akt pathway might be involved in TFPIα and TFPIβ regulated apoptosis in SUM102 cells.

6.1 Further perspectives

- The functional experiments with down-and upregulated TFPIα or TFPIβ on apoptosis and cell growth should be repeated to confirm the results in this study and to draw a clear conclusion.
- Stable HCC1500 cell lines with TFPIα or TFPIβ overexpressed, and SUM102 cell lines with TFPIα downregulated should be tested and compared with the functional effects seen in the transient cells.
- The effect of Akt, TNF-α, PAR-2, TF and NF-κB on TFPI induced apoptosis should also be evaluated in HCC1500 cells with TFPIα or TFPIβ upregulated, and in stable SUM102 cell lines with TFPIα and TFPIβ downregulated. In addition, alternative time points and concentrations of the inhibitors used should be tested.
- Other proteins and pathways that have been found to be involved in other cells in other studies should also be investigated, such as the JAK-2/STAT-3 pathway.
- The effect of the TFPI isoforms on growth and apoptosis should also be examined *in vivo,* for example in a mouse model
- The effects of TFPIα and TFPIβ on tumor characteristics in p53 wild type and mutant cell lines could be compared to investigate the role of p53 in TFPI mediated effects.
- The effect of down- and upregulation of TFPIα and TFPIβ in SUM102 and HCC1500 cell lines, respectively, on other aspects on cancer development should also be investigated, such as adhesion, migration and invasion.

7. References

Agrawal, N., Dasaradhi, P. V. N., Mohmmed, A., Malhotra, P., Bhatnagar, R. K. & Mukherjee, S. K. (2003). RNA Interference: Biology, Mechanism, and Applications. *Microbiology and Molecular Biology Reviews*, 67 (4): 657-685.

Alberts, B., Johnson, A., Lewis, J., Raff, M., Roberts, K. & Walter, P. (2008). *Molecular biology of the cell*. 5 ed. 711 Third Avenue, 8th floor, New York, NY 10017, USA: Garland science. 1267 pp.

Aldridge, G. M., Podrebarac, D. M., Greenough, W. T. & Weiler, I. J. (2008). The use of total protein stains as loading controls: An alternative to high-abundance single-protein controls in semi-quantitative immunoblotting. *Journal of Neuroscience Methods*, 172 (2): 250-254.

Amarzguioui, M., Peng, Q., Wiiger, M. T., Vasovic, V., Babaie, E., Holen, T., Nesland, J. M. & Prydz, H. (2006). Ex vivo and in vivo delivery of anti-tissue factor short interfering RNA inhibits mouse pulmonary metastasis of B16 melanoma cells. *Clin Cancer Res*, 12 (13): 4055-61.

Amirkhosravi, A., Meyer, T., Chang, J. Y., Amaya, M., Siddiqui, F., Desai, H. & Francis, J. L. (2002). Tissue factor pathway inhibitor reduces experimental lung metastasis of B16 melanoma. *Thromb Haemost*, 87 (6): 930-6.

Bacac, M. & Stamenkovic, I. (2008). Metastatic cancer cell. *Annu. Rev. pathmechdis. Mech. Dis.*, 3: 221-247.

Baeriswyl, V. & Christofori, G. (2009). The angiogenic switch in carcinogenesis. *Seminars in Cancer Biology*, 19 (5): 329-337.

Bajaj, M. S., Kuppuswamy, M. N., Saito, H., Spitzer, S. G. & Bajaj, S. P. (1990). Cultured normal human hepatocytes do not synthesize lipoprotein-associated coagulation inhibitor: evidence that endothelium is the principal site of its synthesis. *Proceedings of the National Academy of Sciences*, 87 (22): 8869-8873.

Bergers, G. & Benjamin, L. E. (2003). Tumorigenesis and the angiogenic switch. *Nat Rev Cancer*, 3 (6): 401-10.

Blasco, M. A. (2005). Telomeres and human disease: ageing, cancer and beyond. *Nature Reviews Genetics*, 6 (8): 611-622.

Bos, J. L. (1989). ras Oncogenes in Human Cancer: A Review. *Cancer Research*, 49 (17): 4682-4689.

Broze, G. J., Girard, T. J. & Novotny, W. F. (1990). Regulation of coagulation by a multivalent Kunitz-type inhibitor. *Biochemistry*, 29 (33): 7539-7546.

Broze, G. J., Jr., Lange, G. W., Duffin, K. L. & MacPhail, L. (1994). Heterogeneity of plasma tissue factor pathway inhibitor. *Blood Coagul Fibrinolysis*, 5 (4): 551-9.

Broze, G. J., Jr. & Girard, T. J. (2013). Tissue factor pathway inhibitor: structure-function. *Front Biosci*, 17 (262-280).

Cantley, L. C. (2002). The phosphoinositide 3-kinase pathway. *Science*, 296 (5573): 1655-7.

Carrier, M., Le Gal, G. g., Wells, P. S., Fergusson, D., Ramsay, T. & Rodger, M. A. (2008). Systematic Review: The Trousseau Syndrome Revisited: Should We Screen Extensively for Cancer in Patients with Venous Thromboembolism? *Annals of Internal Medicine*, 149 (5): 323-333.

Carthew, R. W. & Sontheimer, E. J. (2009). Origins and Mechanisms of miRNAs and siRNAs. *Cell*, 136 (4): 642-55.

Chang, J. Y., Monroe, D. M., Oliver, J. A. & Roberts, H. R. (1999). TFPIbeta, a second product from the mouse tissue factor pathway inhibitor (TFPI) gene. *Thromb Haemost*, 81 (1): 45-9.
Chen, A. A., Derfus, A. M., Khetani, S. R. & Bhatia, S. N. (2005). Quantum dots to monitor RNAi delivery and improve gene silencing. *Nucleic Acids Research*, 33 (22): e190.
Chew, H. K., Wun, T., Harvey, D., Zhou, H. & White, R. H. (2006). Incidence of venous thromboembolism and its effect on survival among patients with common cancers. *Archives of Internal Medicine*, 166 (4): 458-464.
Christofori, G. & Semb, H. (1999). The role of the cell-adhesion molecule E-cadherin as a tumour-suppressor gene. *Trends Biochem Sci*, 24 (2): 73-6.
Coussens, L. M. & Werb, Z. (1996). Matrix metalloproteinases and the development of cancer. *Chem Biol*, 3 (11): 895-904.
Covarrubias, L., Nishida, Y., Terao, M., d'Eustachio, P. & Mintz, B. (1987). Cellular DNA rearrangements and early developmental arrest caused by DNA insertion in transgenic mouse embryos. *Molecular and cellular biology*, 7 (6): 2243-2247.
Cunningham, A. C., Hasty, K. A., Enghild, J. J. & Mast, A. E. (2002). Structural and functional characterization of tissue factor pathway inhibitor following degradation by matrix metalloproteinase-8. *Biochem. J.*, 367 (2): 451-458.
Dalby, B., Cates, S., Harris, A., Ohki, E. C., Tilkins, M. L., Price, P. J. & Ciccarone, V. C. (2004). Advanced transfection with Lipofectamine 2000 reagent: primary neurons, siRNA, and high-throughput applications
. *Methods*, 33 (2): 95-103.
Decker, P., Isenberg, D. & Muller, S. (2000). Inhibition of caspase-3-mediated poly (ADP-ribose) polymerase (PARP) apoptotic cleavage by human PARP autoantibodies and effect on cells undergoing apoptosis. *Journal of Biological Chemistry*, 275 (12): 9043-9046.
Di, Y., Liu, Z., Tian, J., Zong, Y., Yang, P. & Qu, S. (2010). TFPI or uPA–PAI-1 complex affect cell function through expression variation of type II very low density lipoprotein receptor. *FEBS Letters*, 584 (15): 3469-3473.
Dominska, M. & Dykxhoorn, D. M. (2010). Breaking down the barriers: siRNA delivery and endosome escape. *J Cell Sci*, 123 (Pt 8): 1183-9.
Dong, X., Song, L. P., Zhu, D. W., Zhang, H. L., Liu, L. X. & Leng, X. G. (2011). Impact of the tissue factor pathway inhibitor gene on apoptosis in human vascular smooth muscle cells. *Genet Mol Biol*, 34 (1): 25-30.
Esmon, C. T. (1989). The roles of protein C and thrombomodulin in the regulation of blood coagulation. *J Biol Chem*, 264 (9): 4743-4746.
Esmon, C. T. (2000). Regulation of blood coagulation. *Biochimica et Biophysica Acta (BBA) - Protein Structure and Molecular Enzymology*, 1477 (1–2): 349-360.
Ferlay, J., Soerjomataram, I., Ervik, M., Dikshit, R., Eser, S., Mathers, C., Rebelo, M., Parkin, D. M., Forman, D. & Bray, F. (2012). *GLOBOCAN 2012 v1.0, Cancer Incidence and Mortality Worldwide: IARC CancerBase No.11*. Lyon, France: International Agency for Research on Cancer; 2013. Available at: http://globocan.iarc.fr (accessed: 08.05).
Fu, Y., Zhao, Y., Liu, Y., Zhu, Y., Chi, J., Hu, J., Zhang, X. & Yin, X. (2012). Adenovirus-mediated tissue factor pathway inhibitor gene transfer induces apoptosis by blocking the phosphorylation of JAK-2/STAT-3 pathway in vascular smooth muscle cells. *Cell Signal*, 24 (10): 1909-17.
Garcia-Echeverria, C. & Sellers, W. R. (2008). Drug discovery approaches targeting the PI3K/Akt pathway in cancer. *Oncogene*, 27 (41): 5511-26.

Gazdar, A. F., Kurvari, V., Virmani, A., Gollahon, L., Sakaguchi, M., Westerfield, M., Kodagoda, D., Stasny, V., Cunningham, H. T., Wistuba, II, et al. (1998). Characterization of paired tumor and non-tumor cell lines established from patients with breast cancer. *Int J Cancer*, 78 (6): 766-74.

GE Healthcare. (2014). *Western Blotting: Principles and Methods*. 28-9998-97 Edition AC.

Girard, T. J., Eddy, R., Wesselschmidt, R. L., MacPhail, L. A., Likert, K. M., Byers, M. G., Shows, T. B. & Broze, G. J., Jr. (1991). Structure of the human lipoprotein-associated coagulation inhibitor gene. Intro/exon gene organization and localization of the gene to chromosome 2. *J Biol Chem*, 266 (8): 5036-41.

GOBO. Available at: http://co.bmc.lu.se/gobo/gsa.pl (accessed: 01.04.14).

Gomez, K. & McVey, J. H. (2006). Tissue Factor Initiated Blood Coagulation. *Frontiers in Bioscience*, 11: 1349-1350.

Hackeng, T. M., Sere, K. M., Tans, G. & Rosing, J. (2006). Protein S stimulates inhibition of the tissue factor pathway by tissue factor pathway inhibitor. *Proc Natl Acad Sci U S A*, 103 (9): 3106-11.

Hamuro, T., Kamikubo, Y.-i., Nakahara, Y., Miyamoto, S. & Funatsu, A. (1998). Human recombinant tissue factor pathway inhibitor induces apoptosis in cultured human endothelial cells. *FEBS Letters*, 421 (3): 197-202.

Hanahan, D. & Weinberg, R. A. (2000). The Hallmarks of Cancer. *Cell*, 100 (1): 57-70.

Hanahan, D. & Weinberg, Robert A. (2011). Hallmarks of Cancer: The Next Generation. *Cell*, 144 (5): 646-674.

Hembrough, T. A., Ruiz, J. F., Papathanassiu, A. E., Green, S. J. & Strickland, D. K. (2001). Tissue factor pathway inhibitor inhibits endothelial cell proliferation via association with the very low density lipoprotein receptor. *J Biol Chem*, 276 (15): 12241-8.

Hembrough, T. A., Swartz, G. M., Papathanassiu, A., Vlasuk, G. P., Rote, W. E., Green, S. J. & Pribluda, V. S. (2003). Tissue Factor/Factor VIIa Inhibitors Block Angiogenesis and Tumor Growth Through a Nonhemostatic Mechanism. *Cancer Research*, 63 (11): 2997-3000.

Hembrough, T. A., Ruiz, J. F., Swerdlow, B. M., Swartz, G. M., Hammers, H. J., Zhang, L., Plum, S. M., Williams, M. S., Strickland, D. K. & Pribluda, V. S. (2004). Identification and characterization of a very low density lipoprotein receptor-binding peptide from tissue factor pathway inhibitor that has antitumor and antiangiogenic activity. *Blood*, 103 (9): 3374-80.

Henriksen, R., Funa, K., Wilander, E., Bäckström, T., Ridderheim, M. & Öberg, K. (1993). Expression and Prognostic Significance of Platelet-derived Growth Factor and Its Receptors in Epithelial Ovarian Neoplasms. *Cancer Research*, 53 (19): 4550-4554.

Higuchi, D. A., Wun, T. C., Likert, K. M. & Broze, G. J., Jr. (1992). The effect of leukocyte elastase on tissue factor pathway inhibitor. *Blood*, 79 (7): 1712-9.

IARC TP53 Database. Available at: http://p53.iarc.fr/ (accessed: 01.04.14).

Iolascon, A., Giordani, L., Borriello, A., Carbone, R., Izzo, A., Tonini, G., Gambini, C. & Della Ragione, F. (2000). Reduced expression of transforming growth factor-beta receptor type III in high stage neuroblastomas. *British journal of cancer*, 82 (6): 1171.

Itakura, J., Ishiwata, T., Shen, B., Kornmann, M. & Korc, M. (2000). Concomitant over-expression of vascular endothelial growth factor and its receptors in pancreatic cancer. *International Journal of Cancer*, 85 (1): 27-34.

Iversen, N., Lindahl Ak Fau - Abildgaard, U. & Abildgaard, U. (1998). Elevated TFPI in malignant disease: relation to cancer type and hypercoagulation. (0007-1048 (Print)).
Jones, R. G. & Thompson, C. B. (2009). Tumor suppressors and cell metabolism: a recipe for cancer growth. *Genes Dev*, 23 (5): 537-48.
Kamikubo, Y.-i., Nakahara, Y., Takemoto, S., Hamuro, T., Miyamoto, S. & Funatsu, A. (1997). Human recombinant tissue-factor pathway inhibitor prevents the proliferation of cultured human neonatal aortic smooth muscle cells. *FEBS Letters*, 407 (1): 116-120.
Kao, J., Salari, K., Bocanegra, M., Choi, Y.-L., Girard, L., Gandhi, J., Kwei, K. A., Hernandez-Boussard, T., Wang, P., Gazdar, A. F., et al. (2009). Molecular Profiling of Breast Cancer Cell Lines Defines Relevant Tumor Models and Provides a Resource for Cancer Gene Discovery. *PLoS ONE*, 4 (7): e6146.
Kaufmann, S. H. & Hengartner, M. O. (2001). Programmed cell death: alive and well in the new millennium. *Trends in Cell Biology*, 11 (12): 526-534.
Kerr, J. F., Wyllie, A. H. & Currie, A. R. (1972). Apoptosis: a basic biological phenomenon with wide-ranging implications in tissue kinetics. *Br J Cancer*, 26 (4): 239-57.
Khorana, A. A., Francis, C. W., Culakova, E., Kuderer, N. M. & Lyman, G. H. (2007). Frequency, risk factors, and trends for venous thromboembolism among hospitalized cancer patients. *Cancer*, 110 (10): 2339-2346.
Kim, D. H., Behlke, M. A., Rose, S. D., Chang, M. S., Choi, S. & Rossi, J. J. (2005). Synthetic dsRNA Dicer substrates enhance RNAi potency and efficacy. *Nat Biotechnol*, 23 (2): 222-6.
Kim, H. E., Du, F., Fang, M. & Wang, X. (2005). Formation of apoptosome is initiated by cytochrome c-induced dATP hydrolysis and subsequent nucleotide exchange on Apaf-1. *Proc Natl Acad Sci U S A*, 102 (49): 17545-50.
Korc, M., Meltzer, P. & Trent, J. (1986). Enhanced expression of epidermal growth factor receptor correlates with alterations of chromosome 7 in human pancreatic cancer. *Proceedings of the National Academy of Sciences*, 83 (14): 5141-5144.
Kulik, G., Klippel, A. & Weber, M. J. (1997). Antiapoptotic signalling by the insulin-like growth factor I receptor, phosphatidylinositol 3-kinase, and Akt. *Molecular and cellular biology*, 17 (3): 1595-1606.
Lawen, A. (2003). Apoptosis—an introduction. *BioEssays*, 25 (9): 888-896.
Lea, T. (2008). *Immunologi og immunologiske teknikker*: Fagbokforlaget Vigmostad & Bjørke AS.
Liang, W., Cheng, J., Liu, R., Wang, J.-p., Mu, J.-g., Wang, Q.-h., Wang, H.-j. & Ma, D. (2009). Peptide corresponding to the C terminus of tissue factor pathway inhibitor inhibits mesangial cell proliferation and activation in vivo. *Peptides*, 30 (12): 2330-2336.
Lima, L. G. & Monteiro, R. Q. (2013). Activation of blood coagulation in cancer: implications for tumour progression. *Biosci Rep*, 33 (5).
Lin, Y. F., Zhang, N., Guo, H. S., Kong, D. S., Jiang, T., Liang, W., Zhao, Z. H., Tang, Q. Q. & Ma, D. (2007). Recombinant tissue factor pathway inhibitor induces apoptosis in cultured rat mesangial cells via its Kunitz-3 domain and C-terminal through inhibiting PI3-kinase/Akt pathway. *Apoptosis*, 12 (12): 2163-73.
Majno, G. & Joris, I. (1995). Apoptosis, oncosis, and necrosis. An overview of cell death. *Am J Pathol*, 146 (1): 3-15.

Mandalà, M., Ferretti, G., Cremonesi, M., Cazzaniga, M., Curigliano, G. & Barni, S. (2003). Venous thromboembolism and cancer:: new issues for an old topic. *Critical Reviews in Oncology/Hematology*, 48 (1): 65-80.

Maroney, S. A., Cunningham, A. C., Ferrel, J., Hu, R., Haberichter, S., Mansbach, C. M., Brodsky, R. A., Dietzen, D. J. & Mast, A. E. (2006). A GPI-anchored co-receptor for tissue factor pathway inhibitor controls its intracellular trafficking and cell surface expression. *J Thromb Haemost*, 4 (5): 1114-24.

Maroney, S. A. & Mast, A. E. (2008). Expression of Tissue Factor Pathway Inhibitor by Endothelial Cells and Platelets. *Transfus Apher Sci*, 38 (1): 9-14.

Maroney, S. A., Ellery, P. E. & Mast, A. E. (2010). Alternatively spliced isoforms of tissue factor pathway inhibitor. *Thrombosis Research*, 125, Supplement 1 (0): S52-S56.

Marques, J. T., Devosse, T., Wang, D., Zamanian-Daryoush, M., Serbinowski, P., Hartmann, R., Fujita, T., Behlke, M. A. & Williams, B. R. (2006). A structural basis for discriminating between self and nonself double-stranded RNAs in mammalian cells. *Nat Biotechnol*, 24 (5): 559-65.

Marusyk, A. & Polyak, K. (2010). Tumor heterogeneity: causes and consequences. *Biochim Biophys Acta*, 1805 (1): 105-17.

Mayor, S. & Riezman, H. (2004). Sorting GPI-anchored proteins. *Nat Rev Mol Cell Biol*, 5 (2): 110-20.

Mizejewski, G. J. (1999). Role of Integrins in Cancer: Survey of Expression Patterns. *Experimental Biology and Medicine*, 222 (2): 124-138.

Mosesson, M. W. (2005). Fibrinogen and fibrin structure and functions. *J Thromb Haemost*, 3 (8): 1894-904.

Ndonwi, M., Tuley, E. A. & Broze, G. J. (2010). The Kunitz-3 domain of TFPI-α is required for protein S–dependent enhancement of factor Xa inhibition. *Blood*, 116 (8): 1344-1351.

Neve, R. M., Chin, K., Fridlyand, J., Yeh, J., Baehner, F. L., Fevr, T., Clark, L., Bayani, N., Coppe, J. P., Tong, F., et al. (2006). A collection of breast cancer cell lines for the study of functionally distinct cancer subtypes. *Cancer Cell*, 10 (6): 515-27.

Nicholson, D. W., Ali, A., Thornberry, N. A., Vaillancourt, J. P., Ding, C. K., Gallant, M., Gareau, Y., Griffin, P. R., Labelle, M., Lazebnik, Y. A., et al. (1995). Identification and inhibition of the ICE/CED-3 protease necessary for mammalian apoptosis. *Nature*, 376 (6535): 37-43.

Ott, I., Fischer, E. G., Miyagi, Y., Mueller, B. M. & Ruf, W. (1998). A role for tissue factor in cell adhesion and migration mediated by interaction with actin-binding protein 280. *J Cell Biol*, 140 (5): 1241-53.

Ott, I., Weigand, B., Michl, R., Seitz, I., Sabbari-Erfani, N., Neumann, F. J. & Schomig, A. (2005). Tissue factor cytoplasmic domain stimulates migration by activation of the GTPase Rac1 and the mitogen-activated protein kinase p38. *Circulation*, 111 (3): 349-55.

Parkin, D. M., Bray, F., Ferlay, J. & Pisani, P. (2005). Global cancer statistics, 2002. *CA: a cancer journal for clinicians*, 55 (2): 74-108.

Peraramelli, S., Thomassen, S., Heinzmann, A., Rosing, J., Hackeng, T. M., Hartmann, R., Scheiflinger, F. & Dockal, M. (2013). Direct inhibition of factor VIIa by TFPI and TFPI constructs. *Journal of Thrombosis and Haemostasis*, 11 (4): 704-714.

Perou, C. M., Sorlie, T., Eisen, M. B., van de Rijn, M., Jeffrey, S. S., Rees, C. A., Pollack, J. R., Ross, D. T., Johnsen, H., Akslen, L. A., et al. (2000). Molecular portraits of human breast tumours. *Nature*, 406 (6797): 747-52.

Piro, O. & Broze, G. J., Jr. (2004). Role for the Kunitz-3 domain of tissue factor pathway inhibitor-alpha in cell surface binding. *Circulation*, 110 (23): 3567-72.
Piro, O. & Broze, G. J., Jr. (2005). Comparison of cell-surface TFPIalpha and beta. *J Thromb Haemost*, 3 (12): 2677-83.
Pitti, R. M., Marsters, S. A., Lawrence, D. A., Roy, M., Kischkel, F. C., Dowd, P., Huang, A., Donahue, C. J., Sherwood, S. W., Baldwin, D. T., et al. (1998). Genomic amplification of a decoy receptor for Fas ligand in lung and colon cancer. *Nature*, 396 (6712): 699-703.
Polyak, K. (2011). Heterogeneity in breast cancer. *The Journal of clinical investigation*, 121 (10): 3786.
Poon, R. T., Lau, C. P., Ho, J. W., Yu, W. C., Fan, S. T. & Wong, J. (2003). Tissue factor expression correlates with tumor angiogenesis and invasiveness in human hepatocellular carcinoma. *Clin Cancer Res*, 9 (14): 5339-45.
Rao, D. D., Vorhies, J. S., Senzer, N. & Nemunaitis, J. (2009). siRNA vs. shRNA: similarities and differences. *Adv Drug Deliv Rev*, 61 (9): 746-59.
Rao, P., Labhart, M., Mayhew, S., Thirumala, S. & Rao, U. S. (2014). Heterogeneity in the expression of receptors in the human breast cancer metastasized to the brain. *Tumor Biology*: 1-7.
Rath, P. & Aggarwal, B. (1999). TNF-Induced Signaling in Apoptosis. *Journal of Clinical Immunology*, 19 (6): 350-364.
Recillas-Targa, F. (2006). Multiple strategies for gene transfer, expression, knockdown, and chromatin influence in mammalian cell lines and transgenic animals. *Molecular Biotechnology*, 34 (3): 337-354.
Remus, R., Kammer, C., Heller, H., Schmitz, B., Schell, G. & Doerfler, W. (1999). Insertion of foreign DNA into an established mammalian genome can alter the methylation of cellular DNA sequences. *J Virol*, 73 (2): 1010-22.
Rickles, F., Shoji, M. & Abe, K. (2001). The Role of the Hemostatic System in Tumor Growth, Metastasis, and Angiogenesis: Tissue factor is a Bifunctional Molecule Capable of Inducing Both Fibrin Deposition and Angiogenesis in Cancer. *International Journal of Hematology*, 73 (2): 145-150.
Rickles, F. R. & Falanga, A. (2001). Molecular basis for the relationship between thrombosis and cancer. *Thromb Res*, 102 (6): V215-24.
Shoji, M., Hancock, W. W., Abe, K., Micko, C., Casper, K. A., Baine, R. M., Wilcox, J. N., Danave, I., Dillehay, D. L., Matthews, E., et al. (1998). Activation of coagulation and angiogenesis in cancer: immunohistochemical localization in situ of clotting proteins and vascular endothelial growth factor in human cancer. *Am J Pathol*, 152 (2): 399-411.
Skretting, G., Iversen, N., Myklebust, C. F., Dahm, A. E. & Sandset, P. M. (2012). Overexpression of tissue factor pathway inhibitor in CHO-K1 cells results in increased activation of NF-kappaB and apoptosis mediated by a caspase-3 independent pathway. *Mol Biol Rep*, 39 (12): 10089-96.
Smith, S. A. (2009). The cell‐based model of coagulation. *Journal of veterinary emergency and critical care*, 19 (1): 3-10.
Soussi, T. & Beroud, C. (2001). Assessing TP53 status in human tumours to evaluate clinical outcome. *Nat Rev Cancer*, 1 (3): 233-40.
Spronk, H. M. H., Govers-Riemslag, J. W. P. & ten Cate, H. (2003). The blood coagulation system as a molecular machine. *BioEssays*, 25 (12): 1220-1228.
Stavik, B., Skretting, G., Sletten, M., Sandset, P. M. & Iversen, N. (2010). Overexpression of both TFPIalpha and TFPIbeta induces apoptosis and expression of genes involved

in the death receptor pathway in breast cancer cells. *Mol Carcinog*, 49 (11): 951-63.
Stavik, B., Skretting, G., Aasheim, H. C., Tinholt, M., Zernichow, L., Sletten, M., Sandset, P. M. & Iversen, N. (2011). Downregulation of TFPI in breast cancer cells induces tyrosine phosphorylation signaling and increases metastatic growth by stimulating cell motility. *BMC Cancer*, 11: 357.
Stavik, B., Tinholt, M., Sletten, M., Skretting, G., Sandset, P. M. & Iversen, N. (2013). TFPIalpha and TFPIbeta are expressed at the surface of breast cancer cells and inhibit TF-FVIIa activity. *J Hematol Oncol*, 6: 5.
Sui, G., Soohoo, C., Affar el, B., Gay, F., Shi, Y., Forrester, W. C. & Shi, Y. (2002). A DNA vector-based RNAi technology to suppress gene expression in mammalian cells. *Proc Natl Acad Sci U S A*, 99 (8): 5515-20.
Sørlie, T., Perou, C. M., Tibshirani, R., Aas, T., Geisler, S., Johnsen, H., Hastie, T., Eisen, M. B., van de Rijn, M., Jeffrey, S. S., et al. (2001). Gene expression patterns of breast carcinomas distinguish tumor subclasses with clinical implications. *Proceedings of the National Academy of Sciences*, 98 (19): 10869-10874.
Tait, S. W. & Green, D. R. (2010). Mitochondria and cell death: outer membrane permeabilization and beyond. *Nat Rev Mol Cell Biol*, 11 (9): 621-32.
Taxman, D. J., Moore, C. B., Guthrie, E. H. & Huang, M. T.-H. (2010). Short hairpin RNA (shRNA): design, delivery, and assessment of gene knockdown. In *RNA Therapeutics*, pp. 139-156: Springer.
Taylor, F. B., Peer, G. T., Lockhart, M. S., Ferrell, G. & Esmon, C. T. (2001). Endothelial cell protein C receptor plays an important role in protein C activation in vivo. *Blood*, 97 (6): 1685-1688.
Taylor, S. C., Berkelman, T., Yadav, G. & Hammond, M. (2013). A defined methodology for reliable quantification of Western blot data. *Mol Biotechnol*, 55 (3): 217-26.
Tinholt, M., Stavik, B., Wiiger, M. T., Louch, W. E., Sletten, M., Skretting, G., Mælandsmo, G. M., Sandset, P. M. & Iversen, N. (2012). *TFPI in targeted cancer therapy?* [Poster]. Personalized cancer care, Oslo September 2012.
Trotter, J., Klein, C. & Krämer, E.-M. (2000). GPI-anchored proteins and glycosphingolipid-rich rafts: Platforms for adhesion and signaling. *The Neuroscientist*, 6 (4): 271-284.
Tsujimoto, Y. (1998). Role of Bcl-2 family proteins in apoptosis: apoptosomes or mitochondria? *Genes Cells*, 3 (11): 697-707.
van den Berg, Y. W., Osanto, S., Reitsma, P. H. & Versteeg, H. H. (2012). The relationship between tissue factor and cancer progression: insights from bench and bedside. *Blood*, 119 (4): 924-32.
Vara, J. Á. F., Casado, E., de Castro, J., Cejas, P., Belda-Iniesta, C. & González-Barón, M. (2004). PI3K/Akt signalling pathway and cancer. *Cancer Treatment Reviews*, 30 (2): 193-204.
Varki, A. (2007). Trousseau's syndrome: multiple definitions and multiple mechanisms. *Blood*, 110 (6): 1723-9.
Vogelstein, B. & Kinzler, K. W. (2004). Cancer genes and the pathways they control. *Nature Medicine*, 10 (8): 789-99.
Watson, J. D., Baker, T. A., Bell, S. P., Gann, A., Levine, M. & Losick, R. (2008). *MOLECULAR BIOLOGY OF THE GENE*. 6 ed. 1301 Sansome Street, San Fransisco, CA 94111: Benjamin Cummings. 841 pp.

Wesselschmidt, R., Likert, K., Girard, T., Wun, T. C. & Broze, G. J., Jr. (1992). Tissue factor pathway inhibitor: the carboxy-terminus is required for optimal inhibition of factor Xa. *Blood*, 79 (8): 2004-10.

Wilson, R. C. & Doudna, J. A. (2013). Molecular Mechanisms of RNA Interference. *Annu. Rev. Biophys.* (42): 217-39.

Wojtukiewicz, M. Z., Tang, D. G., Ciarelli, J. J., Nelson, K. K., Walz, D. A., Diglio, C. A., Mammen, E. F. & Honn, K. V. (1993). Thrombin increases the metastatic potential of tumor cells. *Int J Cancer*, 54 (5): 793-806.

Wood, J. P., Ellery, P. E., Maroney, S. A. & Mast, A. E. (2014). Biology of tissue factor pathway inhibitor. *Blood*.

Wood, J. P., Ellery, P. E., Maroney, S. A. & Mast, A. E. (2014). Protein S Is a Cofactor for Platelet and Endothelial Tissue Factor Pathway Inhibitor-α but Not for Cell Surface–Associated Tissue Factor Pathway Inhibitor. *Arteriosclerosis, thrombosis, and vascular biology*, 34 (1): 169-176.

Würtele, H., Little, K. & Chartrand, P. (2003). Illegitimate DNA integration in mammalian cells. *Gene therapy*, 10 (21): 1791-1799.

Wysoczynski, M., Liu, R., Kucia, M., Drukala, J. & Ratajczak, M. Z. (2010). Thrombin regulates the metastatic potential of human rhabdomyosarcoma cells: distinct role of PAR1 and PAR3 signaling. *Mol Cancer Res*, 8 (5): 677-90.

Yu, J. L., May, L., Lhotak, V., Shahrzad, S., Shirasawa, S., Weitz, J. I., Coomber, B. L., Mackman, N. & Rak, J. W. (2005). Oncogenic events regulate tissue factor expression in colorectal cancer cells: implications for tumor progression and angiogenesis. *Blood*, 105 (4): 1734-41.

Zhang, J., Piro, O., Lu, L. & Broze, G. J. (2003). Glycosyl Phosphatidylinositol Anchorage of Tissue Factor Pathway Inhibitor. *Circulation*, 108: 623-627.

Zhang, X., Xu, H.-J., Murakami, Y., Sachse, R., Yashima, K., Hirohashi, S., Hu, S.-X., Benedict, W. F. & Sekiya, T. (1994). Deletions of Chromosome 13q, Mutations in Retinoblastoma 1, and Retinoblastoma Protein State in Human Hepatocellular Carcinoma. *Cancer Research*, 54 (15): 4177-4182.

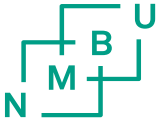

Norwegian University
of Life Sciences

Postboks 5003
NO-1432 Ås, Norway
+47 67 23 00 00
www.nmbu.no